

Kersting, William H. "Distribution Systems"
The Electric Power Engineering Handbook
Ed. L.L. Grigsby
Boca Raton: CRC Press LLC, 2001

6

Distribution Systems

William H. Kersting

New Mexico State University

6.1 Power System Loads *Raymond R. Shoults and Larry D. Swift*

6.2 Distribution System Modeling and Analysis *William H. Kersting*

6.3 Power System Operation and Control *George L. Clark and Simon W. Bowen*

6

Distribution Systems

Raymond R. Shoults

University of Texas at Arlington

Larry D. Swift

University of Texas at Arlington

William H. Kersting

New Mexico State University

George L. Clark

Alabama Power Company

Simon W. Bowen

Alabama Power Company

6.1 Power System Loads

Load Classification • Modeling Applications • Load Modeling
Concepts and Approaches • Load Characteristics and Models •
Static Load Characteristics • Load Window Modeling

6.2 Distribution System Modeling and Analysis

Modeling • Analysis

6.3 Power System Operation and Control

Implementation of Distribution Automation • Distribution
SCADA History • SCADA System Elements • Tactical and
Strategic Implementation Issues • Distribution Management
Platform • Trouble Management Platform • Practical
Considerations

6.1 Power System Loads

Raymond R. Shoults and Larry D. Swift

The physical structure of most power systems consists of generation facilities feeding bulk power into a high-voltage bulk transmission network, that in turn serves any number of distribution substations. A typical distribution substation will serve from one to as many as ten feeder circuits. A typical feeder circuit may serve numerous loads of all types. A light to medium industrial customer may take service from the distribution feeder circuit primary, while a large industrial load complex may take service directly from the bulk transmission system. All other customers, including residential and commercial, are typically served from the secondary of distribution transformers that are in turn connected to a distribution feeder circuit. [Figure 6.1](#) illustrates a representative portion of a typical configuration.

Load Classification

The most common classification of electrical loads follows the billing categories used by the utility companies. This classification includes residential, commercial, industrial, and other. Residential customers are domestic users, whereas commercial and industrial customers are obviously business and industrial users. Other customer classifications include municipalities, state and federal government agencies, electric cooperatives, educational institutions, etc.

Although these load classes are commonly used, they are often inadequately defined for certain types of power system studies. For example, some utilities meter apartments as individual residential customers, while others meter the entire apartment complex as a commercial customer. Thus, the common classifications overlap in the sense that characteristics of customers in one class are not unique to that class. For this reason some utilities define further subdivisions of the common classes.

A useful approach to classification of loads is by breaking down the broader classes into individual load components. This process may altogether eliminate the distinction of certain of the broader classes,

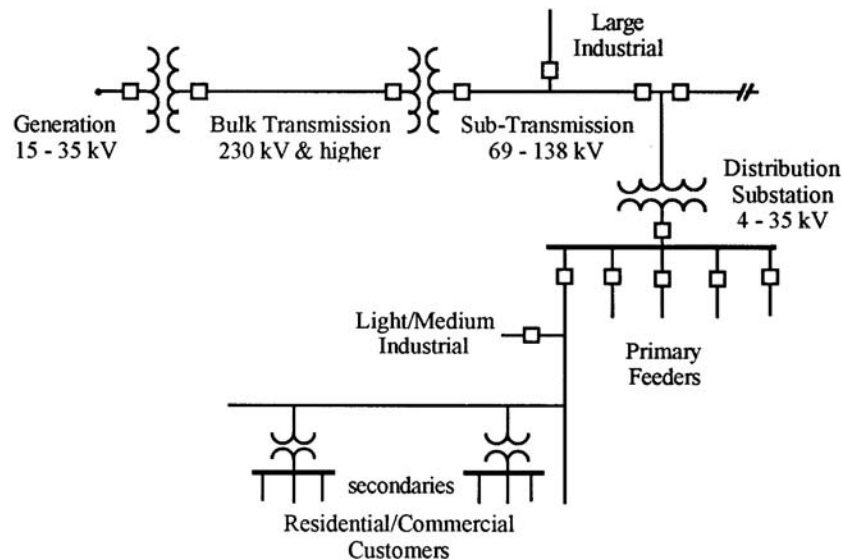


FIGURE 6.1 Representative portion of a typical power system configuration.

but it is a tried and proven technique for many applications. The components of a particular load, be it residential, commercial, or industrial, are individually defined and modeled. These load components as a whole constitute the composite load and can be defined as a “load window.”

Modeling Applications

It is helpful to understand the applications of load modeling before discussing particular load characteristics. The applications are divided into two broad categories: static (“snap-shot” with respect to time) and dynamic (time varying). Static models are based on the steady-state method of representation in power flow networks. Thus, static load models represent load as a function of voltage magnitude. Dynamic models, on the other hand, involve an alternating solution sequence between a time-domain solution of the differential equations describing electromechanical behavior and a steady-state power flow solution based on the method of phasors. One of the important outcomes from the solution of dynamic models is the time variation of frequency. Therefore, it is altogether appropriate to include a component in the static load model that represents variation of load with frequency. The lists below include applications outside of Distribution Systems but are included because load modeling at the distribution level is the fundamental starting point.

Static applications: Models that incorporate only the voltage-dependent characteristic include the following.

- Power flow (PF)
 - Distribution power flow (DPF)
 - Harmonic power flow (HPF)
 - Transmission power flow (TPF)
- Voltage stability (VS)

Dynamic applications: Models that incorporate both the voltage- and frequency-dependent characteristics include the following.

- Transient stability (TS)
- Dynamic stability (DS)
- Operator training simulators (OTS)

Strictly power-flow based solutions utilize load models that include only voltage dependency characteristics. Both voltage and frequency dependency characteristics can be incorporated in load modeling for those hybrid methods that alternate between a time-domain solution and a power flow solution, such as found in Transient Stability and Dynamic Stability Analysis Programs, and Operator Training Simulators.

Load modeling in this section is confined to static representation of voltage and frequency dependencies. The effects of rotational inertia (electromechanical dynamics) for large rotating machines are discussed in Chapters 11 and 12. Static models are justified on the basis that the transient time response of most composite loads to voltage and frequency changes is fast enough so that a steady-state response is reached very quickly.

Load Modeling Concepts and Approaches

There are essentially two approaches to load modeling: component based and measurement based. Load modeling research over the years has included both approaches (EPRI, 1981; 1984; 1985). Of the two, the component-based approach lends itself more readily to model generalization. It is generally easier to control test procedures and apply wide variations in test voltage and frequency on individual components.

The component-based approach is a “bottom-up” approach in that the different load component types comprising load are identified. Each load component type is tested to determine the relationship between real and reactive power requirements versus applied voltage and frequency. A load model, typically in polynomial or exponential form, is then developed from the respective test data. The range of validity of each model is directly related to the range over which the component was tested. For convenience, the load model is expressed on a per-unit basis (i.e., normalized with respect to rated power, rated voltage, rated frequency, rated torque if applicable, and base temperature if applicable). A composite load is approximated by combining appropriate load model types in certain proportions based on load survey information. The resulting composition is referred to as a “load window.”

The measurement approach is a “top-down” approach in that measurements are taken at either a substation level, feeder level, some load aggregation point along a feeder, or at some individual load point. Variation of frequency for this type of measurement is not usually performed unless special test arrangements can be made. Voltage is varied using a suitable means and the measured real and reactive power consumption recorded. Statistical methods are then used to determine load models. A load survey may be necessary to classify the models derived in this manner. The range of validity for this approach is directly related to the realistic range over which the tests can be conducted without damage to customers’ equipment. Both the component and measurement methods were used in the EPRI research projects EL-2036 (1981) and EL-3591 (1984–85). The component test method was used to characterize a number of individual load components that were in turn used in simulation studies. The measurement method was applied to an aggregate of actual loads along a portion of a feeder to verify and validate the component method.

Load Characteristics and Models

Static load models for a number of typical load components appear in [Tables 6.1](#) and [6.2](#) (EPRI 1984–85). The models for each component category were derived by computing a weighted composite from test results of two or more units per category. These component models express per-unit real power and reactive power as a function of per-unit incremental voltage and/or incremental temperature and/or per-unit incremental torque. The incremental form used and the corresponding definition of variables are outlined below:

$$\begin{aligned}\Delta V &= V_{\text{act}} - 1.0 \text{ (incremental voltage in per unit)} \\ \Delta T &= T_{\text{act}} - 95^{\circ}\text{F (incremental temperature for Air Conditioner model)} \\ &= T_{\text{act}} - 47^{\circ}\text{F (incremental temperature for Heat Pump model)} \\ \Delta \tau &= \tau_{\text{act}} - \tau_{\text{rated}} \text{ (incremental motor torque, per unit)}\end{aligned}$$

If ambient temperature is known, it can be used in the applicable models. If it is not known, the temperature difference, ΔT , can be set to zero. Likewise, if motor load torque is known, it can be used in the applicable models. If it is not known, the torque difference, $\Delta \tau$, can be set to zero.

Based on the test results of load components and the developed real and reactive power models as presented in these tables, the following comments on the reactive power models are important.

- The reactive power models vary significantly from manufacturer to manufacturer for the same component. For instance, four load models of single-phase central air-conditioners show a Q/P ratio that varies between 0 and 0.5 at 1.0 p.u. voltage. When the voltage changes, the $\Delta Q/\Delta V$ of each unit is quite different. This situation is also true for all other components, such as refrigerators, freezers, fluorescent lights, etc.
- It has been observed that the reactive power characteristic of fluorescent lights not only varies from manufacturer to manufacturer, from old to new, from long tube to short tube, but also varies from capacitive to inductive depending upon applied voltage and frequency. This variation makes it difficult to obtain a good representation of the reactive power of a composite system and also makes it difficult to estimate the $\Delta Q/\Delta V$ characteristic of a composite system.
- The relationship between reactive power and voltage is more non-linear than the relationship between real power and voltage, making Q more difficult to estimate than P.
- For some of the equipment or appliances, the amount of Q required at the nominal operating voltage is very small; but when the voltage changes, the change in Q with respect to the base Q can be very large.
- Many distribution systems have switchable capacitor banks either at the substations or along feeders. The composite Q characteristic of a distribution feeder is affected by the switching strategy used in these banks.

Static Load Characteristics

The component models appearing in [Tables 6.1](#) and [6.2](#) can be combined and synthesized to create other more convenient models. These convenient models fall into two basic forms: exponential and polynomial.

Exponential Models

The exponential form for both real and reactive power is expressed in Eqs. (6.1) and (6.2) below as a function of voltage and frequency, relative to initial conditions or base values. Note that neither temperature nor torque appear in these forms. Assumptions must be made about temperature and/or torque values when synthesizing from component models to these exponential model forms.

$$P = P_o \left[\frac{V}{V_o} \right]^{\alpha_v} \left[\frac{f}{f_o} \right]^{\alpha_f} \quad (6.1)$$

$$Q = Q_o \left[\frac{V}{V_o} \right]^{\beta_v} \left[\frac{f}{f_o} \right]^{\beta_f} \quad (6.2)$$

The per-unit models of Eqs. (6.1) and (6.2) are as follows.

$$P_u = \frac{P}{P_o} = \left[\frac{V}{V_o} \right]^{\alpha_v} \left[\frac{f}{f_o} \right]^{\alpha_f} \quad (6.3)$$

TABLE 6.1 Static Models of Typical Load Components — AC, Heat Pump, and Appliances

| Load Component | Static Component Model |
|--|--|
| 1- ϕ Central Air Conditioner | $P = 1.0 + 0.4311\Delta V + 0.9507\Delta T + 2.070\Delta V^2 + 2.388\Delta T^2 - 0.900\Delta V\Delta T$ $Q = 0.3152 + 0.6636\Delta V + 0.543\Delta V^2 + 5.422\Delta V^3 + 0.839\Delta T^2 - 1.455\Delta V\Delta T$ |
| 3- ϕ Central Air Conditioner | $P = 1.0 + 0.2693\Delta V + 0.4879\Delta T + 1.005\Delta V^2 - 0.188\Delta T^2 - 0.154\Delta V\Delta T$ $Q = 0.6957 + 2.3717\Delta V + 0.0585\Delta T + 5.81\Delta V^2 + 0.199\Delta T^2 - 0.597\Delta V\Delta T$ |
| Room Air Conditioner (115V Rating) | $P = 1.0 + 0.2876\Delta V + 0.6876\Delta T + 1.241\Delta V^2 + 0.089\Delta T^2 - 0.558\Delta V\Delta T$ $Q = 0.1485 + 0.3709\Delta V + 1.5773\Delta T + 1.286\Delta V^2 + 0.266\Delta T^2 - 0.438\Delta V\Delta T$ |
| Room Air Conditioner (208/230V Rating) | $P = 1.0 + 0.5953\Delta V + 0.5601\Delta T + 2.021\Delta V^2 + 0.145\Delta T^2 - 0.491\Delta V\Delta T$ $Q = 0.4968 + 2.4456\Delta V + 0.0737\Delta T + 8.604\Delta V^2 - 0.125\Delta T^2 - 1.293\Delta V\Delta T$ |
| 3- ϕ Heat Pump (Heating Mode) | $P = 1.0 + 0.4539\Delta V + 0.2860\Delta T + 1.314\Delta V^2 - 0.024\Delta V\Delta T$ $Q = 0.9399 + 3.013\Delta V - 0.1501\Delta T + 7.460\Delta V^2 - 0.312\Delta T^2 - 0.216\Delta V\Delta T$ |
| 3- ϕ Heat Pump (Cooling Mode) | $P = 1.0 + 0.2333\Delta V + 0.5915\Delta T + 1.362\Delta V^2 + 0.075\Delta T^2 - 0.093\Delta V\Delta T$ $Q = 0.8456 + 2.3404\Delta V - 0.1806\Delta T + 6.896\Delta V^2 + 0.029\Delta T^2 - 0.836\Delta V\Delta T$ |
| 1- ϕ Heat Pump (Heating Mode) | $P = 1.0 + 0.3953\Delta V + 0.3563\Delta T + 1.679\Delta V^2 + 0.083\Delta V\Delta T$ $Q = 0.3427 + 1.9522\Delta V - 0.0958\Delta T + 6.458\Delta V^2 - 0.225\Delta T^2 - 0.246\Delta V\Delta T$ |
| 1- ϕ Heat Pump (Cooling Mode) | $P = 1.0 + 0.3630\Delta V + 0.7673\Delta T + 2.101\Delta V^2 + 0.122\Delta T^2 - 0.759\Delta V\Delta T$ $Q = 0.3605 + 1.6873\Delta V + 0.2175\Delta T + 10.055\Delta V^2 - 0.170\Delta T^2 - 1.642\Delta V\Delta T$ |
| Refrigerator | $P = 1.0 + 1.3958\Delta V + 9.881\Delta V^2 + 84.72\Delta V^3 + 293\Delta V^4$ $Q = 1.2507 + 4.387\Delta V + 23.801\Delta V^2 + 1540\Delta V^3 + 555\Delta V^4$ |
| Freezer | $P = 1.0 + 1.3286\Delta V + 12.616\Delta V^2 + 133.6\Delta V^3 + 380\Delta V^4$ $Q = 1.3810 + 4.6702\Delta V + 27.276\Delta V^2 + 293.0\Delta V^3 + 995\Delta V^4$ |
| Washing Machine | $P = 1.0 + 1.2786\Delta V + 3.099\Delta V^2 + 5.939\Delta V^3$ $Q = 1.6388 + 4.5733\Delta V + 12.948\Delta V^2 + 55.677\Delta V^3$ |
| Clothes Dryer | $P = 1.0 - 0.1968\Delta V - 3.6372\Delta V^2 - 28.32\Delta V^3$ $Q = 0.209 + 0.5180\Delta V + 0.363\Delta V^2 - 4.7574\Delta V^3$ |
| Television | $P = 1.0 + 1.2471\Delta V + 0.562\Delta V^2$ $Q = 0.2431 + 0.9830\Delta V + 1.647\Delta V^2$ |
| Fluorescent Lamp | $P = 1.0 + 0.6534\Delta V - 1.65\Delta V^2$ $Q = -0.1535 - 0.0403\Delta V + 2.734\Delta V^2$ |
| Mercury Vapor Lamp | $P = 1.0 + 0.1309\Delta V + 0.504\Delta V^2$ $Q = -0.2524 + 2.3329\Delta V + 7.811\Delta V^2$ |
| Sodium Vapor Lamp | $P = 1.0 + 0.3409\Delta V - 2.389\Delta V^2$ $Q = 0.060 + 2.2173\Delta V + 7.620\Delta V^2$ |
| Incandescent | $P = 1.0 + 1.5209\Delta V + 0.223\Delta V^2$ $Q = 0.0$ |
| Range with Oven | $P = 1.0 + 2.1018\Delta V + 5.876\Delta V^2 + 1.236\Delta V^3$ $Q = 0.0$ |
| Microwave Oven | $P = 1.0 + 0.0974\Delta V + 2.071\Delta V^2$ $Q = 0.2039 + 1.3130\Delta V + 8.738\Delta V^2$ |
| Water Heater | $P = 1.0 + 0.3769\Delta V + 2.003\Delta V^2$ $Q = 0.0$ |
| Resistance Heating | $P = 1.0 + 2\Delta V + \Delta V^2$ $Q = 0.0$ |

$$Q_u = \frac{Q}{P_o} = \frac{Q_o}{P_o} \left[\frac{V}{V_o} \right]^{\beta_v} \left[\frac{f}{f_o} \right]^{\beta_f} \quad (6.4)$$

The ratio Q_o/P_o can be expressed as a function of power factor (pf) where \pm indicates a lagging/leading power factor, respectively.

$$R = \frac{Q_o}{P_o} = \pm \sqrt{\frac{1}{\text{pf}^2} - 1}$$

TABLE 6.2 Static Models of Typical Load Components – Transformers and Induction Motors

| Load Component | Static Component Model |
|---|--|
| Transformer Core Loss Model | $P = \frac{\text{KVA}(\text{rating})}{\text{KVA}(\text{system base})} \left[0.00267V^2 + 0.73 \times 10^{-9} \times e^{13.5V^2} \right]$ $Q = \frac{\text{KVA}(\text{rating})}{\text{KVA}(\text{system base})} \left[0.00167V^2 + 0.268 \times 10^{-13} \times e^{22.76V^2} \right]$ <p style="text-align: center;">where V is voltage magnitude in per unit</p> |
| 1- ϕ Motor Constant Torque | $P = 1.0 + 0.5179\Delta V + 0.9122\Delta\tau + 3.721\Delta V^2 + 0.350\Delta\tau^2 - 1.326\Delta V\Delta\tau$ $Q = 0.9853 + 2.7796\Delta V + 0.0859\Delta\tau + 7.368\Delta V^2 + 0.218\Delta\tau^2 - 1.799\Delta V\Delta\tau$ |
| 3- ϕ Motor (1-10HP) Const. Torque | $P = 1.0 + 0.2250\Delta V + 0.9281\Delta\tau + 0.970\Delta V^2 + 0.086\Delta\tau^2 - 0.329\Delta V\Delta\tau$ $Q = 0.7810 + 2.3532\Delta V + 0.1023\Delta\tau - 5.951\Delta V^2 + 0.446\Delta\tau^2 - 1.48\Delta V\Delta\tau$ |
| 3- ϕ Motor (10HP/Above) Const. Torque | $P = 1.0 + 0.0199\Delta V + 1.0463\Delta\tau + 0.341\Delta V^2 + 0.116\Delta\tau^2 - 0.457\Delta V\Delta\tau$ $Q = 0.6577 + 1.2078\Delta V + 0.3391\Delta\tau + 4.097\Delta V^2 + 0.289\Delta\tau^2 - 1.477\Delta V\Delta\tau$ |
| 1- ϕ Motor Variable Torque | $P = 1.0 + 0.7101\Delta V + 0.9073\Delta\tau + 2.13\Delta V^2 + 0.245\Delta\tau^2 - 0.310\Delta V\Delta\tau$ $Q = 0.9727 + 2.7621\Delta V + 0.077\Delta\tau + 6.432\Delta V^2 + 0.174\Delta\tau^2 - 1.412\Delta V\Delta\tau$ |
| 3- ϕ Motor (1-10HP) Variable Torque | $P = 1.0 + 0.3122\Delta V + 0.9286\Delta\tau + 0.489\Delta V^2 + 0.081\Delta\tau^2 - 0.079\Delta V\Delta\tau$ $Q = 0.7785 + 2.3648\Delta V + 0.1025\Delta\tau + 5.706\Delta V^2 + 0.13\Delta\tau^2 - 1.00\Delta V\Delta\tau$ |
| 3- ϕ Motor (10HP & Above) Variable Torque | $P = 1.0 + 0.1628\Delta V + 1.0514\Delta\tau + 0.099\Delta V^2 + 0.107\Delta\tau^2 + 0.061\Delta V\Delta\tau$ $Q = 0.6569 + 1.2467\Delta V + 0.3354\Delta\tau + 3.685\Delta V^2 + 0.258\Delta\tau^2 - 1.235\Delta V\Delta\tau$ |

After substituting R for Q_o/P_o , Eq. (6.4) becomes the following.

$$Q_u = R \left[\frac{V}{V_o} \right]^{\beta_v} \left[\frac{f}{f_o} \right]^{\beta_f} \quad (6.5)$$

Eqs. (6.1) and (6.2) [or (6.3) and (6.5)] are valid over the voltage and frequency ranges associated with tests conducted on the individual components from which these exponential models are derived. These ranges are typically $\pm 10\%$ for voltage and $\pm 2.5\%$ for frequency. The accuracy of these models outside the test range is uncertain. However, one important factor to note is that in the extreme case of voltage approaching zero, both P and Q approach zero.

EPRI-sponsored research resulted in model parameters such as found in Table 6.3 (EPRI, 1987; Price et al., 1988). Eleven model parameters appear in this table, of which the exponents α and β and the power factor (pf) relate directly to Eqs. (6.3) and (6.5). The first six parameters relate to general load models, some of which include motors, and the remaining five parameters relate to nonmotor loads — typically resistive type loads. The first is load power factor (pf). Next in order (from left to right) are the exponents for the voltage (α_v , α_f) and frequency (β_v , β_f) dependencies associated with real and reactive power, respectively. N_m is the motor-load portion of the load. For example, both a refrigerator and a freezer are 80% motor load. Next in order are the power factor (pf_{nm}) and voltage (α_{vnm} , α_{fnn}) and frequency (β_{vnm} , β_{fnn}) parameters for the nonmotor portion of the load. Since the refrigerator and freezer are 80% motor loads (i.e., $N_m = 0.8$), the nonmotor portion of the load must be 20%.

Polynomial Models

A polynomial form is often used in a Transient Stability program. The voltage dependency portion of the model is typically second order. If the nonlinear nature with respect to voltage is significant, the order can be increased. The frequency portion is assumed to be first order. This model is expressed as follows.

$$P = P_o \left[a_o + a_1 \left(\frac{V}{V_o} \right) + a_2 \left(\frac{V}{V_o} \right)^2 \right] [1 + D_p \Delta f] \quad (6.6)$$

TABLE 6.3 Parameters for Voltage and Frequency Dependencies of Static Loads

| Component/Parameters | pf | α_v | α_f | β_v | β_f | N_m | pf_{nm} | α_{vnm} | α_{fnn} | β_{vnm} | β_{fnn} |
|-------------------------------------|------|------------|------------|-----------|-----------|-------|-----------|----------------|----------------|---------------|---------------|
| Resistance Space Heater | 1.0 | 2.0 | 0.0 | 0.0 | 0.0 | 0.0 | — | — | — | — | — |
| Heat Pump Space Heater | 0.84 | 0.2 | 0.9 | 2.5 | -1.3 | 0.9 | 1.0 | 2.0 | 0.0 | 0.0 | 0.0 |
| Heat Pump/Central A/C | 0.81 | 0.2 | 0.9 | 2.5 | -2.7 | 1.0 | — | — | — | — | — |
| Room Air Conditioner | 0.75 | 0.5 | 0.6 | 2.5 | -2.8 | 1.0 | — | — | — | — | — |
| Water Heater & Range | 1.0 | 2.0 | 0.0 | 0.0 | 0.0 | 0.0 | — | — | — | — | — |
| Refrigerator & Freezer | 0.84 | 0.8 | 0.5 | 2.5 | -1.4 | 0.8 | 1.0 | 2.0 | 0.0 | 0.0 | 0.0 |
| Dish Washer | 0.99 | 1.8 | 0.0 | 3.5 | -1.4 | 0.8 | 1.0 | 2.0 | 0.0 | 0.0 | 0.0 |
| Clothes Washer | 0.65 | 0.08 | 2.9 | 1.6 | 1.8 | 1.0 | — | — | — | — | — |
| Incandescent Lighting | 1.0 | 1.54 | 0.0 | 0.0 | 0.0 | 0.0 | — | — | — | — | — |
| Clothes Dryer | 0.99 | 2.0 | 0.0 | 3.3 | -2.6 | 0.2 | 1.0 | 2.0 | 0.0 | 0.0 | 0.0 |
| Colored Television | 0.77 | 2.0 | 0.0 | 5.2 | -4.6 | 0.0 | — | — | — | — | — |
| Furnace Fan | 0.73 | 0.08 | 2.9 | 1.6 | 1.8 | 1.0 | — | — | — | — | — |
| Commercial Heat Pump | 0.84 | 0.1 | 1.0 | 2.5 | -1.3 | 0.9 | 1.0 | 2.0 | 0.0 | 0.0 | 0.0 |
| Heat Pump Comm. A/C | 0.81 | 0.1 | 1.0 | 2.5 | -1.3 | 1.0 | — | — | — | — | — |
| Commercial Central A/C | 0.75 | 0.1 | 1.0 | 2.5 | -1.3 | 1.0 | — | — | — | — | — |
| Commercial Room A/C | 0.75 | 0.5 | 0.6 | 2.5 | -2.8 | 1.0 | — | — | — | — | — |
| Fluorescent Lighting | 0.90 | 0.08 | 1.0 | 3.0 | -2.8 | 0.0 | — | — | — | — | — |
| Pump, Fan, (Motors) | 0.87 | 0.08 | 2.9 | 1.6 | 1.8 | 1.0 | — | — | — | — | — |
| Electrolysis | 0.90 | 1.8 | -0.3 | 2.2 | 0.6 | 0.0 | — | — | — | — | — |
| Arc Furnace | 0.72 | 2.3 | -1.0 | 1.61 | -1.0 | 0.0 | — | — | — | — | — |
| Small Industrial Motors | 0.83 | 0.1 | 2.9 | 0.6 | -1.8 | 1.0 | — | — | — | — | — |
| Industrial Motors Large | 0.89 | 0.05 | 1.9 | 0.5 | 1.2 | 1.0 | — | — | — | — | — |
| Agricultural H ₂ O Pumps | 0.85 | 1.4 | 5.6 | 1.4 | 4.2 | 1.0 | — | — | — | — | — |
| Power Plant Auxiliaries | 0.80 | 0.08 | 2.9 | 1.6 | 1.8 | 1.0 | — | — | — | — | — |

$$Q = Q_o \left[b_o + b_1 \left(\frac{V}{V_o} \right) + b_2 \left(\frac{V}{V_o} \right)^2 \right] [1 + D_q \Delta f] \quad (6.7)$$

where $a_o + a_1 + a_2 = 1$

$b_o + b_1 + b_2 = 1$

$D_p \equiv$ real power frequency damping coefficient, per unit

$D_q \equiv$ reactive power frequency damping coefficient, per unit

$\Delta f \equiv$ frequency deviation from scheduled value, per unit

The per-unit form of Eqs. (6.6) and (6.7) is the following.

$$P_u = \frac{P}{P_o} = \left[a_o + a_1 \left(\frac{V}{V_o} \right) + a_2 \left(\frac{V}{V_o} \right)^2 \right] [1 + D_p \Delta f] \quad (6.8)$$

$$Q_u = \frac{Q}{P_o} = \frac{Q_o}{P_o} \left[b_o + b_1 \left(\frac{V}{V_o} \right) + b_2 \left(\frac{V}{V_o} \right)^2 \right] [1 + D_q \Delta f] \quad (6.9)$$

Combined Exponential and Polynomial Models

The two previous kinds of models may be combined to form a synthesized static model that offers greater flexibility in representing various load characteristics (EPRI, 1987; Price et al., 1988). The mathematical expressions for these per-unit models are the following.

$$P_u = \frac{P_{\text{poly}} + P_{\text{exp1}} + P_{\text{exp2}}}{P_o} \quad (6.10)$$

$$Q_u = \frac{Q_{\text{poly}} + Q_{\text{exp1}} + Q_{\text{exp2}}}{P_o} \quad (6.11)$$

where

$$P_{\text{poly}} = a_0 + a_1 \left(\frac{V}{V_o} \right) + a_3 \left(\frac{V}{V_o} \right)^2 \quad (6.12)$$

$$P_{\text{exp1}} = a_4 \left(\frac{V}{V_o} \right)^{\alpha_1} [1 + D_{p1} \Delta f] \quad (6.13)$$

$$P_{\text{exp2}} = a_5 \left(\frac{V}{V_o} \right)^{\alpha_2} [1 + D_{p2} \Delta f] \quad (6.14)$$

The expressions for the reactive components have similar structures. Devices used for reactive power compensation are modeled separately.

The flexibility of the component models given here is sufficient to cover most modeling needs. Whenever possible, it is prudent to compare the computer model to measured data for the load.

Table 6.4 provides typical values for the frequency damping characteristic, D , that appears in Eqs. (6.6) through (6.9), (6.13), and (6.14) (EPRI, 1979). Note that nearly all of the damping coefficients for reactive power are negative. This means that as frequency declines, more reactive power is required which can cause an exacerbating effect for low-voltage conditions.

Comparison of Exponential and Polynomial Models

Both models provide good representation around rated or nominal voltage. The accuracy of the exponential form deteriorates when voltage significantly exceeds its nominal value, particularly with exponents (α) greater than 1.0. The accuracy of the polynomial form deteriorates when the voltage falls significantly below its nominal value when the coefficient a_0 is non zero. A nonzero a_0 coefficient represents some portion of the load as constant power. A scheme often used in practice is to use the polynomial form, but switch to the exponential form when the voltage falls below a predetermined value.

TABLE 6.4 Static Load Frequency Damping Characteristics

| Component | Frequency Parameters | |
|--------------------------------|----------------------|-----------|
| | D_p | D_q |
| Three-Phase Central AC | 1.09818 | -0.663828 |
| Single-Phase Central AC | 0.994208 | -0.307989 |
| Window AC | 0.702912 | -1.89188 |
| Duct Heater w/blowers | 0.528878 | -0.140006 |
| Water Heater, Electric Cooking | 0.0 | 0.0 |
| Clothes Dryer | 0.0 | -0.311885 |
| Refrigerator, Ice Machine | 0.664158 | -1.10252 |
| Incandescent Lights | 0.0 | 0.0 |
| Florescent Lights | 0.887964 | -1.16844 |
| Induction Motor Loads | 1.6 | -0.6 |

Devices Contributing to Modeling Difficulties

Some load components have time-dependent characteristics that must be considered if a sequence of studies using static models is performed that represents load changing over time. Examples of such a study include Voltage Stability and Transient Stability. The devices that affect load modeling by contributing abrupt changes in load over periods of time are listed below.

Protective Relays — Protective relays are notoriously difficult to model. The entire load of a substation can be tripped off line or the load on one of its distribution feeders can be tripped off line as a result of protective relay operations. At the utilization level, motors on air conditioner units and motors in many other residential, commercial, and industrial applications contain thermal and/or over-current relays whose operational behavior is difficult to predict.

Thermostatically Controlled Loads — Air conditioning units, space heaters, water heaters, refrigerators, and freezers are all controlled by thermostatic devices. The effects of such devices are especially troublesome to model when a distribution load is reenergized after an extended outage (cold-load pickup). The effect of such devices to cold-load pickup characteristics can be significant.

Voltage Regulation Devices — Voltage regulators, voltage controlled capacitor banks, and automatic LTCs on transformers exhibit time-dependent effects. These devices are present at both the bulk power and distribution system levels.

Discharge Lamps (Mercury Vapor, Sodium Vapor, and Fluorescent Lamps) — These devices exhibit time-dependent characteristics upon restart, after being extinguished by a low-voltage condition — usually about 70% to 80% of rated voltage.

Load Window Modeling

The static load models found in [Tables 6.1](#) and [6.2](#) can be used to define a composite load referred to as the “load window” mentioned earlier. In this scheme, a distribution substation load or one of its feeder loads is defined in as much detail as desired for the model. Using the load window scheme, any number of load windows can be defined representing various composite loads, each having as many load components as deemed necessary for accurate representation of the load. [Figure 6.2](#) illustrates the load window concept. The width of each subwindow denotes the percentage of each load component to the total composite load.

Construction of a load window requires certain load data be available. For example, load saturation and load diversity data are needed for various classes of customers. These data allow one to (1) identify the appropriate load components to be included in a particular load window, (2) assign their relative percentage of the total load, and (3) specify the diversified total amount of load for that window. If load modeling is being used for Transient Stability or Operator Training Simulator programs, frequency dependency can be added. Let $P(V)$ and $Q(V)$ represent the composite load models for P and Q ,

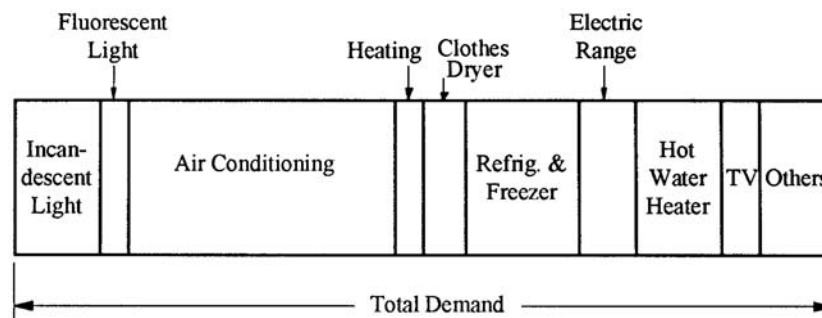


FIGURE 6.2 A typical load window with % composition of load components.

TABLE 6.5 Composition of Six Different Load Window Types

| Load Window Type | LW 1 | LW 2 | LW 3 | LW 4 | LW 5 | LW 6 |
|----------------------------|--------|--------|--------|-------|-------|--------|
| Load Component | Res. 1 | Res. 2 | Res. 3 | Com 1 | Com 2 | Indust |
| | (%) | (%) | (%) | (%) | (%) | (%) |
| 3-Phase Central AC | 25 | 30 | 10 | 35 | 40 | 20 |
| Window Type AC | 5 | 0 | 20 | 0 | 0 | 0 |
| Duct Heater with Blower | 5 | 0 | 0 | 0 | 0 | 0 |
| Water Heater, Range Top | 10 | 10 | 10 | 0 | 0 | 0 |
| Clothes Dryer | 10 | 10 | 10 | 0 | 0 | 0 |
| Refrigerator, Ice Machine | 15 | 15 | 10 | 30 | 0 | 0 |
| Incandescent Lights | 10 | 5 | 10 | 0 | 0 | 0 |
| Fluorescent Lights | 20 | 30 | 30 | 25 | 30 | 10 |
| Industrial (Induct. Motor) | 0 | 0 | 0 | 10 | 30 | 70 |

respectively, with only voltage dependency (as developed using components taken from [Tables 6.1](#) and [6.2](#)). Frequency dependency is easily included as illustrated below.

$$P = P(V) \times (1 + D_p \Delta f)$$

$$Q = Q(V) \times (1 + D_q \Delta f)$$

[Table 6.5](#) shows six different composite loads for a summer season in the southwestern portion of the U.S. This “window” serves as an example to illustrate the modeling process. Note that each column must add to 100%. The entries across from each component load for a given window type represent the percentage of that load making up the composite load.

References

- EPRI User's Manual — Extended Transient/Midterm Stability Program Package*, version 3.0, June 1992.
- General Electric Company, Load modeling for power flow and transient stability computer studies, *EPRI Final Report EL-5003*, January 1987 (four volumes describing LOADSYN computer program).
- Kundur, P., *Power System Stability and Control*, EPRI Power System Engineering Series, McGraw-Hill, Inc., 271–314, 1994.
- Price, W. W., Wirgau, K. A., Murdoch, A., Mitsche, J. V., Vaahedi, E., and El-Kady, M. A., Load Modeling for Power Flow and Transient Stability Computer Studies, *IEEE Trans. on Power Syst.*, 3(1), 180–187, February 1988.
- Taylor, C. W., *Power System Voltage Stability*, EPRI Power System Engineering Series, McGraw-Hill, Inc., 67–107, 1994.
- University of Texas at Arlington, Determining Load Characteristics for Transient Performances, *EPRI Final Report EL-848*, May 1979 (three volumes).
- University of Texas at Arlington, Effect of Reduced Voltage on the Operation and Efficiency of Electrical Loads, *EPRI Final Report EL-2036*, September 1981 (two volumes).
- University of Texas at Arlington, Effect of Reduced Voltage on the Operation and Efficiency of Electrical Loads, *EPRI Final Report EL-3591*, June 1984 and July 1985 (three volumes).
- Warnock, V. J. and Kirkpatrick, T. L., Impact of Voltage Reduction on Energy and Demand: Phase II, *IEEE Trans. on Power Syst.*, 3(2), 92–97, May 1986.

6.2 Distribution System Modeling and Analysis

William H. Kersting

Modeling

Radial distribution feeders are characterized by having only one path for power to flow from the source (“distribution substation”) to each customer. A typical distribution system will consist of one or more distribution substations consisting of one or more “feeders”. Components of the feeder may consist of the following:

- Three-phase primary “main” feeder
- Three-phase, two-phase (“V” phase), and single-phase laterals
- Step-type voltage regulators or load tap changing transformer (LTC)
- In-line transformers
- Shunt capacitor banks
- Three-phase, two-phase, and single-phase loads

The loading of a distribution feeder is inherently unbalanced because of the large number of unequal single-phase loads that must be served. An additional unbalance is introduced by the nonequilateral conductor spacings of the three-phase overhead and underground line segments.

Because of the nature of the distribution system, conventional power-flow and short-circuit programs used for transmission system studies are not adequate. Such programs display poor convergence characteristics for radial systems. The programs also assume a perfectly balanced system so that a single-phase equivalent system is used.

If a distribution engineer is to be able to perform accurate power-flow and short-circuit studies, it is imperative that the distribution feeder be modeled as accurately as possible. This means that three-phase models of the major components must be utilized. Three-phase models for the major components will be developed in the following sections. The models will be developed in the “phase frame” rather than applying the method of symmetrical components.

Figure 6.3 shows a simple one-line diagram of a three-phase feeder; it illustrates the major components of a distribution system. The connecting points of the components will be referred to as “nodes.” Note in the figure that the phasing of the line segments is shown. This is important if the most accurate models are to be developed.

The following sections will present generalized three-phase models for the “series” components of a feeder (line segments, voltage regulators, transformer banks). Additionally, models are presented for the “shunt” components (loads, capacitor banks). Finally, the “ladder iterative technique” for power-flow studies using the models is presented along with a method for computing short-circuit currents for all types of faults.

Line Impedance

The determination of the impedances for overhead and underground lines is a critical step before analysis of distribution feeder can begin. Depending upon the degree of accuracy required, impedances can be calculated using Carson’s equations where no assumptions are made, or the impedances can be determined from tables where a wide variety of assumptions are made. Between these two limits are other techniques, each with their own set of assumptions.

Carson’s Equations

Since a distribution feeder is inherently unbalanced, the most accurate analysis should not make any assumptions regarding the spacing between conductors, conductor sizes, or transposition. In a classic paper, John Carson developed a technique in 1926 whereby the self and mutual impedances for **ncond**

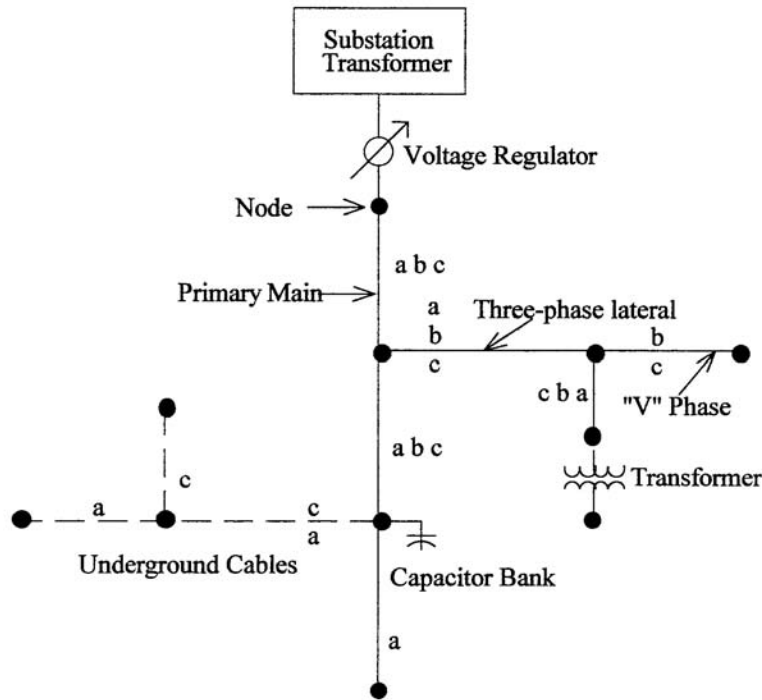


FIGURE 6.3 Distribution feeder.

overhead conductors can be determined. The equations can also be applied to underground cables. In 1926, this technique was not met with a lot of enthusiasm because of the tedious calculations that had to be done on the slide rule and by hand. With the advent of the digital computer, Carson's equations have now become widely used.

In his paper, Carson assumes the earth is an infinite, uniform solid, with a flat uniform upper surface and a constant resistivity. Any "end effects" introduced at the neutral grounding points are not large at power frequencies, and therefore are neglected. The original Carson equations are given in Eqs. (6.15) and (6.16).

Self-impedance:

$$\hat{z}_{ii} = r_i + 4\omega P_{ii}G + j \left(X_i + 2\omega G_{ii} \cdot \ln \frac{S_{ii}}{R_i} + 4\omega Q_{ii}G \right) \text{ Ohms/mile} \quad (6.15)$$

Mutual impedance:

$$\hat{z}_{ij} = 4\omega P_{ij}G + j \left(2\omega G \cdot \ln \frac{S_{ij}}{D_{ij}} + 4\omega Q_{ij}G \right) \text{ Ohms/mile} \quad (6.16)$$

where \hat{z}_{ii} = self-impedance of conductor i in Ohms/mile
 \hat{z}_{ij} = mutual impedance between conductors i and j in ohms/mile
 r_i = resistance of conductor i in Ohms/mile
 ω = system angular frequency in radians per second
 G = 0.1609347×10^{-7} Ohm-cm/abohm-mile
 R_i = radius of conductor i in feet
 GMR_i = geometric mean radius of conductor i in feet

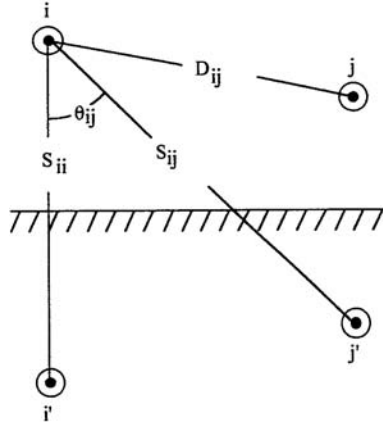


FIGURE 6.4 Conductors and images.

- f = system frequency in Hertz
 ρ = resistivity of earth in ohm-meters
 D_{ij} = distance between conductors i and j in feet
 S_{ij} = distance between conductor i and image j in feet
 θ_{ij} = angle between a pair of lines drawn from conductor i to its own image and to the image of conductor j

$$X_i = 2\omega G \cdot \ln \frac{R_i}{GMR_i} \text{ Ohms/mile} \quad (6.17)$$

$$P_{ij} = \frac{\pi}{8} - \frac{1}{3\sqrt{2}} k_{ij} \cos(\theta_{ij}) + \frac{k_{ij}^2}{16} \cos(2\theta_{ij}) \cdot \left(0.6728 + \ln \frac{2}{k_{ij}} \right) \quad (6.18)$$

$$Q_{ij} = -0.0386 + \frac{1}{2} \ln \frac{2}{k_{ij}} + \frac{1}{3\sqrt{2}} k_{ij} \cos(\theta_{ij}) \quad (6.19)$$

$$k_{ij} = 8.565 \times 10^{-4} \cdot S_{ij} \cdot \sqrt{\frac{f}{\rho}} \quad (6.20)$$

As indicated above, Carson made use of conductor images; that is, every conductor at a given distance above ground has an image conductor the same distance below ground. This is illustrated in Fig. 6.4.

Modified Carson's Equations

Only two approximations are made in deriving the "Modified Carson Equations." These approximations involve the terms associated with P_{ij} and Q_{ij} . The approximations are shown below:

$$P_{ij} = \frac{\pi}{8} \quad (6.21)$$

$$Q_{ij} = -0.03860 + \frac{1}{2} \ln \frac{2}{k_{ij}} \quad (6.22)$$

It is also assumed:

f = frequency = 60 Hertz

ρ = resistivity = 100 Ohm-meter

Using these approximations and assumptions, Carson's equations reduce to:

$$\hat{z}_{ii} = r_i + 0.0953 + j0.12134 \left(\ln \frac{1}{GMR_i} + 7.93402 \right) \text{ Ohms/mile} \quad (6.23)$$

$$\hat{z}_{ij} = 0.0953 + j0.12134 \left(\ln \frac{1}{D_{ij}} + 7.93402 \right) \text{ Ohms/mile} \quad (6.24)$$

Overhead and Underground Lines

Equations (6.23) and (6.24) can be used to compute an $\mathbf{ncond} \times \mathbf{ncond}$ “primitive impedance” matrix. For an overhead four wire, grounded wye distribution line segment, this will result in a 4×4 matrix. For an underground grounded wye line segment consisting of three concentric neutral cables, the resulting matrix will be 6×6 . The primitive impedance matrix for a three-phase line consisting of \mathbf{m} neutrals will be of the form:

$$[z_{primitive}] = \begin{bmatrix} \hat{z}_{aa} & \hat{z}_{ab} & \hat{z}_{ac} & | & \hat{z}_{an1} & \bullet & \hat{z}_{anm} \\ \hat{z}_{ba} & \hat{z}_{bb} & \hat{z}_{bc} & | & \hat{z}_{bn1} & \bullet & \hat{z}_{bnm} \\ \hat{z}_{ca} & \hat{z}_{cb} & \hat{z}_{cc} & | & \hat{z}_{cn1} & \bullet & \hat{z}_{cnm} \\ \hline \hat{z}_{n1a} & \hat{z}_{n1b} & \hat{z}_{n1c} & | & \hat{z}_{n1n1} & \bullet & \hat{z}_{n1nm} \\ \bullet & \bullet & \bullet & | & \bullet & \bullet & \bullet \\ \hat{z}_{nma} & \hat{z}_{nmb} & \hat{z}_{nmc} & | & \hat{z}_{nmn1} & \bullet & \hat{z}_{nmnm} \end{bmatrix} \quad (6.25)$$

In partitioned form Eq. 6.11 becomes:

$$[z_{primitive}] = \begin{bmatrix} [\hat{z}_{ij}] & [\hat{z}_{in}] \\ [\hat{z}_{nj}] & [\hat{z}_{nn}] \end{bmatrix} \quad (6.26)$$

Phase Impedance Matrix

For most applications, the primitive impedance matrix needs to be reduced to a 3×3 “phase frame” matrix consisting of the self and mutual equivalent impedances for the three phases. One standard method of reduction is the “Kron” reduction (1952) where the assumption is made that the line has a multi-grounded neutral. The Kron reduction results in the “phase impedances matrix” determined by using Eq. 6.27 below:

$$[z_{abc}] = [\hat{z}_{ij}] - [\hat{z}_{in}] \cdot [\hat{z}_{nn}]^{-1} \cdot [\hat{z}_{nj}] \quad (6.27)$$

For two-phase (V-phase) and single-phase lines in grounded wye systems, the modified Carson equations can be applied, which will lead to initial 3×3 and 2×2 primitive impedance matrices. Kron reduction will reduce the matrices to 2×2 and a single element. These matrices can be expanded to 3×3 “phase frame” matrices by the addition of rows and columns consisting of zero elements for the missing phases.

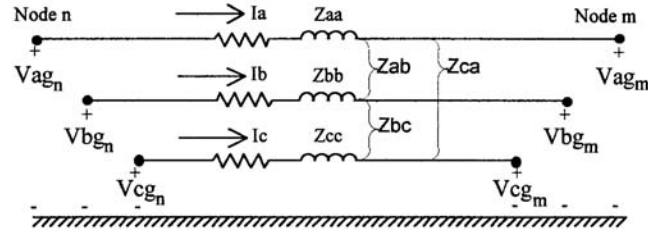


FIGURE 6.5 Three-phase line segment.

The phase frame matrix for a three-wire delta line is determined by the application of Carson's equations without the Kron reduction step.

The phase frame matrix can be used to accurately determine the voltage drops on the feeder line segments once the currents flowing have been determined. Since no approximations (transposition, for example) have been made regarding the spacing between conductors, the effect of the mutual coupling between phases is accurately taken into account. The application of Carson's equations and the phase frame matrix leads to the most accurate model of a line segment.

Figure 6.5 shows the equivalent circuit of a line segment.

The voltage equation in matrix form for the line segment is given by Eq. (6.28).

$$\begin{bmatrix} V_{ag} \\ V_{bg} \\ V_{cg} \end{bmatrix}_n = \begin{bmatrix} V_{ag} \\ V_{bg} \\ V_{cg} \end{bmatrix}_m + \begin{bmatrix} Z_{aa} & Z_{ab} & Z_{ac} \\ Z_{ba} & Z_{bb} & Z_{bc} \\ Z_{ca} & Z_{cb} & Z_{cc} \end{bmatrix} \cdot \begin{bmatrix} I_a \\ I_b \\ I_c \end{bmatrix} \quad (6.28)$$

where $Z_{ij} = z_{ij} \cdot \text{length}$

The "phase impedance matrix" is defined in Eq. (6.29). The phase impedance matrix for single-phase and "V"-phase lines will have a row and column of zeros for each missing phase.

$$\begin{bmatrix} Z_{abc} \end{bmatrix} = \begin{bmatrix} Z_{aa} & Z_{ab} & Z_{ac} \\ Z_{ba} & Z_{bb} & Z_{bc} \\ Z_{ca} & Z_{cb} & Z_{cc} \end{bmatrix} \quad (6.29)$$

Equation (6.28) can be written in "condensed" form as:

$$\begin{bmatrix} VLG_{abc} \end{bmatrix}_n = \begin{bmatrix} VLG_{abc} \end{bmatrix}_m + \begin{bmatrix} Z_{abc} \end{bmatrix} \cdot \begin{bmatrix} I_{abc} \end{bmatrix} \quad (6.30)$$

This condensed notation will be used throughout the document.

Sequence Impedances

Many times the analysis of a feeder will use the positive and zero sequence impedances for the line segments. There are basically two methods for obtaining these impedances. The first method incorporates the application of Carson's equations and the Kron reduction to obtain the phase frame impedance matrix. The 3×3 "sequence impedance matrix" can be obtained by:

$$\begin{bmatrix} z_{012} \end{bmatrix} = \begin{bmatrix} A_s \end{bmatrix}^{-1} \cdot \begin{bmatrix} z_{abc} \end{bmatrix} \cdot \begin{bmatrix} A_s \end{bmatrix} \quad \text{Ohms/mile} \quad (6.31)$$

where

$$[A_s] = \begin{bmatrix} 1 & 1 & 1 \\ 1 & a^2 & a \\ 1 & a & a^2 \end{bmatrix} \quad (6.32)$$

$$a = 1.0/\underline{120} \quad a^2 = 1.0/\underline{240}$$

The resulting sequence impedance matrix is of the form:

$$[Z_{012}] = \begin{bmatrix} z_{00} & z_{01} & z_{02} \\ z_{10} & z_{11} & z_{12} \\ z_{20} & z_{21} & z_{22} \end{bmatrix} \text{ Ohms/mile} \quad (6.33)$$

where z_{00} = the zero sequence impedance
 z_{11} = the positive sequence impedance
 z_{22} = the negative sequence impedance

In the idealized state, the off diagonal terms of Eq. (6.33) would be zero. When the off diagonal terms of the phase impedance matrix are all equal, the off diagonal terms of the sequence impedance matrix will be zero. For high voltage transmission lines, this will generally be the case because these lines are transposed, which causes the mutual coupling between phases (off diagonal terms) to be equal. Distribution lines are rarely if ever transposed. This causes unequal mutual coupling between phases, which causes the off diagonal terms of the phase impedance matrix to be unequal. For the nontransposed line, the diagonal terms of the phase impedance matrix will also be unequal. In most cases, the off diagonal terms of the sequence impedance matrix are very small compared to the diagonal terms and errors made by ignoring the off diagonal terms are small.

Sometimes the phase impedance matrix is modified such that the three diagonal terms are equal and all of the off diagonal terms are equal. The usual procedure is to set the three diagonal terms of the phase impedance matrix equal to the average of the diagonal terms of Eq. (6.29) and the off diagonal terms equal to the average of the off diagonal terms of Eq. (6.29). When this is done, the self and mutual impedances are defined as:

$$z_s = \frac{1}{3} \cdot (z_{aa} + z_{bb} + z_{cc}) \quad (6.34)$$

$$z_m = \frac{1}{3} (z_{ab} + z_{bc} + z_{ca}) \quad (6.35)$$

The phase impedance matrix is now defined as:

$$[Z_{abc}] = \begin{bmatrix} z_s & z_m & z_m \\ z_m & z_s & z_m \\ z_m & z_m & z_s \end{bmatrix} \text{ Ohms/mile} \quad (6.36)$$

When Eq. (6.31) is used with this phase impedance matrix, the resulting sequence matrix is diagonal (off diagonal terms are zero). The sequence impedances can be determined directly as:

$$z_{00} = z_s + 2 \cdot z_m \quad (6.37)$$

$$z_{11} = z_{22} = z_s - z_m$$

A second method that is commonly used to determine the sequence impedances directly is to employ the concept of Geometric Mean Distances (GMD). The GMD between phases is defined as:

$$D_{ij} = GMD_{ij} = \sqrt[3]{D_{ab} \cdot D_{bc} \cdot D_{ca}} \quad (6.38)$$

The GMD between phases and neutral is defined as:

$$D_{in} = GMD_{in} = \sqrt[3]{D_{an} \cdot D_{bn} \cdot D_{cn}} \quad (6.39)$$

The GMDs as defined above are used in Eqs. (6.23) and (6.24) to determine the various self and mutual impedances of the line resulting in:

$$\hat{z}_{ii} = r_i + 0.0953 + j0.12134 \cdot \left[\ln \left(\frac{1}{GMR_i} \right) + 7.93402 \right] \quad (6.40)$$

$$\hat{z}_{nn} = r_n + 0.0953 + j0.12134 \cdot \left[\ln \left(\frac{1}{GMR_n} \right) + 7.93402 \right] \quad (6.41)$$

$$\hat{z}_{ij} = 0.0953 + j0.12134 \cdot \left[\ln \left(\frac{1}{D_{ij}} \right) + 7.93402 \right] \quad (6.42)$$

$$\hat{z}_{in} = 0.0953 + j0.12134 \cdot \left[\ln \left(\frac{1}{D_{in}} + 7.93402 \right) \right] \quad (6.43)$$

Equations (6.40) through (6.43) will define a matrix of order **ncond** \times **ncond**, where ncond is the number of conductors (phases plus neutrals) in the line segment. Application of the Kron reduction (Eq. 6.27) and the sequence impedance transformation [Eq. (6.37)] leads to the following expressions for the zero, positive, and negative sequence impedances:

$$z_{00} = \hat{z}_{ii} + 2 \cdot \hat{z}_{ij} - 3 \cdot \left(\frac{\hat{z}_{in}^2}{\hat{z}_{nn}} \right) \text{ Ohms/mile} \quad (6.44)$$

$$z_{11} = z_{22} = \hat{z}_{ii} - \hat{z}_{ij} \quad (6.45)$$

$$z_{11} = z_{22} = r_i + j0.12134 \cdot \ln \left(\frac{D_{ij}}{GMR_i} \right) \text{ Ohms/mile}$$

Eq. (6.45) is recognized as the standard equation for the calculation of the line impedances when a balanced three-phase system and transposition are assumed.

Example 1

The spacings for an overhead three-phase distribution line is constructed as shown in Fig. 6.6. The phase conductors are 336,400 26/7 ACSR (Linnet) and the neutral conductor is 4/0 6/1 ACSR.

- Determine the phase impedance matrix.
- Determine the positive and zero sequence impedances.

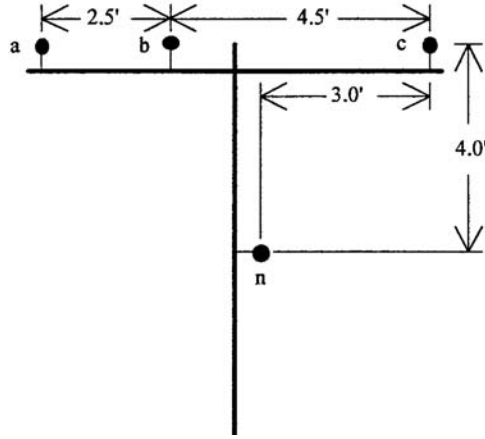


FIGURE 6.6 Three-phase distribution line spacings.

From the table of standard conductor data, it is found that:

336,400 26/7 ACSR: GMR = 0.0244 ft
Resistance = 0.306 Ohms/mile
4/0 6/1 ACSR: GMR = 0.00814 ft
Resistance = 0.5920 Ohms/mile

From Fig. 6.6 the following distances between conductors can be determined:

$D_{ab} = 2.5$ ft $D_{bc} = 4.5$ ft $D_{ca} = 7.0$ ft
 $D_{an} = 5.6569$ ft $D_{bn} = 4.272$ ft $D_{cn} = 5.0$ ft

Applying Carson's modified equations [Eqs. (6.23) and (6.24)] results in the "primitive impedance matrix."

$$[\hat{z}] = \begin{bmatrix} 0.4013 + j1.4133 & 0.0953 + j0.8515 & 0.0953 + j0.7266 & 0.0953 + j0.7524 \\ 0.0953 + j0.8515 & 0.4013 + j1.4133 & 0.0953 + j0.7802 & 0.0953 + j0.7865 \\ 0.0953 + j0.7266 & 0.0953 + j0.7802 & 0.4013 + j1.4133 & 0.0953 + j0.7674 \\ 0.0953 + j0.7524 & 0.0953 + j0.7865 & 0.0953 + j0.7674 & 0.6873 + j1.5465 \end{bmatrix} \quad (6.46)$$

The "Kron" reduction of Eq. (6.27) results in the "phase impedance matrix."

$$[z_{abc}] = \begin{bmatrix} 0.4576 + j1.0780 & 0.1560 + j0.5017 & 0.1535 + j0.3849 \\ 0.1560 + j0.5017 & 0.4666 + j1.0482 & 0.1580 + j0.4236 \\ 0.1535 + j0.3849 & 0.1580 + j0.4236 & 0.4615 + j1.0651 \end{bmatrix} \text{ Ohms/mile} \quad (6.47)$$

The phase impedance matrix of Eq. (6.47) can be transformed into the "sequence impedance matrix" with the application of Eq. (6.31).

$$[z_{012}] = \begin{bmatrix} 0.7735 + j1.9373 & 0.0256 + j0.0115 & -0.0321 + j0.0159 \\ -0.0321 + j0.0159 & 0.3061 + j0.6270 & -0.0723 - j0.0060 \\ 0.0256 + j0.0115 & 0.0723 - j0.0059 & 0.3061 + j0.6270 \end{bmatrix} \text{ Ohms/mile} \quad (6.48)$$

In Eq. (6.48), the 1,1 term is the zero sequence impedance, the 2,2 term is the positive sequence impedance, and the 3,3 term is the negative sequence impedance. Note that the off-diagonal terms are not zero, which implies that there is mutual coupling between sequences. This is a result of the nonsymmetrical spacing between phases. With the off-diagonal terms nonzero, the three sequence networks representing the line will not be independent. However, it is noted that the off-diagonal terms are small relative to the diagonal terms.

In high voltage transmission lines, it is usually assumed that the lines are transposed and that the phase currents represent a balanced three-phase set. The transposition can be simulated in this example by replacing the diagonal terms of Eq. (6.47) with the average value of the diagonal terms ($0.4619 + j1.0638$) and replacing each off-diagonal term with the average of the off-diagonal terms ($0.1558 + j0.4368$). This modified phase impedance matrix becomes:

$$[z1_{abc}] = \begin{bmatrix} 0.3619 + j1.0638 & 0.1558 + j0.4368 & 0.1558 + j0.4368 \\ 0.1558 + j0.4368 & 0.3619 + j1.0638 & 0.1558 + j0.4368 \\ 0.1558 + j0.4368 & 0.1558 + j0.4368 & 0.3619 + j1.0638 \end{bmatrix} \text{ Ohms/mile} \quad (6.49)$$

Using this modified phase impedance matrix in the symmetrical component transformation, Eq. (6.31) results in the modified sequence impedance matrix.

$$[z1_{012}] = \begin{bmatrix} 0.7735 + j1.9373 & 0 & 0 \\ 0 & 0.3061 + j0.6270 & 0 \\ 0 & 0 & 0.3061 + j0.6270 \end{bmatrix} \text{ Ohms/mile} \quad (6.50)$$

Note now that the off-diagonal terms are all equal to zero, meaning that there is no mutual coupling between sequence networks. It should also be noted that the zero, positive, and negative sequence impedances of Eq. (6.50) are exactly equal to the same sequence impedances of Eq. (6.48).

The results of this example should not be interpreted to mean that a three-phase distribution line can be assumed to have been transposed. The original phase impedance matrix of Eq. (6.47) must be used if the correct effect of the mutual coupling between phases is to be modeled.

Underground Lines

Figure 6.7 shows the general configuration of three underground cables (concentric neutral, or tape shielded) with an additional neutral conductor.

Carson's equations can be applied to underground cables in much the same manner as for overhead lines. The circuit of Fig. 6.7 will result in a 7×7 primitive impedance matrix. For underground circuits that do not have the additional neutral conductor, the primitive impedance matrix will be 6×6 .

Two popular types of underground cables in use today are the "concentric neutral cable" and the "tape shield cable." To apply Carson's equations, the resistance and GMR of the phase conductor and the equivalent neutral must be known.

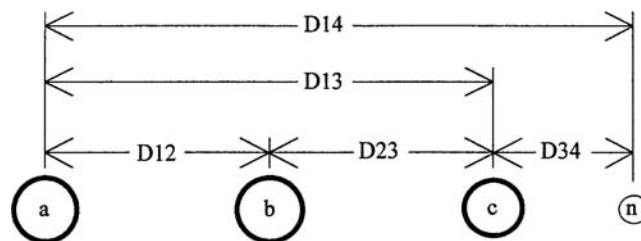


FIGURE 6.7 Three-phase underground with additional neutral.

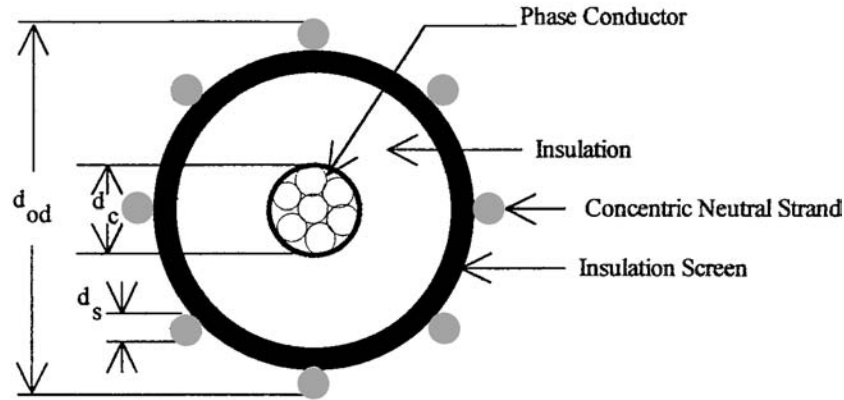


FIGURE 6.8 Concentric neutral cable.

Concentric Neutral Cable

Figure 6.8 shows a simple detail of a concentric neutral cable. The cable consists of a central “phase conductor” covered by a thin layer of nonmetallic semiconducting screen to which is bonded the insulating material. The insulation is then covered by a semiconducting insulation screen. The solid strands of concentric neutral are spiralled around the semiconducting screen with a uniform spacing between strands. Some cables will also have an insulating “jacket” encircling the neutral strands.

In order to apply Carson’s equations to this cable, the following data needs to be extracted from a table of underground cables.

- d_c = phase conductor diameter (inches)
- d_{od} = nominal outside diameter of the cable (inches)
- d_s = diameter of a concentric neutral strand (inches)
- GMR_c = geometric mean radius of the phase conductor (ft)
- GMR_s = geometric mean radius of a neutral strand (ft)
- r_c = resistance of the phase conductor (Ohms/mile)
- r_s = resistance of a solid neutral strand (Ohms/mile)
- k = number of concentric neutral strands

The geometric mean radii of the phase conductor and a neutral strand are obtained from a standard table of conductor data. The equivalent geometric mean radius of the concentric neutral is given by:

$$GMR_{cn} = \sqrt[k]{GMR_s \cdot k \cdot R^{k-1}} \quad (6.51)$$

where R = radius of a circle passing through the center of the concentric neutral strands

$$R = \frac{d_{od} - d_s}{24} \text{ ft} \quad (6.52)$$

The equivalent resistance of the concentric neutral is:

$$r_{cn} = \frac{r_s}{k} \text{ Ohms/mile} \quad (6.53)$$

The various spacings between a concentric neutral and the phase conductors and other concentric neutrals are as follows:

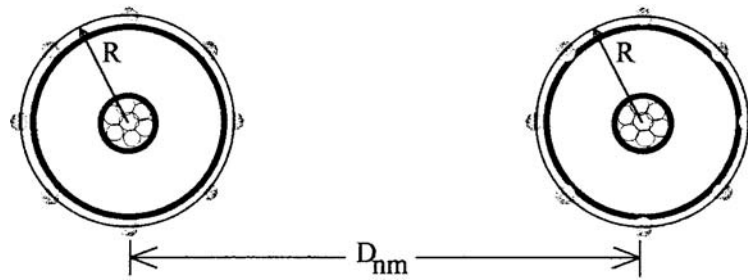


FIGURE 6.9 Distances between concentric neutral cables.

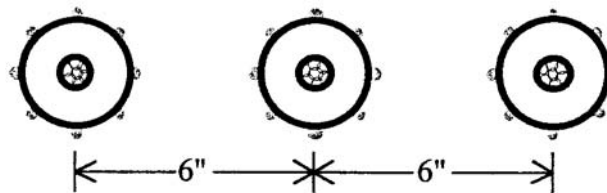


FIGURE 6.10 Three-phase concentric neutral cable spacing.

Concentric neutral to its own phase conductor

$$D_{ij} = R \quad [\text{Eq. (6.52) above}]$$

Concentric neutral to an adjacent concentric neutral

$$D_{ij} = \text{center-to-center distance of the phase conductors}$$

Concentric neutral to an adjacent phase conductor

Figure 6.9 shows the relationship between the distance between centers of concentric neutral cables and the radius of a circle passing through the centers of the neutral strands.

The geometric mean distance between a concentric neutral and an adjacent phase conductor is given by Eq. (6.54).

$$D_{ij} = \sqrt[k]{D_{nm}^k - R^k} \quad (\text{ft}) \quad (6.54)$$

where D_{nm} = center-to-center distance between phase conductors

For cables buried in a trench, the distance between cables will be much greater than the radius R and therefore very little error is made if D_{ij} in Eq. (6.54) is set equal to D_{nm} . For cables in conduit, that assumption is not valid.

Example 2

Three concentric neutral cables are buried in a trench with spacings as shown in Fig. 6.10. The cables are 15 kV, 250,000 CM stranded all aluminum with 13 strands of #14 annealed coated copper wires (1/3 neutral). The data for the phase conductor and neutral strands from a conductor data table are:

250,000 AA phase conductor: $\text{GMR}_p = 0.0171$ ft, resistance = 0.4100 Ohms/mile

14 copper neutral strands: $\text{GMR}_s = 0.00208$ ft, resistance = 14.87 Ohms/mile

Diameter (d_s) = 0.0641 in.

The equivalent GMR of the concentric neutral [Eq. (6.51)] = 0.04864 ft

The radius of the circle passing through strands [Eq. (6.52)] = 0.0511 ft

The equivalent resistance of the concentric neutral [Eq. (6.53)] = 1.1440 Ohms/mile

Since R (0.0511 ft) is much less than D_{12} (0.5 ft) and D_{13} (1.0 ft), then the distances between concentric neutrals and adjacent phase conductors are the center-to-center distances of the cables.

Applying Carson's equations results in a 6×6 primitive impedance matrix. This matrix in partitioned form [Eq. (6.26)] is:

$$\begin{bmatrix} Z_{ij} \end{bmatrix} = \begin{bmatrix} 0.5053 + j1.4564 & 0.0953 + j1.0468 & 0.0953 + j0.9627 \\ 0.0953 + j1.0468 & 0.5053 + j1.4564 & 0.0953 + j1.0468 \\ 0.0953 + j0.9627 & 0.0953 + j1.0468 & 0.5053 + j1.4564 \end{bmatrix}$$

$$\begin{bmatrix} Z_{in} \end{bmatrix} = \begin{bmatrix} 0.0953 + j1.3236 & 0.0953 + j1.0468 & 0.0953 + j0.9627 \\ 0.0953 + j1.0468 & 0.0953 + j1.3236 & 0.0953 + j1.0468 \\ 0.0953 + j0.9627 & 0.0953 + j1.0468 & 0.0953 + j1.3236 \end{bmatrix}$$

$$\begin{bmatrix} z_{nj} \end{bmatrix} = \begin{bmatrix} z_{in} \end{bmatrix}$$

$$\begin{bmatrix} Z_{nn} \end{bmatrix} = \begin{bmatrix} 1.2393 + j1.3296 & 0.0953 + j1.0468 & 0.0953 + j0.9627 \\ 0.0953 + j1.0468 & 1.2393 + j1.3296 & 0.0953 + j1.0468 \\ 0.0953 + j0.9627 & 0.0953 + j1.0468 & 1.2393 + j1.3296 \end{bmatrix}$$

Using the Kron reduction [Eq. (6.27)] results in the phase impedance matrix:

$$\begin{bmatrix} z_{abc} \end{bmatrix} = \begin{bmatrix} 0.7982 + j0.4463 & 0.3192 + j0.0328 & 0.2849 - j0.0143 \\ 0.3192 + j0.0328 & 0.7891 + j0.4041 & 0.3192 + j0.0328 \\ 0.2849 - j0.0143 & 0.3192 + j0.0328 & 0.7982 + j0.4463 \end{bmatrix} \text{ Ohms/mile}$$

The sequence impedance matrix for the concentric neutral three-phase line is determined using Eq. (6.17). The resulting sequence impedance matrix is:

$$\begin{bmatrix} z_{012} \end{bmatrix} = \begin{bmatrix} 1.4106 + j0.4665 & -0.0028 - j0.0081 & -0.0056 + j0.0065 \\ -0.0056 + j0.0065 & 0.4874 + j0.4151 & -0.0264 + j0.0451 \\ -0.0028 - j0.0081 & 0.0523 + j0.0003 & 0.4867 + j0.4151 \end{bmatrix} \text{ Ohms/mile}$$

Tape Shielded Cables

Figure 6.11 shows a simple detail of a tape shielded cable.

Parameters of Fig. 6.11 are:

- d_c = diameter of phase conductor (in.)
- d_s = inside diameter of tape shield (in.)
- d_{od} = outside diameter over jacket (in.)
- T = thickness of copper tape shield in mils
- = 5 mils (standard)

Once again, Carson's equations will be applied to calculate the self-impedances of the phase conductor and the tape shield as well as the mutual impedance between the phase conductor and the tape shield.

The resistance and GMR of the phase conductor are found in a standard table of conductor data.

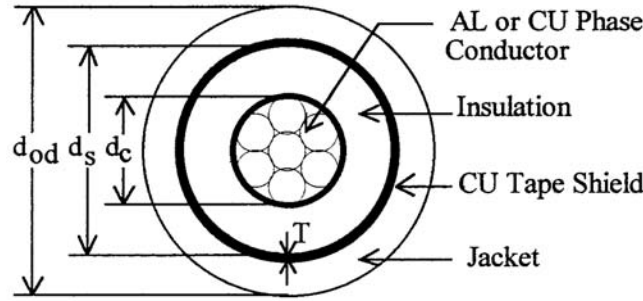


FIGURE 6.11 Taped shielded cable.

The resistance of the tape shield is given by:

$$r_{shield} = \frac{18.826}{d_s \cdot T} \text{ Ohms/mile} \quad (6.55)$$

The resistance of the tape shield given in Eq. (6.55) assumes a resistivity of 100 Ohm-meter and a temperature of 50°C. The diameter of the tape shield d_s is given in inches and the thickness of the tape shield T is in mils.

The GMR of the tape shield is given by:

$$GMR_{shield} = \frac{\frac{d_s}{2} - \frac{T}{12}}{2000} \text{ ft} \quad (6.56)$$

The various spacings between a tape shield and the conductors and other tape shields are as follows:
Tape shield to its own phase conductor

$$D_{ij} = GMR_{tape} = \text{radius to midpoint of the shield} \quad (6.57)$$

Tape shield to an adjacent tape shield

$$D_{ij} = \text{center-to-center distance of the phase conductors} \quad (6.58)$$

Tape shield to an adjacent phase or neutral conductor

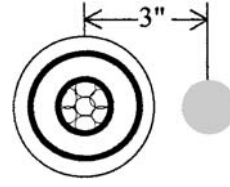
$$D_{ij} = D_{nm} \quad (6.59)$$

where D_{nm} = center to center distance between phase conductors.

In applying Carson's equations for both concentric neutral and tape shielded cables, the numbering of conductors and neutrals is important. For example, a three-phase underground circuit with an additional neutral conductor must be numbered as:

- 1 = phase conductor #1
- 2 = phase conductor #2
- 3 = phase conductor #3
- 4 = neutral of conductor #1

FIGURE 6.12 Single-phase tape shield with neutral.



- 5 = neutral of conductor #2
- 6 = neutral of conductor #3
- 7 = additional neutral conductor (if present)

Example 3

A single-phase circuit consists of a 1/0 AA tape shielded cable and a 1/0 CU neutral conductor as shown in Fig. 6.12.

Cable Data: 1/0 AA
 Inside diameter of tape shield = $d_s = 1.084$ in.
 Resistance = 0.97 Ohms/mi
 $GMR_p = 0.0111$ ft
 Tape shield thickness = $T = 8$ mils

Neutral Data: 1/0 Copper, 7 strand
 Resistance = 0.607 Ohms/mi
 $GMR_n = 0.01113$ ft

Distance between cable and neutral = $D_{nm} = 3$ in.

The resistance of the tape shield is computed according to Eq. (6.55):

$$r_{shield} = \frac{18.826}{d_s \cdot T} = \frac{18.826}{1.084 \cdot 8} = 2.1705 \text{ Ohms/mile}$$

The GMR of the tape shield is computed according to Eq. (6.56):

$$GMR_{shield} = \frac{\frac{d_s}{2} - \frac{T}{2000}}{12} = \frac{\frac{1.084}{2} - \frac{8}{2000}}{12} = 0.0455 \text{ ft}$$

Using the relations defined in Eqs. (6.57) to (6.59) and Carson's equations results in a 3×3 primitive impedance matrix:

$$z_{primitive} = \begin{bmatrix} 1.0653 + j1.5088 & 0.0953 + j1.3377 & 0.0953 + j1.1309 \\ 0.0953 + j1.3377 & 2.2658 + j1.3377 & 0.0953 + j1.1309 \\ 0.0953 + j1.1309 & 0.0953 + j1.1309 & 0.7023 + j1.5085 \end{bmatrix} \text{ Ohms/mile}$$

Applying Kron's reduction method will result in a single impedance which represents the equivalent single-phase impedance of the tape shield cable and the neutral conductor.

$$z_{1p} = 1.3368 + j0.6028 \text{ Ohms/mile}$$

Shunt Admittance

When a high-voltage transmission line is less than 50 miles in length, the shunt capacitance of the line is typically ignored. For lightly loaded distribution lines, particularly underground lines, the shunt capacitance should be modeled.

The basic equation for the relationship between the charge on a conductor to the voltage drop between the conductor and ground is given by:

$$Q_n = C_{ng} \cdot V_{ng} \quad (6.60)$$

where Q_n = charge on the conductor
 C_{ng} = capacitance between the conductor and ground
 V_{ng} = voltage between the conductor and ground

For a line consisting of **ncond** (number of phase plus number of neutral) conductors, Eq. (6.60) can be written in condensed matrix form as:

$$[Q] = [C] \cdot [V] \quad (6.61)$$

where $[Q]$ = column vector of order **ncond**
 $[C]$ = **ncond** \times **ncond** matrix
 $[V]$ = column vector of order **ncond**

Equation (6.61) can be solved for the voltages:

$$[V] = [C]^{-1} \cdot [Q] = [P] \cdot [Q] \quad (6.62)$$

where $[P] = [C]^{-1}$ = "Potential Coefficient Matrix" (6.63)

Overhead Lines

The determination of the shunt admittance of overhead lines starts with the calculation of the "potential coefficient matrix" (Glover and Sarma, 1994). The elements of the matrix are determined by:

$$P_{ii} = 11.17689 \cdot \ln \frac{S_{ii}}{RD_i} \quad (6.64)$$

$$P_{ij} = 11.17689 \cdot \ln \frac{S_{ij}}{D_{ij}} \quad (6.65)$$

See Fig. 6.4 for the following definitions.

S_{ii} = distance between a conductor and its image below ground in ft
 S_{ij} = distance between conductor **i** and the image of conductor **j** below ground in ft
 D_{ij} = overhead spacing between two conductors in ft
 RD_i = radius of conductor **i** in ft

The potential coefficient matrix will be an **ncond** \times **ncond** matrix. If one or more of the conductors is a grounded neutral, then the matrix must be reduced using the "Kron" method to an **nphase** \times **nphase** matrix $[P_{abc}]$.

The inverse of the potential coefficient matrix will give the **nphase** \times **nphase** capacitance matrix $[C_{abc}]$. The shunt admittance matrix is given by:

$$[Y_{abc}] = j \cdot \omega \cdot [C_{abc}] \quad \text{micro-S/mile} \quad (6.66)$$

where $\omega = 2 \cdot \pi f = 376.9911$

Example 4

Determine the shunt admittance matrix for the overhead line of Example 1. Assume that the neutral conductor is 25 ft above ground.

For this configuration, the image spacing matrix is computed to be:

$$[S] = \begin{bmatrix} 58 & 58.0539 & 58.4209 & 54.1479 \\ 58.0539 & 58 & 58.1743 & 54.0208 \\ 58.4209 & 58.1743 & 58 & 54.0833 \\ 54.1479 & 54.0208 & 54.0833 & 58 \end{bmatrix} \text{ ft}$$

The primitive potential coefficient matrix is computed to be:

$$[P_{\text{primitive}}] = \begin{bmatrix} 84.56 & 35.1522 & 23.7147 & 25.2469 \\ 35.4522 & 84.56 & 28.6058 & 28.359 \\ 23.7147 & 28.6058 & 84.56 & 26.6131 \\ 25.2469 & 28.359 & 26.6131 & 85.6659 \end{bmatrix}$$

“Kron” reduce to a 3×3 matrix:

$$[P] = \begin{bmatrix} 77.1194 & 26.7944 & 15.8714 \\ 26.7944 & 75.172 & 19.7957 \\ 15.8714 & 19.7957 & 76.2923 \end{bmatrix}$$

Invert $[P]$ to determine the shunt capacitance matrix:

$$[C_{abc}] = [P]^{-1} = \begin{bmatrix} 0.015 & -0.0049 & -0.0019 \\ -0.0019 & 0.0159 & -0.0031 \\ -0.0019 & -0.0031 & 0.0143 \end{bmatrix}$$

Multiply $[C_{abc}]$ by the radian frequency to determine the final three-phase shunt admittance matrix.

$$[Y_{abc}] = j \cdot 376.9911 \cdot [C_{abc}] = \begin{bmatrix} j5.6711 & -j1.8362 & -j0.7033 \\ -j1.8362 & j5.9774 & -j1.169 \\ -j0.7033 & -j1.169 & j5.391 \end{bmatrix} \mu\text{S/mile}$$

Underground Lines

Because the electric fields of underground cables are confined to the space between the phase conductor and its concentric neutral to tape shield, the calculation of the shunt admittance matrix requires only the determination of the “self” admittance terms.

Concentric Neutral

The self-admittance in micro-S/mile for a concentric neutral cable is given by:

$$Y_{cn} = j \frac{77.582}{\ln\left(\frac{R_b}{R_a}\right) - \frac{1}{k} \cdot \ln\left(\frac{k \cdot R_n}{R_b}\right)} \quad (6.67)$$

where R_b = radius of a circle to center of concentric neutral strands (ft)

R_a = radius of phase conductor (ft)

R_n = radius of concentric neutral strand (ft)

k = number of concentric neutral strands

Example 5

Determine the three-phase shunt admittance matrix for the concentric neutral line of Example 2.

$$R_b = R = 0.0511 \text{ ft}$$

Diameter of the 250,000 AA phase conductor = 0.567 in.

$$R_a = \frac{0.567}{24} = 0.0236 \text{ ft}$$

Diameter of the #14 CU concentric neutral strand = 0.0641 in.

$$R_n = \frac{0.0641}{24} = 0.0027 \text{ ft}$$

Substitute into Eq. (6.67):

$$Y_{cn} = j \frac{77.582}{\ln\left(\frac{R_b}{R_a}\right) - \frac{1}{k} \cdot \ln\left(\frac{k \cdot R_n}{R_b}\right)} = j \frac{77.582}{\ln\left(\frac{0.0511}{0.0236}\right) - \frac{1}{13} \cdot \ln\left(\frac{13 \cdot 0.0027}{0.0511}\right)} = j96.8847$$

The three-phase shunt admittance matrix is:

$$[Y_{abc}] = \begin{bmatrix} j96.8847 & 0 & 0 \\ 0 & j96.8847 & 0 \\ 0 & 0 & j96.8847 \end{bmatrix} \mu\text{S/mile}$$

Tape Shield Cable

The shunt admittance in micro-S/mile for tape shielded cables is given by:

$$Y_{ts} = j \frac{77.586}{\ln\left(\frac{R_b}{R_a}\right)} \mu\text{S/mile} \quad (6.68)$$

where R_b = inside radius of the tape shield

R_a = radius of phase conductor

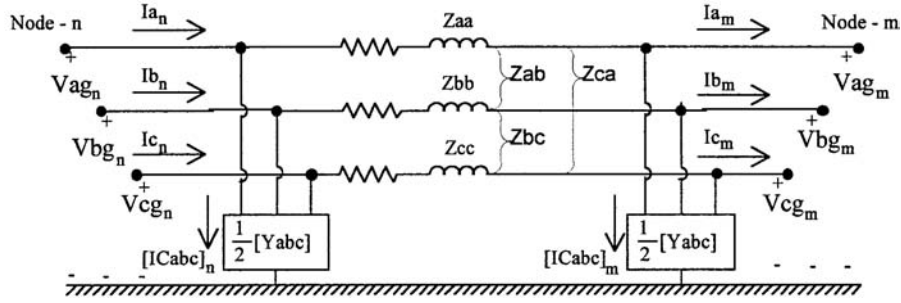


FIGURE 6.13 Three-phase line segment model.

Example 6

Determine the shunt admittance of the single-phase tape shielded cable of Example 3 in the section “Line Impedance”.

$$R_b = \frac{d_s}{24} = \frac{1.084}{24} = 0.0452$$

The diameter of the 1/0 AA phase conductor = 0.368 in.

$$R_a = \frac{d_p}{24} = \frac{0.368}{24} = 0.0153$$

Substitute into Eq. (6.68):

$$Y_{ts} = j \frac{77.586}{\ln\left(\frac{R_b}{R_a}\right)} = j \frac{77.586}{\ln\left(\frac{0.0452}{0.0153}\right)} = j71.8169 \text{ } \mu\text{S/mile}$$

Line Segment Models

Exact Line Segment Model

The exact model of a three-phase line segment is shown in Fig. 6.13.

For the line segment in Fig. 6.13, the equations relating the input (Node n) voltages and currents to the output (Node m) voltages and currents are:

$$[VLG_{abc}]_n = [a] \cdot [VLG_{abc}]_m + [b] \cdot [I_{abc}]_m \quad (6.69)$$

$$[I_{abc}]_n = [c] \cdot [VLG_{abc}]_m + [d] \cdot [I_{abc}]_m \quad (6.70)$$

where

$$[a] = [U] - \frac{1}{2} \cdot [Z_{abc}] \cdot [Y_{abc}] \quad (6.71)$$

$$[b] = [Z_{abc}] \quad (6.72)$$

$$[c] = [Y_{abc}] - \frac{1}{4} \cdot [Z_{abc}] \cdot [Y_{abc}]^2 \quad (6.73)$$

$$[d] = [U] - \frac{1}{2} \cdot [Z_{abc}] \cdot [Y_{abc}] \quad (6.74)$$

In Eqs. (6.71) through (6.74), the impedance matrix $[Z_{abc}]$ and the admittance matrix $[Y_{abc}]$ are defined earlier in this document.

Sometimes it is necessary to determine the voltages at node-m as a function of the voltages at node-n and the output currents at node-m. The necessary equation is:

$$[VLG_{abc}]_m = [A] \cdot [VLG_{abc}]_n - [B] \cdot [I_{abc}]_m \quad (6.75)$$

where

$$[A] = \left([U] + \frac{1}{2} \cdot [Z_{abc}] \cdot [Y_{abc}] \right)^{-1} \quad (6.76)$$

$$[B] = \left([U] + \frac{1}{2} \cdot [Z_{abc}] \cdot [Y_{abc}] \right)^{-1} \cdot [Z_{abc}] \quad (6.77)$$

$$[U] = \begin{bmatrix} 1 & 0 & 0 \\ 0 & 1 & 0 \\ 0 & 0 & 1 \end{bmatrix} \quad (6.78)$$

In most cases the shunt admittance is so small that it can be neglected. When this is the case, the $[a]$, $[b]$, $[c]$, $[d]$, $[A]$, and $[B]$ matrices become:

$$[a] = [U] \quad (6.79)$$

$$[b] = [Z_{abc}] \quad (6.80)$$

$$[c] = [0] \quad (6.81)$$

$$[d] = [U] \quad (6.82)$$

$$[A] = [U] \quad (6.83)$$

$$[B] = [Z_{abc}] \quad (6.84)$$

When the shunt admittance is neglected, Eqs. (6.69), (6.70), and (6.75) become:

$$[VLG_{abc}]_n = [VLG_{abc}]_m + [Z_{abc}] \cdot [I_{abc}]_m \quad (6.85)$$

$$[I_{abc}]_n = [I_{abc}]_m \quad (6.86)$$

$$[VLG_{abc}]_m = [VLG_{abc}]_n - [Z_{abc}] \cdot [I_{abc}]_m \quad (6.87)$$

It is usually safe to neglect the shunt capacitance of overhead line segments for segments less than 25 miles in total length and for voltages less than 25 kV. For underground lines, the shunt admittance should be included.

If an accurate determination of the voltage drops down a line segment is to be made, it is essential that the phase impedance matrix $[Z_{abc}]$ be computed based on the actual configuration and spacings of the overhead or underground lines. No assumptions should be made, such as transposition. The reason for this is best demonstrated by an example.

Example 7

The phase impedance matrix for the line configuration in Example 1 was computed to be:

$$[Z_{abc}] = \begin{bmatrix} 0.4576 + j1.0780 & 0.1560 + j0.5017 & 0.1535 + j0.3849 \\ 0.1560 + j0.5017 & 0.466 + j1.0482 & 0.1580 + j0.4236 \\ 0.1535 + j0.3849 & 0.1580 + j0.4236 & 0.4615 + j1.0651 \end{bmatrix} \text{ Ohms/mile}$$

Assume that a 12.47-kV substation serves a load 1.5 miles from the substation. The metered output at the substation is balanced 10,000 kVA at 12.47 kV and 0.9 lagging power factor. Compute the three-phase line-to-ground voltages at the load end of the line and the voltage unbalance at the load.

The line-to-ground voltages and line currents at the substation are:

$$[VLG_{abc}] = \begin{bmatrix} 7200/0 \\ 7200/-120 \\ 7200/120 \end{bmatrix} \quad [I_{abc}]_n = \begin{bmatrix} 463/-25.84 \\ 463/-145.84 \\ 463/94.16 \end{bmatrix}$$

Solve Eq. (6.85) for the load voltages:

$$[VLG_{abc}]_m = [VLG_{abc}]_n - 1.5 \cdot [Z_{abc}] \cdot [I_{abc}]_n = \begin{bmatrix} 6761.10/2.32 \\ 6877.7/-122.43 \\ 6836.33/117.21 \end{bmatrix}$$

The voltage unbalance at the load using the NEMA definition is:

$$V_{unbalance} = \frac{\max(V_{deviation})}{V_{avg}} \cdot 100 = 0.937\%$$

The point of Example 1 is to demonstrate that even though the system is perfectly balanced at the substation, the unequal mutual coupling between phases results in a significant voltage unbalance at the load. Significant because NEMA requires that induction motors be derated when the voltage unbalance is 1% or greater.

Approximate Line Segment Model

Many times the only data available for a line segment will be the positive and zero sequence impedances. An approximate three-phase line segment model can be developed by applying the “reverse impedance transformation” from symmetrical component theory.

Using the known positive and zero sequence impedances, the “sequence impedance matrix” is given by:

$$[Z_{seq}] = \begin{bmatrix} Z_0 & 0 & 0 \\ 0 & Z_+ & 0 \\ 0 & 0 & Z_+ \end{bmatrix} \quad (6.88)$$

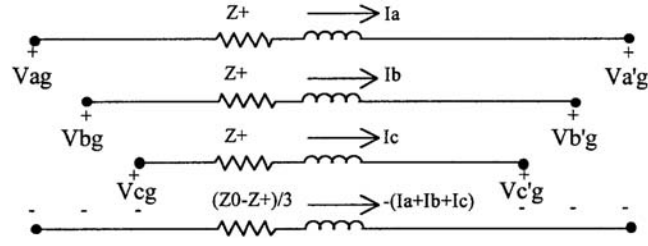


FIGURE 6.14 Approximate line segment model.

The “reverse impedance transformation” results in the following “approximate phase impedance matrix.”

$$[Z_{approx}] = [A_s] \cdot [Z_{seq}] \cdot [A_s]^{-1} = \frac{1}{3} \cdot \begin{bmatrix} (2 \cdot Z_+ - Z_0) & (Z_0 - Z_+) & (Z_0 - Z_+) \\ (Z_0 - Z_+) & (2 \cdot Z_+ - Z_0) & (Z_0 - Z_+) \\ (Z_0 - Z_+) & (Z_0 - Z_+) & (2 \cdot Z_+ - Z_0) \end{bmatrix} \quad (6.89)$$

Notice that the approximate phase impedance matrix is characterized by the three diagonal terms being equal and all mutual terms being equal. This is the same result that is achieved if the line is assumed to be transposed. Substituting the approximate phase impedance matrix into Eq. (6.85) results in:

$$\begin{bmatrix} V_{an} \\ V_{bn} \\ V_{cn} \end{bmatrix}_n = \begin{bmatrix} V_{an} \\ V_{bn} \\ V_{cn} \end{bmatrix}_m + \frac{1}{3} \cdot \begin{bmatrix} (2 \cdot Z_+ - Z_0) & (Z_0 - Z_+) & (Z_0 - Z_+) \\ (Z_0 - Z_+) & (2 \cdot Z_+ - Z_0) & (Z_0 - Z_+) \\ (Z_0 - Z_+) & (Z_0 - Z_+) & (2 \cdot Z_+ - Z_0) \end{bmatrix} \cdot \begin{bmatrix} I_a \\ I_b \\ I_c \end{bmatrix}_n \quad (6.90)$$

Eq. (6.90) can be expanded and an equivalent circuit for the approximate line segment model can be developed. This approximate model is shown in Fig. 6.14.

The errors made by using this approximate line segment model are demonstrated in Example 8.

Example 8

For the line of Example 7, the positive and zero sequence impedances were determined to be:

$$Z_+ = 0.3061 + j0.6270 \text{ Ohms/mile}$$

$$Z_0 = 0.7735 + j1.9373 \text{ Ohms/mile}$$

The sequence impedance matrix is:

$$[Z_{seq}] = \begin{bmatrix} 0.7735 + j1.9373 & 0 & 0 \\ 0 & 0.3061 + j0.6270 & 0 \\ 0 & 0 & 0.3061 + j0.6270 \end{bmatrix}$$

Performing the reverse impedance transformation results in the approximate phase impedance matrix.

$$[Z_{approx}] = [A_s] \cdot [Z_{seq}] \cdot [A_s]^{-1} = \begin{bmatrix} 0.4619 + j1.0638 & 0.1558 + j0.4368 & 0.1558 + j0.4368 \\ 0.1558 + j0.4368 & 0.4619 + j1.0638 & 0.1558 + j0.4368 \\ 0.1558 + j0.4368 & 0.1558 + j0.4368 & 0.4619 + j1.0638 \end{bmatrix}$$

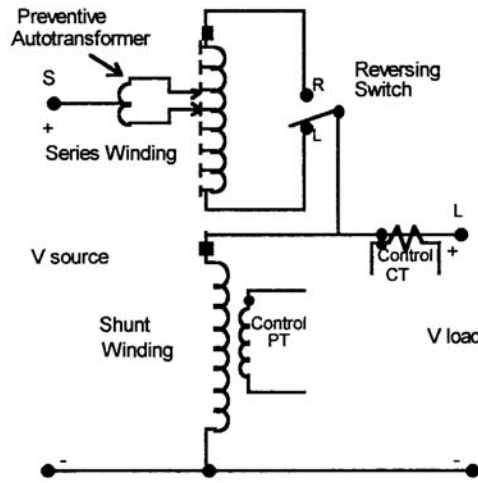


FIGURE 6.15 Step voltage regulator.

Note in the approximate phase impedance matrix that the three diagonal terms are equal and all of the mutual terms are equal.

Use the approximate impedance matrix to compute the load voltage and voltage unbalance as specified in Example 1.

$$\begin{bmatrix} VLG_{abc} \end{bmatrix}_m = \begin{bmatrix} VLG_{abc} \end{bmatrix}_n - 1.5 \cdot \begin{bmatrix} z_{approx} \end{bmatrix} \cdot \begin{bmatrix} I_{abc} \end{bmatrix}_n = \begin{bmatrix} 6825.01/-2.51 \\ 6825.01/-122.51 \\ 6825.01/117.49 \end{bmatrix}$$

Note that the voltages are computed to be balanced. In the previous example it was shown that when the line is modeled accurately, there is a voltage unbalance of almost 1%.

Step-Voltage Regulators

A step voltage regulator consists of an autotransformer and a load tap changing mechanism. The voltage change is obtained by changing the taps of the series winding of the autotransformer. The position of the tap is determined by a control circuit (line drop compensator). Standard step regulators contain a reversing switch enabling a $\pm 10\%$ regulator range, usually in 32 steps. This amounts to a $5/8\%$ change per step or 0.75 volt change per step on a 120-volt base.

A typical step voltage regulator is shown in Fig. 6.15. The tap changing is controlled by a control circuit shown in the block diagram of Fig. 6.16.

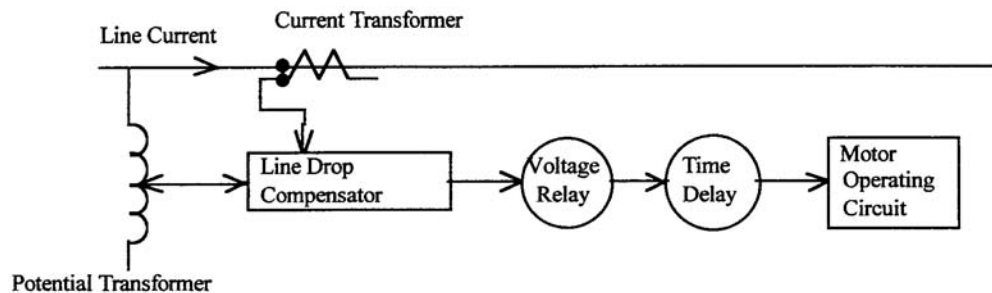


FIGURE 6.16 Regulator control circuit.

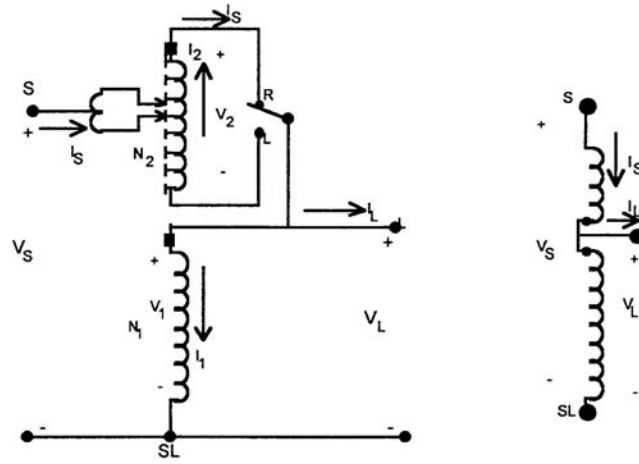


FIGURE 6.17 Voltage regulator in the raise position.

The control circuit requires the following settings:

1. Voltage Level — The desired voltage (on 120-volt base) to be held at the “load center.” The load center may be the output terminal of the regulator or a remote node on the feeder.
2. Bandwidth — The allowed variance of the load center voltage from the set voltage level. The voltage held at the load center will be plus or minus one-half the bandwidth. For example, if the voltage level is set to 122 volts and the bandwidth set to 2 volts, the regulator will change taps until the load center voltage lies between 121 volts and 123 volts.
3. Time Delay — Length of time that a raise or lower operation is called for before the actual execution of the command. This prevents taps changing during a transient or short time change in current.
4. Line Drop Compensator — Set to compensate for the voltage drop (line drop) between the regulator and the load center. The settings consist of R and X settings in volts corresponding to the *equivalent* impedance between the regulator and the load center. This setting may be zero if the regulator output terminals are the “load center.”

The rating of a regulator is based on the kVA transformed, not the kVA rating of the line. In general this will be 10% of the line rating since rated current flows through the series winding which represents the $\pm 10\%$ voltage change.

Voltage Regulator in the Raise Position

Figure 6.17 shows a detailed and abbreviated drawing of a regulator in the raise position.

The defining voltage and current equations for the regulator in the raise position are as follows:

Voltage Equations

$$\frac{V_1}{N_1} = \frac{V_2}{N_2}$$

$$V_S = V_1 - V_2$$

$$V_L = V_1$$

$$V_2 = \frac{N_2}{N_1} \cdot V_1 = \frac{N_2}{N_1} \cdot V_L$$

Current Equations

$$N_1 \cdot I_1 = N_2 \cdot I_2 \quad (6.91)$$

$$I_L = I_S - I_1 \quad (6.92)$$

$$I_2 = I_S \quad (6.93)$$

$$I_1 = \frac{N_2}{N_1} \cdot I_2 = \frac{N_2}{N_1} \cdot I_S \quad (6.94)$$

$$V_S = \left(1 - \frac{N_2}{N_1}\right) \cdot V_1 \quad I_L = \left(1 - \frac{N_2}{N_1}\right) \cdot I_S \quad (6.95)$$

$$V_S = a_R \cdot V_L \quad I_L = a_R \cdot I_S \quad (6.96)$$

$$a_R = 1 - \frac{N_2}{N_1} \quad (6.97)$$

Equations (6.96) and (6.97) are the necessary defining equations for modeling a regulator in the raise position.

Voltage Regulator in the Lower Position

Figure 6.18 shows the detailed and abbreviated drawings of a regulator in the lower position. Note in the figure that the only difference between the lower and raise models is that the polarity of the series winding and how it is connected to the shunt winding is reversed.

The defining voltage and current equations for a regulator in the lower position are as follows:

| <i>Voltage Equations</i> | <i>Current Equations</i> | |
|-------------------------------------|---------------------------------|--------|
| $\frac{V_1}{N_1} = \frac{V_2}{N_2}$ | $N_1 \cdot I_1 = N_2 \cdot I_2$ | (6.98) |

| | | |
|-------------------|-------------------|--------|
| $V_S = V_1 + V_2$ | $I_L = I_S - I_1$ | (6.99) |
|-------------------|-------------------|--------|

| | | |
|-------------|--------------|---------|
| $V_L = V_1$ | $I_2 = -I_S$ | (6.100) |
|-------------|--------------|---------|

| | | |
|---|--|---------|
| $V_2 = \frac{N_2}{N_1} \cdot V_1 = \frac{N_2}{N_1} \cdot V_L$ | $I_1 = \frac{N_2}{N_1} \cdot I_2 = \frac{N_2}{N_1} \cdot (-I_S)$ | (6.101) |
|---|--|---------|

| | | |
|--|--|---------|
| $V_S = \left(1 + \frac{N_2}{N_1}\right) \cdot V_L$ | $I_L = \left(1 + \frac{N_2}{N_1}\right) \cdot I_S$ | (6.102) |
|--|--|---------|

| | | |
|-----------------------|-----------------------|---------|
| $V_S = a_R \cdot V_L$ | $I_L = a_R \cdot I_S$ | (6.103) |
|-----------------------|-----------------------|---------|

$$a_R = 1 + \frac{N_2}{N_1} \quad (6.104)$$

Equations (6.97) and (6.104) give the value of the effective regulator ratio as a function of the ratio of the number of turns on the series winding (N_2) to the number of turns on the shunt winding (N_1). The actual turns ratio of the windings is not known. However, the particular position will be known. Equations (6.97) and (6.104) can be modified to give the effective regulator ratio as a function of the tap position. Each tap changes the voltage by 5/8% or 0.00625 per unit. Therefore, the effective regulator ratio can be given by:

$$a_R = 1 \mp 0.00625 \cdot \text{Tap} \quad (6.105)$$

In Eq. (6.105), the minus sign applies to the “raise” position and the positive sign for the “lower” position.

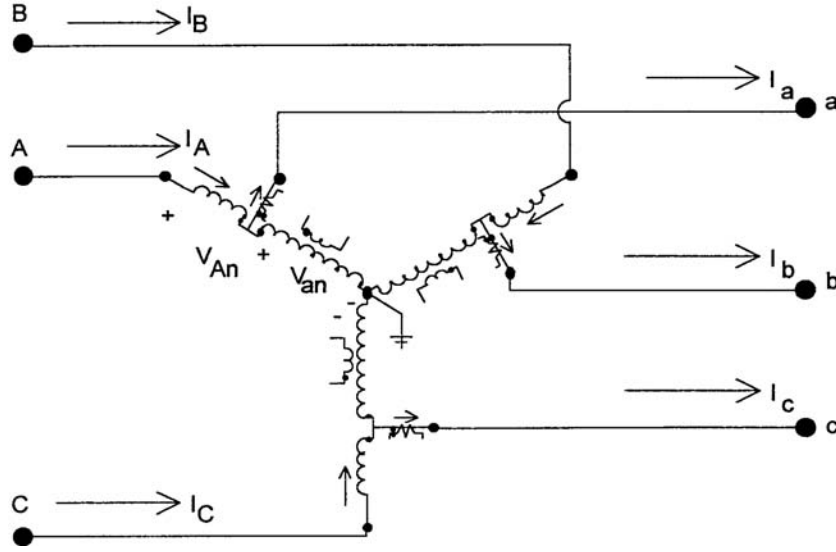


FIGURE 6.20 Wye connected regulators.

The value of the compensator settings in ohms are determined by:

$$R'_{ohms} + jX'_{ohms} = \frac{R'_{volts} + jX'_{volts}}{Ct_s} \text{ Ohms} \quad (6.107)$$

It is important to understand that the value of $R_{line_ohms} + jX_{line_ohms}$ is not the impedance of the line between the regulator and the load center. Typically the load center is located down the primary main feeder after several laterals have been tapped. As a result, the current measured by the CT of the regulator is not the current that flows all the way from the regulator to the load center. The proper way to determine the line impedance values is to run a power-flow program of the feeder without the regulator operating. From the output of the program, the voltages at the regulator output and the load center are known. Now the “equivalent” line impedance can be computed as:

$$R_{line} + jX_{line} = \frac{V_{regulator_output} - V_{load_center}}{I_{line}} \text{ ohms} \quad (6.108)$$

In Eq. (6.108), the voltages must be specified in system volts and the current in system amps.

Wye Connected Regulators

Three single-phase regulators connected in wye are shown in Fig. 6.20.

In Fig. 6.20 the polarities of the windings are shown in the “raise” position. When the regulator is in the “lower” position, a reversing switch will have reconnected the series winding so that the polarity on the series winding is now at the output terminal.

Regardless of whether the regulator is raising or lowering the voltage, the following equations apply:

Voltage Equations

$$\begin{bmatrix} V_{An} \\ V_{Bn} \\ V_{Cn} \end{bmatrix} = \begin{bmatrix} a_{R_a} & 0 & 0 \\ 0 & a_{R_b} & 0 \\ 0 & 0 & a_{R_c} \end{bmatrix} \cdot \begin{bmatrix} V_{an} \\ V_{bn} \\ V_{cn} \end{bmatrix} \quad (6.109)$$

Equation (6.109) can be written in condensed form as:

$$[VLN_{ABC}] = [aRV_{abc}] \cdot [VLN_{abc}] \quad (6.110)$$

Also:
$$[VLN_{abc}] = [aRV_{ABC}] \cdot [VLN_{ABC}] \quad (6.111)$$

where
$$[aRV_{ABC}] = [aRV_{abc}]^{-1} \quad (6.112)$$

Current Equations

$$\begin{bmatrix} I_A \\ I_B \\ I_C \end{bmatrix} = \begin{bmatrix} \frac{1}{a_{R_a}} & 0 & 0 \\ 0 & \frac{1}{a_{R_b}} & 0 \\ 0 & 0 & \frac{1}{a_{R_c}} \end{bmatrix} \cdot \begin{bmatrix} I_a \\ I_b \\ I_c \end{bmatrix} \quad (6.113)$$

Or:
$$[I_{ABC}] = [aRI_{abc}] \cdot [I_{abc}] \quad (6.114)$$

Also:
$$[I_{abc}] = [aRI_{ABC}] \cdot [I_{ABC}] \quad (6.115)$$

where
$$[aRI_{ABC}] = [aRI_{abc}]^{-1} \quad (6.116)$$

where $0.9 \leq a_{R_{abc}} \leq 1.1$ in 32 steps of 0.625%/step (0.75 volts/step on 120 volt base).

Note: The effective turn ratios (a_{R_a} , a_{R_b} , and a_{R_c}) can take on different values when three single-phase regulators are connected in wye. It is also possible to have a three-phase regulator connected in wye where the voltage and current are sampled on only one phase and then all three phases are changed by the same value of a_R (number of taps).

Closed Delta Connected Regulators

Three single-phase regulators can be connected in a closed delta as shown in Fig. 6.21. In the figure, the regulators are shown in the “raise” position.

The closed delta connection is typically used in three-wire delta feeders. Note that the potential transformers for this connection are monitoring the load side line-to-line voltages and the current transformers are monitoring the load side line currents.

Applying the basic voltage and current Eqs. (6.91) through (6.97) of the regulator in the raise position, the following voltage and current relations are derived for the closed delta connection.

$$\begin{bmatrix} V_{AB} \\ V_{BC} \\ V_{CA} \end{bmatrix} = \begin{bmatrix} a_{R_{ab}} & 1-a_{R_{bc}} & 0 \\ 0 & a_{R_{bc}} & 1-a_{R_{ca}} \\ 1-a_{R_{ab}} & 0 & a_{R_{ca}} \end{bmatrix} \cdot \begin{bmatrix} V_{ab} \\ V_{bc} \\ V_{ca} \end{bmatrix} \quad (6.117)$$

Equation (6.115) in abbreviated form can be written as:

$$[VLL_{ABC}] = [aRVD_{abc}] \cdot [VLL_{abc}] \quad (6.118)$$

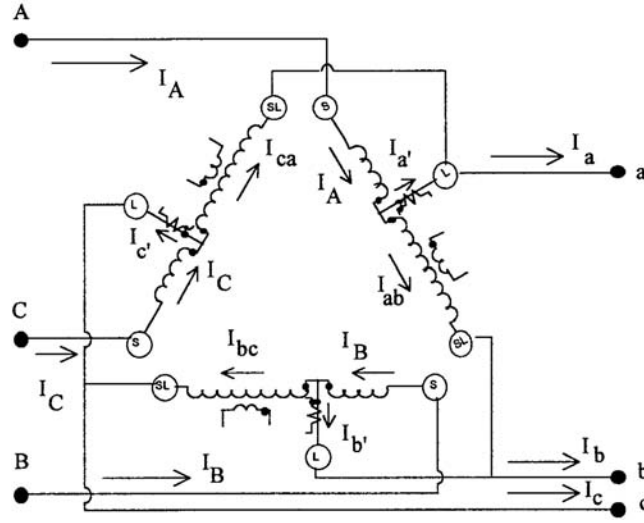


FIGURE 6.21 Delta connected regulators.

When the load side voltages are known, the source side voltages can be determined by:

$$[VLL_{abc}] = [aRVD_{ABC}] \cdot [VLL_{ABC}] \quad (6.119)$$

where

$$[aRVD_{ABC}] = [aRVD_{abc}]^{-1} \quad (6.120)$$

In similar manner the relationships between the load side and source side line currents are given by:

$$\begin{bmatrix} I_a \\ I_b \\ I_c \end{bmatrix} = \begin{bmatrix} a_{R_{ab}} & 0 & 1 - a_{R_{ca}} \\ 1 - a_{R_{ab}} & a_{R_{bc}} & 0 \\ 0 & 1 - a_{R_{bc}} & a_{R_{ca}} \end{bmatrix} \cdot \begin{bmatrix} I_A \\ I_B \\ I_C \end{bmatrix} \quad (6.121)$$

Or:
$$[I_{abc}] = [AID_{ABC}] \cdot [I_{ABC}] \quad (6.122)$$

Also:
$$[I_{ABC}] = [AID_{abc}] \cdot [I_{abc}] \quad (6.123)$$

where
$$[IAD_{abc}] = [IAD_{ABC}]^{-1} \quad (6.124)$$

The closed delta connection can be difficult to apply. Note in both the voltage and current equations that a change of the tap position in one regulator will affect voltages and currents in two phases. As a result, increasing the tap in one regulator will affect the tap position of the second regulator. In most cases the bandwidth setting for the closed delta connection will have to be wider than that for wye connected regulators.

Open Delta Connection

Two single-phase regulators can be connected in the “open” delta connection. Shown in Fig. 6.22 is an open delta connection where two single-phase regulators have been connected between phases AB and CB.

Two other open connections can also be made where the single-phase regulators are connected between phases BC and AC and also between phases CA and BA.

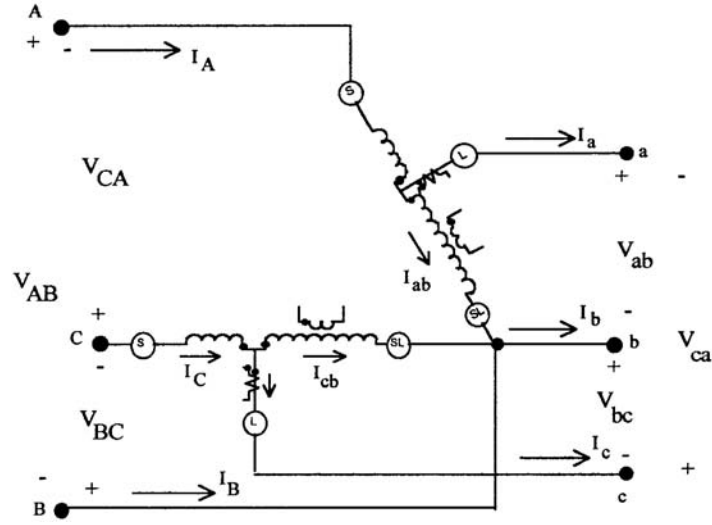


FIGURE 6.22 Open delta connection.

The open delta connection is typically applied to three-wire delta feeders. Note that the potential transformers monitor the line-to-line voltages and the current transformers monitor the line currents. Once again, the basic voltage and current relations of the individual regulators are used to determine the relationships between the source side and load side voltages and currents.

For all three open connections, the following general equations will apply:

$$[VLL_{ABC}] = [aRV_{abc}] \cdot [VLL_{abc}] \quad (6.125)$$

$$[VLL_{abc}] = [aRV_{ABC}] \cdot [VLL_{ABC}] \quad (6.126)$$

$$[I_{ABC}] = [aRI_{abc}] \cdot [I_{abc}] \quad (6.127)$$

$$[I_{abc}] = [aRI_{ABC}] \cdot [I_{ABC}] \quad (6.128)$$

The matrices for the three open connections are defined as follows:

Phases AB & CB

$$[aRV_{abc}] = \begin{bmatrix} a_{R_A} & 0 & 0 \\ 0 & a_{R_C} & 0 \\ -a_{R_A} & -a_{R_C} & 0 \end{bmatrix} \quad (6.129)$$

$$[aRV_{ABC}] = \begin{bmatrix} \frac{1}{a_{R_A}} & 0 & 0 \\ a_{R_A} & \frac{1}{a_{R_C}} & 0 \\ -\frac{1}{a_{R_A}} & -\frac{1}{a_{R_C}} & 0 \end{bmatrix} \quad (6.130)$$

$$\begin{bmatrix} aRI_{abc} \end{bmatrix} = \begin{bmatrix} \frac{1}{a_{R_A}} & 0 & 0 \\ -\frac{1}{a_{R_A}} & 0 & -\frac{1}{a_{R_C}} \\ 0 & 0 & \frac{1}{a_{R_C}} \end{bmatrix} \quad (6.131)$$

$$\begin{bmatrix} aRI_{ABC} \end{bmatrix} = \begin{bmatrix} a_{R_A} & 0 & 0 \\ -a_{R_A} & 0 & a_{R_C} \\ 0 & 0 & a_{R_C} \end{bmatrix} \quad (6.132)$$

Phases BC & AC

$$\begin{bmatrix} aRV_{abc} \end{bmatrix} = \begin{bmatrix} 0 & -a_{R_B} & -a_{R_A} \\ 0 & a_{R_B} & 0 \\ 0 & 0 & a_{R_A} \end{bmatrix} \quad (6.133)$$

$$\begin{bmatrix} aRV_{ABC} \end{bmatrix} = \begin{bmatrix} 0 & -\frac{1}{a_{R_B}} & -\frac{1}{a_{R_A}} \\ 0 & \frac{1}{a_{R_B}} & 0 \\ 0 & 0 & \frac{1}{a_{R_A}} \end{bmatrix} \quad (6.134)$$

$$\begin{bmatrix} aRI_{abc} \end{bmatrix} = \begin{bmatrix} \frac{1}{a_{R_A}} & 0 & 0 \\ 0 & \frac{1}{a_{R_B}} & 0 \\ -\frac{1}{a_{R_A}} & -\frac{1}{a_{R_B}} & 0 \end{bmatrix} \quad (6.135)$$

$$\begin{bmatrix} aRI_{ABC} \end{bmatrix} = \begin{bmatrix} a_{R_A} & 0 & 0 \\ 0 & a_{R_B} & 0 \\ -a_{R_A} & -a_{R_B} & 0 \end{bmatrix} \quad (6.136)$$

Phases CA & BA

$$\begin{bmatrix} aRV_{abc} \end{bmatrix} = \begin{bmatrix} a_{R_B} & 0 & 0 \\ -a_{R_B} & 0 & -a_{R_C} \\ 0 & 0 & a_{R_C} \end{bmatrix} \quad (6.137)$$

$$[aRV_{ABC}] = \begin{bmatrix} \frac{1}{a_{R_B}} & 0 & 0 \\ -\frac{1}{a_{R_B}} & 0 & -\frac{1}{a_{R_C}} \\ 0 & 0 & \frac{1}{a_{R_C}} \end{bmatrix} \quad (6.138)$$

$$[aRI_{abc}] = \begin{bmatrix} 0 & -\frac{1}{a_{R_B}} & -\frac{1}{a_{R_C}} \\ 0 & \frac{1}{a_{R_B}} & 0 \\ 0 & 0 & \frac{1}{a_{R_C}} \end{bmatrix} \quad (6.139)$$

$$[aRI_{ABC}] = \begin{bmatrix} 0 & -a_{R_B} & -a_{R_C} \\ 0 & a_{R_B} & 0 \\ 0 & 0 & a_{R_C} \end{bmatrix} \quad (6.140)$$

Generalized Equations

The voltage regulator models used in power-flow studies are generalized for the various connections in a form similar to the ABCD parameters that are used in transmission line analysis. The general form of the power-flow models in matrix form are:

$$[V_{ABC}] = [a] \cdot [V_{abc}] + [b] \cdot [I_{abc}] \quad (6.141)$$

$$[I_{ABC}] = [c] \cdot [V_{abc}] + [d] \cdot [I_{abc}] \quad (6.142)$$

$$[V_{abc}] = [A] \cdot [V_{ABC}] - [B] \cdot [I_{abc}] \quad (6.143)$$

Depending upon the connection, the matrices $[V_{ABC}]$ and $[V_{abc}]$ can be either line-to-line or line-to-ground. The current matrices represent the line currents regardless of the regulator connection. For all voltage regulator connections, the generalized constants are defined as:

$$[a] = [aRV_{abc}] \quad (6.144)$$

$$[b] = [0] \quad (6.145)$$

$$[c] = [0] \quad (6.146)$$

$$[d] = [aRI_{abc}] \quad (6.147)$$

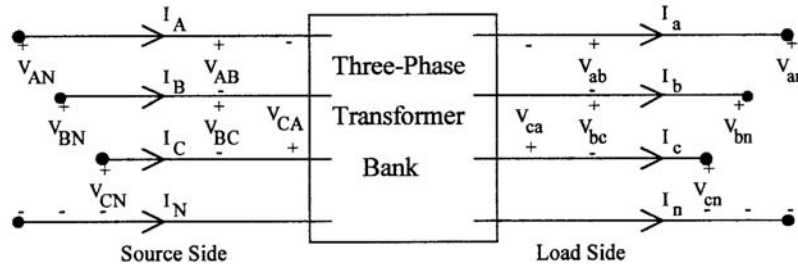


FIGURE 6.23 General transformer bank.

$$[A] = [aRV_{ABC}] \quad (6.148)$$

$$[B] = [0] \quad (6.149)$$

Transformer Bank Connections

Unique models of three-phase transformer banks applicable to radial distribution feeders have been developed (Kersting, 1999). Models for the following three-phase connections are included in this document:

- Delta-Grounded Wye
- Grounded Wye-Delta
- Ungrounded Wye-Delta
- Grounded Wye-Grounded Wye
- Delta-Delta

Figure 6.23 defines the various voltages and currents for the transformer bank models.

The models can represent a step-down (source side to load side) or a step-up (source side to load side) transformer bank. The notation is such that the capital letters **A,B,C,N** will always refer to the **source** side of the bank and the lower case letters **a,b,c,n** will always refer to the **load** side of the bank. It is assumed that all variations of the wye-delta connections are connected in the “American Standard Thirty Degree” connection. The standard is such that:

Step-down connection

V_{AB} leads V_{ab} by 30°

I_A leads I_a by 30°

Step-up connection

V_{ab} leads V_{AB} by 30°

I_a leads I_A by 30°

Generalized Equations

The models to be used in power-flow studies are generalized for the connections in a form similar to the ABCD parameters that are used in transmission line analysis. The general form of the power-flow models in matrix form are:

$$[V_{ABC}] = [a] \cdot [V_{abc}] + [b] \cdot [I_{abc}] \quad (6.150)$$

$$[I_{ABC}] = [c] \cdot [V_{abc}] + [d] \cdot [I_{abc}] \quad (6.151)$$

$$[V_{abc}] = [A] \cdot [V_{ABC}] - [B] \cdot [I_{abc}] \quad (6.152)$$

In Eqs. (6.150), (6.151), and (6.152), the matrices $[V_{ABC}]$ and $[V_{abc}]$ can be either line-to-line voltages (delta connection) or line-to-ground voltages (wye connection). The current matrices represent the line currents regardless of the transformer winding connection.

Common Variable and Matrices

All transformer models will use the following common variable and matrices:

- Transformer turns ratio:
$$a_T = \frac{V_{\text{rated_source}}}{V_{\text{rated_load}}} \quad (6.153)$$

where $V_{\text{rated_source}}$ = transformer winding rating on the source side

$V_{\text{rated_load}}$ = transformer winding rating on the load side

Note that the transformer “winding” ratings may be either line-to-line or line-to-neutral, depending upon the connection. The winding ratings can be specified in actual volts or per-unit volts using the appropriate base line-to-neutral voltages.

- Source to load matrix voltage relations:
$$[V_{ABC}] = [AV] \cdot [V_{abc}] \quad (6.154)$$

The voltage matrices may be line-to-line or line-to-neutral voltages depending upon the connection.

- Load to source matrix current relations:
$$[I_{abc}] = [AI] \cdot [I_{ABC}] \quad (6.155)$$

The current matrices may be line currents or delta currents depending upon the connection.

- Transformer impedance matrix:
$$[Zt_{abc}] = \begin{bmatrix} Zt_a & 0 & 0 \\ 0 & Zt_b & 0 \\ 0 & 0 & Zt_c \end{bmatrix} \quad (6.156)$$

The impedance elements in the matrix will be the per-unit impedance of the transformer windings on the load side of the transformer whether it is connected in wye or delta.

- Symmetrical component transformation matrix:
$$[A_s] = \begin{bmatrix} 1 & 1 & 1 \\ 1 & a^2 & a \\ 1 & a & a^2 \end{bmatrix} \quad (6.157)$$

where $a = 1/\underline{120}$

- Phase shift matrix:
$$[T] = \begin{bmatrix} 1 & 0 & 0 \\ 0 & t & 0 \\ 0 & 0 & t^* \end{bmatrix} \quad (6.158)$$

where
$$t = \frac{1}{\sqrt{3}} \cdot \angle -30$$

- Matrix to convert line-to-line voltages to equivalent line-to-neutral voltages:

$$[W] = [A_s] \cdot [T] \cdot [A_s]^{-1} = \frac{1}{3} \cdot \begin{bmatrix} 2 & 1 & 0 \\ 0 & 2 & 1 \\ 1 & 0 & 2 \end{bmatrix} \quad (6.159)$$

Example: $[VLN] = [W] \cdot [VLL]$

- Matrix to convert delta currents into line currents:

$$[DI] = \begin{bmatrix} 1 & 0 & -1 \\ -1 & 1 & 0 \\ 0 & -1 & 1 \end{bmatrix} \quad (6.160)$$

Example: $[I_{abc}] = [DI] \cdot [ID_{abc}]$

- Matrix to convert line-to-ground or line-to-neutral voltages to line-to-line voltages:

$$[D] = \begin{bmatrix} 1 & -1 & 0 \\ 0 & 1 & -1 \\ -1 & 0 & 1 \end{bmatrix} \quad (6.161)$$

Example: $[VLL_{abc}] = [D] \cdot [VLN_{abc}]$

The matrices $[a]$, $[b]$, $[c]$, $[d]$, $[A]$, and $[B]$ [see Eqs. (6.150), (6.151), and (6.152)] for each connection are defined at the end of this section.

The Per-Unit System

All transformer models were developed so that they can be applied using either “actual” or “per-unit” values of voltages, currents, and impedances. When the per-unit system is used, all per-unit voltages (line-to-line and line-to-neutral) use the line-to-neutral base as the base voltage. In other words, for a balanced set of three-phase voltages, the per-unit line-to-neutral voltage magnitude will be 1.0 at rated voltage and the per-unit line-to-line voltage magnitude will be the square root of 3 (1.732). In similar fashion, all currents (line currents and delta currents) are based on the base line current. Again, a square root of 3 relationship will exist between the line and delta currents under balanced conditions. The base “line” impedance will be used for all line impedances and for wye and delta connected transformer impedances. There will be different base values on the two sides of the transformer bank.

Base values are computed following the steps listed below:

- Select a base three-phase kVA_{base} and the rated line-to-line voltage, $kVLL_{source}$, on the source side as the base line-to-line voltage.
- Based upon the voltage ratings of the transformer bank, determine the “rated” line-to-line voltage, $kVLL_{load}$, on the load side.
- Determine the “transformer ratio”, n_T , as:

$$n_T = \frac{kVLL_{source}}{kVLL_{load}} \quad (6.162)$$

- The “source” side base values are computed as:

$$kVLN_s = \frac{kVLL_s}{\sqrt{3}} \quad (6.163)$$

$$I_s = \frac{kVA_{base}}{\sqrt{3} \cdot kVLL_{source}} \quad (6.164)$$

$$Z_S = \frac{kVLL_{source}^2 \cdot 1000}{kVA_B} \quad (6.165)$$

- The load side base values are computed by:

$$kVLN_L = \frac{kVLN_S}{n_T} \quad (6.166)$$

$$I_L = n_T \cdot I_S \quad (6.167)$$

$$Z_L = \frac{Z_S}{n_T^2} \quad (6.168)$$

Thevenin Equivalent Circuit

The study of short circuit studies that occur on the load side of a transformer bank requires the three-phase Thevenin equivalent circuit referenced to the load-side terminals of the transformer. In order to determine this equivalent circuit, the Thevenin equivalent circuit up to the primary terminals of the “feeder” transformer must be determined. A block diagram of the total system is shown in Fig. 6.24.

In Fig. 6.24 the system voltage source will typically be a balanced set of per-unit voltages such that:

$$[Eth_{ABC}] = \begin{bmatrix} E_{AN} \\ E_{BN} \\ E_{CN} \end{bmatrix} = \begin{bmatrix} 1.0/0 \\ 1.0/-120 \\ 1.0/120 \end{bmatrix} \text{ per-unit} \quad (6.169)$$

The Thevenin equivalent impedance from the source to the primary terminals of the feeder transformer is given by:

$$[Zth_{ABC}] = [Zsys_{ABC}] + [Zsub_{ABC}] + [ZeqS_{ABC}] \quad (6.170)$$

The values of the source side Thevenin equivalent circuit will be the same regardless of the type of connection of the feeder transformer. The three-phase Thevenin equivalent circuit referenced to the load side of the feeder transformer is shown in Fig. 6.25.

For each three-phase transformer connection, unique values of the matrices $[Eth_{abc}]$ and $[Zth_{abc}]$ are defined as functions of the source side Thevenin equivalent circuit. These definitions are shown for each transformer connection below.

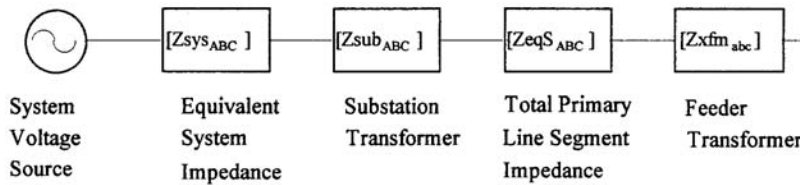


FIGURE 6.24 Total system.

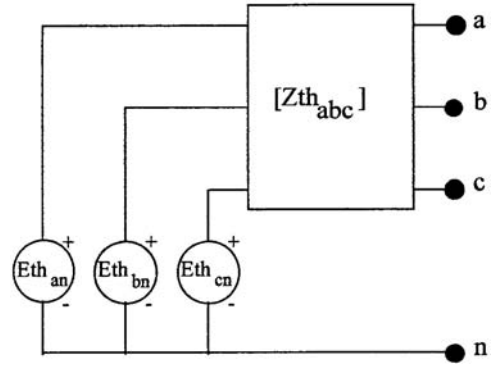


FIGURE 6.25 Three-phase Thevenin equivalent circuit.

Matrix Definitions

Delta-Grounded Wye

Power flow equations:

$$\begin{bmatrix} VLL_{ABC} \end{bmatrix} = \begin{bmatrix} a \end{bmatrix} \cdot \begin{bmatrix} VLG_{abc} \end{bmatrix} + \begin{bmatrix} b \end{bmatrix} \cdot \begin{bmatrix} I_{abc} \end{bmatrix}$$

$$\begin{bmatrix} I_{ABC} \end{bmatrix} = \begin{bmatrix} c \end{bmatrix} \cdot \begin{bmatrix} VLG_{abc} \end{bmatrix} + \begin{bmatrix} d \end{bmatrix} \cdot \begin{bmatrix} I_{abc} \end{bmatrix}$$

$$\begin{bmatrix} a \end{bmatrix} = \begin{bmatrix} AV0 \end{bmatrix}$$

$$\begin{bmatrix} b \end{bmatrix} = \begin{bmatrix} AV0 \end{bmatrix} \cdot \begin{bmatrix} ZNt_{abc} \end{bmatrix}$$

$$\begin{bmatrix} c \end{bmatrix} = \begin{bmatrix} 0 \end{bmatrix}$$

$$\begin{bmatrix} d \end{bmatrix} = \begin{bmatrix} DY \end{bmatrix}$$

$$\begin{bmatrix} VLG_{abc} \end{bmatrix} = \begin{bmatrix} A \end{bmatrix} \cdot \begin{bmatrix} VLL_{ABC} \end{bmatrix} - \begin{bmatrix} B \end{bmatrix} \cdot \begin{bmatrix} I_{abc} \end{bmatrix}$$

$$\begin{bmatrix} A \end{bmatrix} = \begin{bmatrix} AV \end{bmatrix}^{-1}$$

$$\begin{bmatrix} B \end{bmatrix} = \begin{bmatrix} ZNt_{abc} \end{bmatrix}$$

Thevenin equations:

$$\begin{bmatrix} Eth_{abc} \end{bmatrix} = \begin{bmatrix} AV \end{bmatrix}^{-1} \cdot \begin{bmatrix} D \end{bmatrix} \cdot \begin{bmatrix} Eth_{ABC} \end{bmatrix}$$

$$\begin{bmatrix} Zth_{abc} \end{bmatrix} = \begin{bmatrix} AV \end{bmatrix}^{-1} \cdot \begin{bmatrix} D \end{bmatrix} \cdot \begin{bmatrix} Zth_{ABC} \end{bmatrix} \cdot \begin{bmatrix} DY \end{bmatrix} + \begin{bmatrix} Zt_{abc} \end{bmatrix}$$

The matrices used for the step-down connection are:

$$\begin{bmatrix} AV0 \end{bmatrix} = \frac{a_T}{3} \cdot \begin{bmatrix} 1 & -2 & 1 \\ 1 & 1 & -2 \\ -2 & 1 & 1 \end{bmatrix} \quad \begin{bmatrix} AV \end{bmatrix}^{-1} = \begin{bmatrix} 0 & 0 & -\frac{1}{a_T} \\ -\frac{1}{a_T} & 0 & 0 \\ 0 & -\frac{1}{a_T} & 0 \end{bmatrix}$$

$$[DY] = \begin{bmatrix} \frac{1}{a_T} & -\frac{1}{a_T} & 0 \\ 0 & \frac{1}{a_T} & -\frac{1}{a_T} \\ -\frac{1}{a_T} & 0 & \frac{1}{a_T} \end{bmatrix} \quad [D] = \begin{bmatrix} 1 & -1 & 0 \\ 0 & 1 & -1 \\ -1 & 0 & 1 \end{bmatrix}$$

$$[ZNt_{abc}] = \begin{bmatrix} Zt_a & 0 & 0 \\ 0 & Zt_b & 0 \\ 0 & 0 & Zt_c \end{bmatrix}$$

The matrices used for the step-up connection are:

$$[AV0] = \frac{a_T}{3} \cdot \begin{bmatrix} 2 & -1 & -1 \\ -1 & 2 & -1 \\ -1 & -1 & 2 \end{bmatrix} \quad [AV]^{-1} = \begin{bmatrix} \frac{1}{a_T} & 0 & 0 \\ 0 & \frac{1}{a_T} & 0 \\ 0 & 0 & \frac{1}{a_T} \end{bmatrix}$$

$$[DY] = \begin{bmatrix} \frac{1}{a_T} & 0 & -\frac{1}{a_T} \\ -\frac{1}{a_T} & \frac{1}{a_T} & 0 \\ 0 & -\frac{1}{a_T} & \frac{1}{a_T} \end{bmatrix} \quad [D] = \begin{bmatrix} 1 & -1 & 0 \\ 0 & 1 & -1 \\ -1 & 0 & 1 \end{bmatrix}$$

$$[ZNt_{abc}] = [Zt_{abc}] = \begin{bmatrix} Zt_a & 0 & 0 \\ 0 & Zt_b & 0 \\ 0 & 0 & Zt_c \end{bmatrix}$$

Grounded Wye-Delta

Power flow equations:

$$[VLG_{ABC}] = [a] \cdot [VLL_{abc}] + [b] \cdot [I_{abc}]$$

$$[I_{ABC}] = [c] \cdot [VLL_{abc}] + [d] \cdot [I_{abc}]$$

$$[a] = [EV] \cdot [AV]$$

$$[b] = [EV] \cdot [AV] \cdot [ZNt_{abc}] \cdot [H1]$$

$$[c] = [H2] \cdot [EV] \cdot [AV]$$

$$[d] = [H1] - [H2] \cdot [EV] \cdot [AV] \cdot [ZNt_{abc}] \cdot [H1]$$

$$\begin{bmatrix} VLL_{abc} \end{bmatrix} = \begin{bmatrix} A \end{bmatrix} \cdot \begin{bmatrix} VLG_{ABC} \end{bmatrix} - \begin{bmatrix} B \end{bmatrix} \cdot \begin{bmatrix} I_{abc} \end{bmatrix}$$

$$\begin{bmatrix} A \end{bmatrix} = \begin{bmatrix} AV \end{bmatrix}^{-1} - \begin{bmatrix} ZNt_{abc} \end{bmatrix} \cdot \begin{bmatrix} H2 \end{bmatrix}$$

$$\begin{bmatrix} B \end{bmatrix} = \begin{bmatrix} ZNt_{abc} \end{bmatrix} \cdot \begin{bmatrix} H1 \end{bmatrix}$$

Thevenin equations:

$$\begin{bmatrix} Eth_{abc} \end{bmatrix} = \begin{bmatrix} Eth_{ABC} \end{bmatrix} / \pm 30, \quad +30 \text{ for step-up, } -30 \text{ for step-down}$$

$$\begin{bmatrix} Zth_{abc} \end{bmatrix} = \begin{bmatrix} W \end{bmatrix} \cdot \left(\begin{bmatrix} K1 \end{bmatrix} \cdot \begin{bmatrix} K \end{bmatrix}^{-1} \cdot \begin{bmatrix} ZeqS_{ABC} \end{bmatrix} + \begin{bmatrix} ZNt_{abc} \end{bmatrix} \right) \cdot \begin{bmatrix} H1 \end{bmatrix}$$

Sub-matrices used for the step-down and the step-up connections are:

$$\begin{bmatrix} ZNt_{abc} \end{bmatrix} = \begin{bmatrix} Zt_{abc} \end{bmatrix} \cdot \begin{bmatrix} AI \end{bmatrix}$$

$$\begin{bmatrix} K1 \end{bmatrix} = \begin{bmatrix} AV \end{bmatrix}^{-1} - \begin{bmatrix} ZNt_{abc} \end{bmatrix} \cdot \begin{bmatrix} H2 \end{bmatrix}$$

$$\begin{bmatrix} K \end{bmatrix} = \begin{bmatrix} U \end{bmatrix} + \begin{bmatrix} Zth_{ABC} \end{bmatrix} \cdot \begin{bmatrix} H2 \end{bmatrix}$$

$$\begin{bmatrix} EV \end{bmatrix} = \begin{bmatrix} U \end{bmatrix} - \begin{bmatrix} AV \end{bmatrix} \cdot \begin{bmatrix} ZNt_{abc} \end{bmatrix} \cdot \begin{bmatrix} H2 \end{bmatrix}$$

Matrices used for the step-down connection are:

$$\begin{bmatrix} AV \end{bmatrix} = \begin{bmatrix} a_T & 0 & 0 \\ 0 & a_T & 0 \\ 0 & 0 & a_T \end{bmatrix} \quad \begin{bmatrix} AI \end{bmatrix} = \begin{bmatrix} a_T & 0 & 0 \\ 0 & a_T & 0 \\ 0 & 0 & a_T \end{bmatrix}$$

$$\begin{bmatrix} DY \end{bmatrix} = \begin{bmatrix} a_T & 0 & -a_T \\ -a_T & a_T & 0 \\ 0 & -a_T & a_T \end{bmatrix} \quad \begin{bmatrix} U \end{bmatrix} = \begin{bmatrix} 1 & 0 & 0 \\ 0 & 1 & 0 \\ 0 & 0 & 1 \end{bmatrix}$$

$$\begin{bmatrix} Zt_{abc} \end{bmatrix} = \begin{bmatrix} Zt_{ab} & 0 & 0 \\ 0 & Zt_{bc} & 0 \\ 0 & 0 & Zt_{ca} \end{bmatrix}$$

$$\begin{bmatrix} H1 \end{bmatrix} = \frac{1}{a_T \cdot (Zt_{ab} + Zt_{bc} + Zt_{ca})} \cdot \begin{bmatrix} Zt_{ca} & -Zt_{bc} & 0 \\ Zt_{ca} & Zt_{ab} + Zt_{cb} & 0 \\ -Zt_{ab} - Zt_{bc} & -Zt_{bc} & 0 \end{bmatrix}$$

$$\begin{bmatrix} H2 \end{bmatrix} = \frac{1}{a_T \cdot (Zt_{ab} + Zt_{bc} + Zt_{ca})} \cdot \begin{bmatrix} 1 & 1 & 1 \\ 1 & 1 & 1 \\ 1 & 1 & 1 \end{bmatrix}$$

The matrices used for the step-up connection are:

$$[AV] = \begin{bmatrix} 0 & 0 & -a_T \\ -a & 0 & 0 \\ 0 & -a & 0 \end{bmatrix} \quad [AI] = \begin{bmatrix} 0 & -a_T & 0 \\ 0 & 0 & -a_T \\ -a_T & 0 & 0 \end{bmatrix}$$

$$[DY] = \begin{bmatrix} a_T & -a_T & 0 \\ 0 & a_T & -a_T \\ -a_T & 0 & a_T \end{bmatrix} \quad [U] = \begin{bmatrix} 1 & 0 & 0 \\ 0 & 1 & 0 \\ 0 & 0 & 1 \end{bmatrix}$$

$$[Zt_{abc}] = \begin{bmatrix} Zt_{ab} & 0 & 0 \\ 0 & Zt_{bc} & 0 \\ 0 & 0 & Zt_{ca} \end{bmatrix}$$

$$[H1] = \frac{1}{a_T \cdot (Zt_{ab} + Zt_{bc} + Zt_{ca})} \cdot \begin{bmatrix} Zt_{ab} + Zt_{bc} & Zt_{bc} & 0 \\ -Zt_{ca} & Zt_{bc} & 0 \\ -Zt_{ca} & -(Zt_{ab} + Zt_{ca}) & 0 \end{bmatrix}$$

$$[H2] = \frac{1}{a_T \cdot (Zt_{ab} + Zt_{bc} + Zt_{ca})} \cdot \begin{bmatrix} -1 & -1 & -1 \\ -1 & -1 & -1 \\ -1 & -1 & -1 \end{bmatrix}$$

Ungrounded Wye-Delta

Power flow equations:

$$[VLN_{ABC}] = [a] \cdot [VLL_{abc}] + [b] \cdot [I_{abc}]$$

$$[I_{ABC}] = [c] \cdot [VLL_{abc}] + [d] \cdot [I_{abc}]$$

$$[a] = [AV]$$

$$[b] = [ZDt_{abc}]$$

$$[c] = [0]$$

$$[d] = [H]$$

$$[VLL_{abc}] = [A] \cdot [VLN_{ABC}] - [B] \cdot [I_{abc}]$$

$$[A] = [AV]^{-1}$$

$$[B] = [ZNt_{abc}] \cdot [H]$$

Thevenin equations:

$$[Eth_{abc}] = [Eth_{ABC}] / \pm 30, \quad +30 \text{ for step-up, } -30 \text{ for step-down}$$

$$[Zth_{abc}] = [W] \cdot \left([AV]^{-1} \cdot [W0] \cdot [ZeqS_{ABC}] + [ZNt_{ABC}] \right) \cdot [H]$$

The matrices used for the step-down connection are:

$$[AV] = \begin{bmatrix} a_T & 0 & 0 \\ 0 & a_T & 0 \\ 0 & 0 & a_T \end{bmatrix} \quad [AI] = \begin{bmatrix} a_T & 0 & 0 \\ 0 & a_T & 0 \\ 0 & 0 & a_T \end{bmatrix}$$

$$[DY] = \begin{bmatrix} a_T & 0 & -a_T \\ -a_T & a_T & 0 \\ 0 & -a_T & a_T \end{bmatrix} \quad [H] = \frac{1}{3 \cdot a_T} \cdot \begin{bmatrix} 1 & -1 & 0 \\ 1 & 2 & 0 \\ -2 & -1 & 0 \end{bmatrix}$$

$$[ZNt_{abc}] = \begin{bmatrix} a_T \cdot Zt_{ab} & 0 & 0 \\ 0 & a_T \cdot Zt_{bc} & 0 \\ 0 & 0 & a_T \cdot Zt_{ca} \end{bmatrix}$$

$$[ZDt_{abc}] = \frac{a_T}{3} \cdot \begin{bmatrix} Zt_{ab} & -Zt_{ab} & 0 \\ Zt_{bc} & 2 \cdot Zt_{bc} & 0 \\ -2 \cdot Zt_{ca} & -Zt_{ca} & 0 \end{bmatrix}$$

The matrices used for the step-up connection are:

$$[AV] = \begin{bmatrix} 0 & 0 & -a_T \\ -a_T & 0 & 0 \\ 0 & -a_T & 0 \end{bmatrix} \quad [AI] = \begin{bmatrix} 0 & -\frac{1}{a_T} & 0 \\ 0 & 0 & -\frac{1}{a_T} \\ -\frac{1}{a_T} & 0 & 0 \end{bmatrix}$$

$$[DY] = \begin{bmatrix} a_T & -a_T & 0 \\ 0 & a_T & -a_T \\ -a_T & 0 & a_T \end{bmatrix} \quad [H] = \frac{1}{3 \cdot a_T} \cdot \begin{bmatrix} 2 & 1 & 0 \\ -1 & 1 & 0 \\ -1 & -2 & 0 \end{bmatrix}$$

$$[ZDt_{abc}] = \frac{a_T}{3} \cdot \begin{bmatrix} 2 \cdot Zt_{ca} & Zt_{ca} & 0 \\ -Zt_{ab} & Zt_{ab} & 0 \\ -Zt_{bc} & -2 \cdot Zt_{bc} & 0 \end{bmatrix}$$

$$\begin{bmatrix} ZNt_{abc} \end{bmatrix} = \begin{bmatrix} 0 & -a_T \cdot Zt_{ab} & 0 \\ 0 & 0 & -a_T \cdot Zt_{bc} \\ a_T \cdot Zt_{ca} & 0 & 0 \end{bmatrix}$$

The Grounded Wye-Grounded Wye Connection

Power flow equations:

$$\begin{bmatrix} VLG_{ABC} \end{bmatrix} = \begin{bmatrix} a \end{bmatrix} \cdot \begin{bmatrix} VLG_{abc} \end{bmatrix} + \begin{bmatrix} b \end{bmatrix} \cdot \begin{bmatrix} I_{abc} \end{bmatrix}$$

$$\begin{bmatrix} I_{ABC} \end{bmatrix} = \begin{bmatrix} c \end{bmatrix} \cdot \begin{bmatrix} VLG_{abc} \end{bmatrix} + \begin{bmatrix} d \end{bmatrix} \cdot \begin{bmatrix} I_{abc} \end{bmatrix}$$

$$\begin{bmatrix} a \end{bmatrix} = \begin{bmatrix} AV \end{bmatrix}$$

$$\begin{bmatrix} b \end{bmatrix} = \begin{bmatrix} ZNt_{abc} \end{bmatrix}$$

$$\begin{bmatrix} c \end{bmatrix} = \begin{bmatrix} 0 \end{bmatrix}$$

$$\begin{bmatrix} d \end{bmatrix} = \begin{bmatrix} AI \end{bmatrix}^{-1}$$

$$\begin{bmatrix} VLG_{abc} \end{bmatrix} = \begin{bmatrix} A \end{bmatrix} \cdot \begin{bmatrix} VLG_{ABC} \end{bmatrix} - \begin{bmatrix} B \end{bmatrix} \cdot \begin{bmatrix} I_{ABC} \end{bmatrix}$$

$$\begin{bmatrix} A \end{bmatrix} = \begin{bmatrix} AV \end{bmatrix}^{-1}$$

$$\begin{bmatrix} B \end{bmatrix} = \begin{bmatrix} AV \end{bmatrix}^{-1} \cdot \begin{bmatrix} ZNt_{abc} \end{bmatrix}$$

Thevenin equations

$$\begin{bmatrix} Eth_{abc} \end{bmatrix} = \begin{bmatrix} AV \end{bmatrix}^{-1} \cdot \begin{bmatrix} Eth_{ABC} \end{bmatrix}$$

$$\begin{bmatrix} Zth_{abc} \end{bmatrix} = \begin{bmatrix} AV \end{bmatrix}^{-1} \cdot \left(\begin{bmatrix} ZeqS_{ABC} \end{bmatrix} \cdot \begin{bmatrix} AV \end{bmatrix}^{-1} + \begin{bmatrix} ZNt_{abc} \end{bmatrix} \right)$$

The matrices used are:

$$\begin{bmatrix} AV \end{bmatrix} = \begin{bmatrix} AI \end{bmatrix} = \begin{bmatrix} a_T & 0 & 0 \\ 0 & a_T & 0 \\ 0 & 0 & a_T \end{bmatrix} \quad \begin{bmatrix} AV \end{bmatrix}^{-1} = \begin{bmatrix} AI \end{bmatrix}^{-1} \cdot \begin{bmatrix} \frac{1}{a_T} & 0 & 0 \\ 0 & \frac{1}{a_T} & 0 \\ 0 & 0 & \frac{1}{a_T} \end{bmatrix}$$

$$\begin{bmatrix} Zt_{abc} \end{bmatrix} = \begin{bmatrix} Zt_a & 0 & 0 \\ 0 & Zt_b & 0 \\ 0 & 0 & Zt_c \end{bmatrix} \quad \begin{bmatrix} ZNt_{abc} \end{bmatrix} = \begin{bmatrix} a_T \cdot Zt_a & 0 & 0 \\ 0 & a_T \cdot Zt_b & 0 \\ 0 & 0 & a_T \cdot Zt_c \end{bmatrix}$$

Delta-Delta

Power flow equations:

$$\begin{aligned}
 [VLL_{ABC}] &= [a] \cdot [VLL_{abc}] + [b] \cdot [I_{abc}] \\
 [I_{ABC}] &= [c] \cdot [VLL_{abc}] + [d] \cdot [I_{abc}] \\
 [a] &= [AV] \\
 [b] &= [Zt_{abc}] \cdot [G1] \\
 [c] &= [0] \\
 [d] &= [AI]^{-1} \\
 [VLL_{abc}] &= [A] \cdot [VLL_{ABC}] - [B] \cdot [I_{abc}] \\
 [A] &= [AV]^{-1} \\
 [B] &= [Zt_{abc}] \cdot [G1]
 \end{aligned}$$

Thevenin equations:

$$\begin{aligned}
 [Eth_{abc}] &= [W] \cdot [AV]^{-1} \cdot [D] \cdot [W] \cdot [ELL_S] \\
 [Zth_{abc}] &= [W] \cdot \left([AV]^{-1} \cdot [D] \cdot [ZeqS_{ABC}] \cdot [AV]^{-1} + [Zt_{abc}] \cdot [G1] \right)
 \end{aligned}$$

The matrices used are:

$$[AV] = \begin{bmatrix} a_T & 0 & 0 \\ 0 & a_T & 0 \\ 0 & 0 & a_T \end{bmatrix} \quad [AI] = \begin{bmatrix} a_T & 0 & 0 \\ 0 & a_T & 0 \\ 0 & 0 & a_T \end{bmatrix}$$

$$[D] = \begin{bmatrix} 1 & -1 & 0 \\ 0 & 1 & -1 \\ -1 & 0 & 1 \end{bmatrix} \quad [W] = \frac{1}{3} \cdot \begin{bmatrix} 2 & 1 & 0 \\ 0 & 2 & 1 \\ 1 & 0 & 2 \end{bmatrix}$$

$$[Zt_{abc}] = \begin{bmatrix} Zt_{ab} & 0 & 0 \\ 0 & Zt_{bc} & 0 \\ 0 & 0 & Zt_{ca} \end{bmatrix}$$

$$[G1] = \frac{1}{Zt_{ab} + Zt_{bc} + Zt_{ca}} \cdot \begin{bmatrix} Zt_{ca} & -Zt_{bc} & 0 \\ Zt_{ca} & Zt_{ab} + Zt_{ca} & 0 \\ -Zt_{ab} - Zt_{bc} & -Zt_{bc} & 0 \end{bmatrix}$$

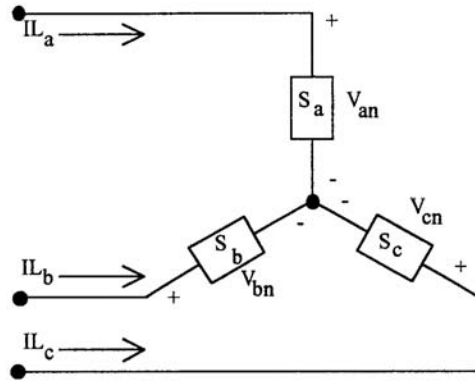


FIGURE 6.26 Wye connected load.

Load Models

Loads can be represented as being connected phase-to-phase or phase-to-neutral in a four-wire wye systems or phase-to-phase in a three-wire delta system. The loads can be three-phase, two-phase, or single-phase with any degree of unbalance and can be modeled as:

- Constant real and reactive power (constant PQ)
- Constant current
- Constant impedance
- Any combination of the above

The load models developed in this document are used in the iterative process of a power-flow program. All models are initially defined by a complex power per phase and either a line-to-neutral (wye load) or a line-to-line voltage (delta load). The units of the complex power can be in volt-amperes and volts or per-unit volt-amperes and per-unit volts.

For both the wye and delta connected loads, the basic requirement is to determine the load component of the line currents coming into the loads. It is assumed that all loads are initially specified by their complex power ($S = P + jQ$) per phase and a line-to-neutral or line-to-line voltage.

Wye Connected Loads

Figure 6.26 shows the model of a wye connected load.

The notation for the specified complex powers and voltages are as follows:

$$\text{Phase a: } |S_a|/\theta_a = P_a + jQ_a \text{ and } |V_{an}|/\delta_a \quad (6.171)$$

$$\text{Phase b: } |S_b|/\theta_b = P_b + jQ_b \text{ and } |V_{bn}|/\delta_b \quad (6.172)$$

$$\text{Phase c: } |S_c|/\theta_c = P_c + jQ_c \text{ and } |V_{cn}|/\delta_c \quad (6.173)$$

1. Constant Real and Reactive Power Loads

$$IL_a = \left(\frac{S_a}{V_{an}} \right)^* = \frac{|S_a|}{|V_{an}|} / \delta_a - \theta_a = |IL_a| / \alpha_a \quad (6.174)$$

$$IL_b = \left(\frac{S_b}{V_{bn}} \right)^* = \frac{|S_b|}{|V_{bn}|} / \underline{\delta_b - \theta_b} = |IL_b| / \underline{\alpha_b}$$

$$IL_c = \left(\frac{S_c}{V_{cn}} \right)^* = \frac{|S_c|}{|V_{cn}|} / \underline{\delta_c - \theta_c} = |IL_c| / \underline{\alpha_c}$$

In this model the line-to-neutral voltages will change during each iteration until convergence is achieved.

2. Constant Impedance Loads

The “constant load impedance” is first determined from the specified complex power and line-to-neutral voltages according to Eq. (6.175).

$$Z_a = \frac{|V_{an}|^2}{S_a^*} = \frac{|V_{an}|^2}{|S_a|} / \underline{\theta_a} = |Z_a| / \underline{\theta_a}$$

$$Z_b = \frac{|V_{bn}|^2}{S_b^*} = \frac{|V_{bn}|^2}{|S_b|} / \underline{\theta_b} = |Z_b| / \underline{\theta_b}$$

$$Z_c = \frac{|V_{cn}|^2}{S_c^*} = \frac{|V_{cn}|^2}{|S_c|} / \underline{\theta_c} = |Z_c| / \underline{\theta_c}$$
(6.175)

The load currents as a function of the “constant load impedances” are given by Eq. (6.176).

$$IL_a = \frac{V_{an}}{Z_a} = \frac{|V_{an}|}{|Z_a|} / \underline{\delta_a - \theta_a} = |IL_a| / \underline{\alpha_a}$$

$$IL_b = \frac{V_{bn}}{Z_b} = \frac{|V_{bn}|}{|Z_b|} / \underline{\delta_b - \theta_b} = |IL_b| / \underline{\alpha_b}$$

$$IL_c = \frac{V_{cn}}{Z_c} = \frac{|V_{cn}|}{|Z_c|} / \underline{\delta_c - \theta_c} = |IL_c| / \underline{\alpha_c}$$
(6.176)

In this model the line-to-neutral voltages in Eq. (6.176) will change during each iteration until convergence is achieved.

3. Constant Current Loads

In this model the magnitudes of the currents are computed according to Eq. (6.174) and then held constant while the angle of the voltage (δ) changes during each iteration. This keeps the power factor of the load constant.

$$IL_a = |IL_a| / \underline{\delta_a - \theta_a}$$

$$IL_b = |IL_b| / \underline{\delta_b - \theta_b}$$

$$IL_c = |IL_c| / \underline{\delta_c - \theta_c}$$
(6.177)

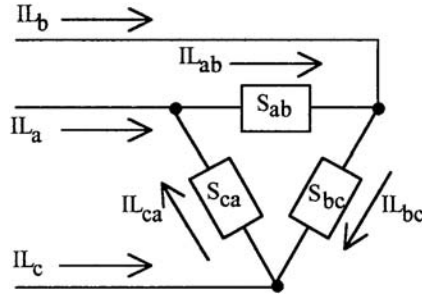


FIGURE 6.27 Delta connected load.

4. Combination Loads

Combination loads can be modeled by assigning a percentage of the total load to each of the above three load models. The total line current entering the load is the sum of the three components.

Delta Connected Loads

Figure 6.27 shows the model of a delta connected load.

The notation for the specified complex powers and voltages are as follows:

$$\text{Phase ab: } |S_{ab}|/\theta_{ab} = P_{ab} + jQ_{ab} \quad \text{and} \quad |V_{ab}|/\delta_{ab} \quad (6.178)$$

$$\text{Phase bc: } |S_{bc}|/\theta_{bc} = P_{bc} + jQ_{bc} \quad \text{and} \quad |V_{bc}|/\delta_{bc} \quad (6.179)$$

$$\text{Phase ca: } |S_{ca}|/\theta_{ca} = P_{ca} + jQ_{ca} \quad \text{and} \quad |V_{ca}|/\delta_{ca} \quad (6.180)$$

1. Constant Real and Reactive Power Loads

$$\begin{aligned} IL_{ab} &= \left(\frac{S_{ab}}{V_{ab}} \right)^* = \frac{|S_{ab}|}{|V_{ab}|} / \delta_{ab} - \theta_{ab} = |IL_{ab}| / \alpha_{ab} \\ IL_{bc} &= \left(\frac{S_{bc}}{V_{bc}} \right)^* = \frac{|S_{bc}|}{|V_{bc}|} / \delta_{bc} - \theta_{bc} = |IL_{bc}| / \alpha_{bc} \\ IL_{ca} &= \left(\frac{S_{ca}}{V_{ca}} \right)^* = \frac{|S_{ca}|}{|V_{ca}|} / \delta_{ca} - \theta_{ca} = |IL_{ca}| / \alpha_{ca} \end{aligned} \quad (6.181)$$

In this model the line-to-line voltages will change during each iteration until convergence is achieved.

2. Constant Impedance Loads

The “constant load impedance” is first determined from the specified complex power and line-to-neutral voltages according to Eq. (6.182).

$$Z_{ab} = \frac{|V_{ab}|^2}{S_{ab}^*} = \frac{|V_{ab}|^2}{|S_{ab}|} / \theta_{ab} = |Z_{ab}| / \theta_{ab} \quad (6.182)$$

$$Z_{bc} = \frac{|V_{bc}|^2}{S_{bc}^*} = \frac{|V_{bc}|^2}{|S_{bc}|} / \theta_{bc} = |Z_{bc}| / \theta_{bc}$$

$$Z_{ca} = \frac{|V_{ca}|^2}{S_{ca}^*} = \frac{|V_{ca}|^2}{|S_{ca}|} / \theta_{ca} = |Z_{ca}| / \theta_{ca}$$

The load currents as a function of the “constant load impedances” are given by Eq. (6.173).

$$IL_{ab} = \frac{V_{ab}}{Z_{ab}} = \frac{|V_{ab}|}{|Z_{ab}|} / \delta_{ab} - \theta_{ab} = |IL_{ab}| / \alpha_{ab}$$

$$IL_{bc} = \frac{V_{bc}}{Z_{bc}} = \frac{|V_{bc}|}{|Z_{bc}|} / \delta_{bc} - \theta_{bc} = |IL_{bc}| / \alpha_{bc} \quad (6.183)$$

$$IL_{ca} = \frac{V_{ca}}{Z_{ca}} = \frac{|V_{ca}|}{|Z_{ca}|} / \delta_{ca} - \theta_{ca} = |IL_{ca}| / \alpha_{ca}$$

In this model the line-to-neutral voltages in Eq. (6.183) will change during each iteration until convergence is achieved.

3. Constant Current Loads

In this model the magnitudes of the currents are computed according to Eq. (6.181) and then held constant while the angle of the voltage (δ) changes during each iteration. This keeps the power factor of the load constant.

$$IL_{ab} = |IL_{ab}| / \delta_{ab} - \theta_{ab}$$

$$IL_{bc} = |IL_{bc}| / \delta_{bc} - \theta_{bc} \quad (6.184)$$

$$IL_{ca} = |IL_{ca}| / \delta_{ca} - \theta_{ca}$$

4. Combination Loads

Combination loads can be modeled by assigning a percentage of the total load to each of the above three load models. The total delta current for each load is the sum of the three components.

The line currents entering the delta connected load are determined by:

$$\begin{bmatrix} IL_a \\ IL_b \\ IL_c \end{bmatrix} = \begin{bmatrix} 1 & 0 & -1 \\ -1 & 1 & 0 \\ 0 & -1 & 1 \end{bmatrix} \cdot \begin{bmatrix} IL_{ab} \\ IL_{bc} \\ IL_{ca} \end{bmatrix} \quad (6.185)$$

In both the wye and delta connected loads, single-phase and two-phase loads are modeled by setting the complex powers of the missing phases to zero. In other words, all loads are modeled as three-phase loads and by setting the complex power of the missing phases to zero, the only load currents computed using the above equations will be for the non-zero loads.

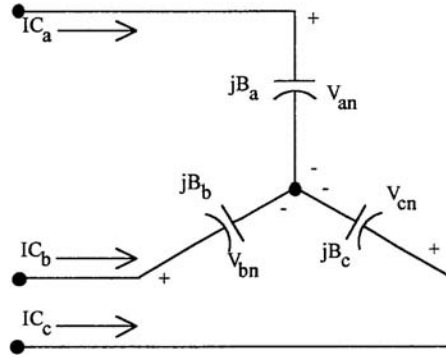


FIGURE 6.28 Wye connected capacitor bank.

Shunt Capacitor Models

Shunt capacitor banks are commonly used in a distribution system to help in voltage regulation and to provide reactive power support. The capacitor banks are modeled as constant susceptances connected in either wye or delta. Similar to the load model, all capacitor banks are modeled as three-phase banks with the kVAr of missing phases set to zero for single-phase and two-phase banks.

Wye Connected Capacitor Bank

A wye connected capacitor bank is shown in Fig. 6.28.

The individual phase capacitor units are specified in kVAr and kV. The constant susceptance for each unit can be computed in either Siemens or per-unit. When per-unit is desired, the specified kVAr of the capacitor must be divided by the base single-phase kVAr and the kV must be divided by the base line-to-neutral kV.

The susceptance of a capacitor unit is computed by:

$$B_{actual} = \frac{kVAr}{kV^2 \cdot 1000} \quad \text{Siemens} \quad (6.186)$$

$$B_{pu} = \frac{kVAr_{pu}}{V_{pu}^2} \quad \text{Per-unit} \quad (6.187)$$

where

$$kVAr_{pu} = \frac{kVAr_{actual}}{kVA_{single_phase_base}} \quad (6.188)$$

$$V_{pu} = \frac{kV_{actual}}{kV_{line_to_neutral_base}} \quad (6.189)$$

The per-unit value of the susceptance can also be determined by first computing the actual value [Eq. (6.186)] and then dividing by the base admittance of the system.

With the susceptance computed, the line currents serving the capacitor bank are given by:

$$\begin{aligned} IC_a &= jB_a \cdot V_{an} \\ IC_b &= jB_b \cdot V_{bn} \\ IC_c &= jB_c \cdot V_{cn} \end{aligned} \quad (6.190)$$

Delta Connected Capacitor Bank

A delta connected capacitor bank is shown in Fig. 6.29.

Equations (6.186) through (6.189) can be used to determine the value of the susceptance in actual Siemens and/or per-unit. It should be pointed out that in this case, the kV will be a line-to-line value of the voltage. Also, it should be noted that in Eq. (6.189), the base line-to-neutral voltage is used to compute the per-unit line-to-line voltage. This is a variation from the usual application of the per-unit system where the actual line-to-line voltage would be divided by a base line-to-line voltage in order to get the per-unit line-to-line voltage. That is not done here so that under normal conditions, the per-unit line-to-line voltage will have a magnitude of $\sqrt{3}$ rather than 1.0. This is done so that KCL at each node of the delta connection will apply for either the actual or per-unit delta currents.

The currents flowing in the delta connected capacitors are given by:

$$\begin{aligned} IC_{ab} &= jB_{ab} \cdot V_{ab} \\ IC_{bc} &= jB_{bc} \cdot V_{bc} \\ IC_{ca} &= jB_{ca} \cdot V_{ca} \end{aligned} \quad (6.191)$$

The line currents feeding the delta connected capacitor bank are given by:

$$\begin{bmatrix} IC_a \\ IC_b \\ IC_c \end{bmatrix} = \begin{bmatrix} 1 & 0 & -1 \\ -1 & 1 & 0 \\ 0 & -1 & 1 \end{bmatrix} \cdot \begin{bmatrix} IC_{ab} \\ IC_{bc} \\ IC_{ca} \end{bmatrix} \quad (6.192)$$

Analysis

Power Flow Analysis

The power-flow analysis of a distribution feeder is similar to that of an interconnected transmission system. Typically what will be known prior to the analysis will be the three-phase voltages at the substation and the complex power of all of the loads and the load model (constant complex power, constant impedance, constant current or a combination). Sometimes, the input complex power supplied to the feeder from the substation is also known.

In the areas of this section entitled “Line Segment Models”, “Step-Voltage Regulators”, and “Transformer Bank Connections”, phase frame models were presented for the series components of a distribution feeder. In the areas entitled “Load Models” and “Shunt Capacitor Models”, models were presented for the shunt components (loads and capacitor banks). These models are used in the “power-flow” analysis of a distribution feeder.

A power-flow analysis of a feeder can determine the following by phase and total three-phase:

- Voltage magnitudes and angles at all nodes of the feeder
- Line flow in each line section specified in kW and kVAr, amps and degrees or amps and power factor
- Power loss in each line section
- Total feeder input kW and kVAr
- Total feeder power losses
- Load kW and kVAr based upon the specified model for the load

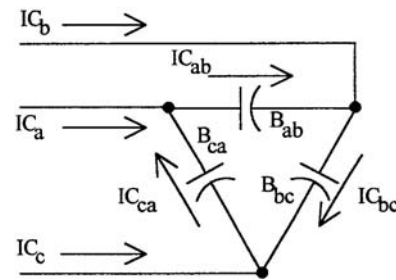


FIGURE 6.29 Delta connected capacitor bank.

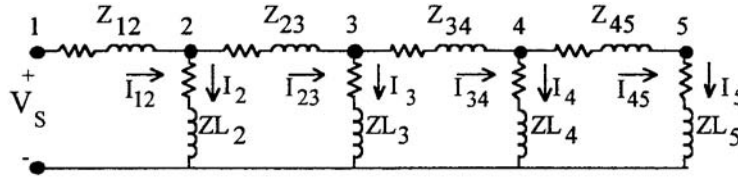


FIGURE 6.30 Linear ladder network.

Because the feeder is radial, iterative techniques commonly used in transmission network power-flow studies are not used because of poor convergence characteristics (Trevino, 1970). Instead, an iterative technique specifically designed for a radial system is used. The “ladder iterative technique” (Kersting and Mendive, 1976) will be presented here.

The Ladder Iterative Technique

Linear Network

A modification of the “ladder” network theory of linear systems provides a robust iterative technique for power-flow analysis. A distribution feeder is non-linear because most loads are assumed to be constant kW and kVar. However, the approach taken for the linear system can be modified to take into account the non-linear characteristics of the distribution feeder.

For the ladder network in Fig. 6.30 it is assumed that all of the line impedances and load impedances are known along with the voltage at the source (V_s). The solution for this network is to assume a voltage at the most remote load (V_5). The load current I_5 is then determined as:

$$I_5 = \frac{V_5}{ZL_5} \quad (6.193)$$

For this “end node” case, the line current I_{45} is equal to the load current I_5 . The voltage at node 4 (V_4) can be determined using Kirchhoff’s Voltage Law:

$$V_4 = V_5 + Z_{45} \cdot I_{45} \quad (6.194)$$

The load current I_4 can be determined and then Kirchhoff’s Current Law applied to determine the line current I_{34} .

$$I_{34} = I_{45} + I_4 \quad (6.195)$$

Kirchhoff’s Voltage Law is applied to determine the node voltage V_3 . This procedure is continued until a voltage (V_1) has been computed at the source. The computed voltage V_1 is compared to the specified voltage V_s . There will be a difference between these two voltages. The ratio of the specified voltage to the compute voltage can be determined as:

$$Ratio = \frac{V_s}{V_1} \quad (6.196)$$

Since the network is linear, all of the line and load currents and node voltages in the network can be multiplied by the Ratio for the final solution to the network.

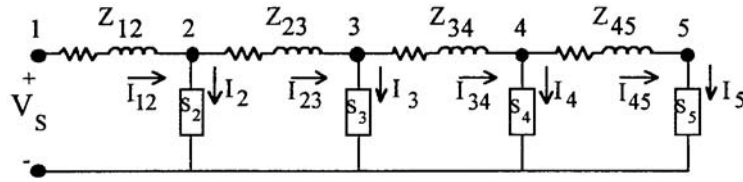


FIGURE 6.31 Non-linear ladder network.

Non-Linear Network

The linear network of Fig. 6.30 is modified to a non-linear network by replacing all of the constant load impedances by constant complex power loads as shown in Fig. 6.31.

The procedure outlined for the linear network is applied initially to the non-linear network. The only difference being that the load current at each node is computed by:

$$I_n = \left(\frac{S_n}{V_n} \right)^* \quad (6.197)$$

The “forward sweep” will determine a computed source voltage V_1 . As in the linear case, this first “iteration” will produce a voltage that is not equal to the specified source voltage V_s . Because the network is non-linear, multiplying currents and voltages by the ratio of the specified voltage to the computed voltage will not give the solution. The most direct modification to the ladder network theory is to perform a “backward sweep.” The backward sweep commences by using the specified source voltage and the line currents from the “forward sweep.” Kirchhoff’s Voltage Law is used to compute the voltage at node 2 by:

$$V_2 = V_s - Z_{12} \cdot I_{12} \quad (6.198)$$

This procedure is repeated for each line segment until a “new” voltage is determined at node 5. Using the “new” voltage at node 5, a second “forward sweep” is started that will lead to a “new” computed voltage at the source.

The forward and backward sweep process is continued until the difference between the computed and specified voltage at the source is within a given tolerance.

General Feeder

A typical distribution feeder will consist of the “primary main” with laterals tapped off the primary main, and sublaterals tapped off the laterals, etc. Figure 6.32 shows an example of a typical feeder.

The ladder iterative technique for the feeder of Fig. 6.32 would proceed as follows:

1. Assume voltages (1.0 per-unit) at the “end” nodes (6, 8, 9, 11, and 13).
2. Starting at node 13, compute the node current (load current plus capacitor current if present).
3. With this current, apply Kirchhoff’s Voltage Law (KVL) to calculate the node voltages at 12 and 10.
4. Node 10 is referred to as a “junction” node since laterals branch in two directions from the node. This feeder goes to node 11 and computes the node current. Use that current to compute the voltage at node 10. This will be referred to as “the most recent voltage at node 10.”
5. Using the most recent value of the voltage at node 10, the node current at node 10 (if any) is computed.
6. Apply Kirchhoff’s Current Law (KCL) to determine the current flowing from node 4 towards node 10.
7. Compute the voltage at node 4.
8. Node 4 is a “junction node.” An end node downstream from node 4 is selected to start the forward sweep toward node 4.

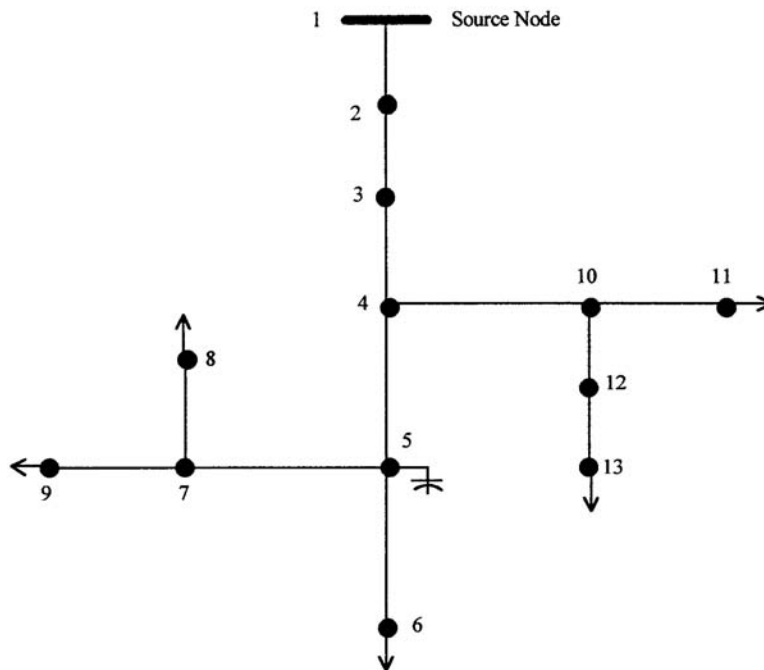


FIGURE 6.32 Typical distribution feeder.

9. Select node 6, compute the node current, and then compute the voltage at “junction node” 5.
10. Go to downstream end node 8. Compute the node current and then the voltage at junction node 7.
11. Go to downstream end node 9. Compute the node current and then the voltage at junction node 7.
12. Compute the node current at node 7 using the most recent value of node 7 voltage.
13. Apply KCL at node 7 to compute the current flowing on the line segment from node 5 to node 7.
14. Compute the voltage at node 5.
15. Compute the node current at node 5.
16. Apply KCL at node 5 to determine the current flowing from node 4 toward node 5.
17. Compute the voltage at node 4.
18. Compute the node current at node 4.
19. Apply KCL at node 4 to compute the current flowing from node 3 to node 4.
20. Calculate the voltage at node 3.
21. Compute the node current at node 3.
22. Apply KCL at node 3 to compute the current flowing from node 2 to node 3.
23. Calculate the voltage at node 2.
24. Compute the node current at node 2.
25. Apply KCL at node 2.
26. Calculate the voltage at node 1.
27. Compare the calculated voltage at node 1 to the specified source voltage.
28. If not within tolerance, use the specified source voltage and the forward sweep current flowing from node 1 to node 2 and compute the new voltage at node 2.
29. The backward sweep continues using the new upstream voltage and line segment current from the forward sweep to compute the new downstream voltage.
30. The backward sweep is completed when new voltages at all end nodes have been completed.
31. This completes the first iteration.
32. Now repeat the forward sweep using the new end voltages rather than the assumed voltages as was done in the first iteration.

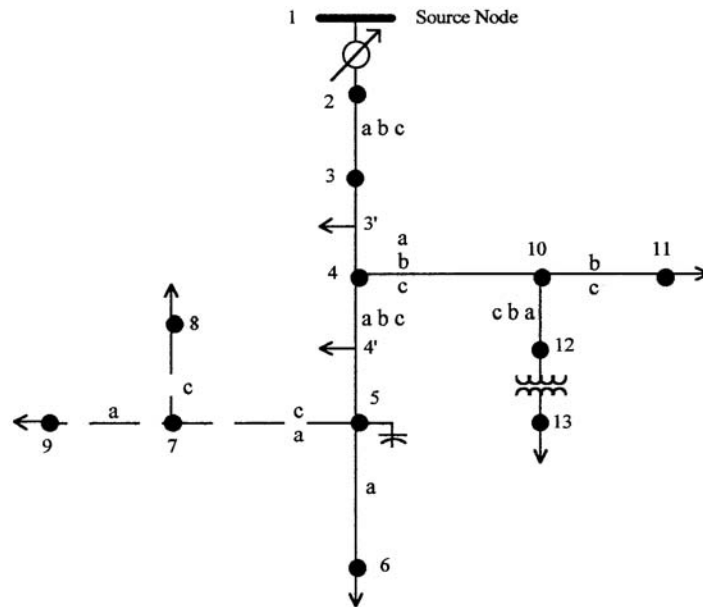


FIGURE 6.33 Unbalanced three-phase distribution feeder.

33. Continue the forward and backward sweeps until the calculated voltage at the source is within a specified tolerance of the source voltage
34. At this point the voltages are known at all nodes and the currents flowing in all line segments are known. An output report can be produced giving all desired results.

The Unbalanced Three-Phase Distribution Feeder

The previous section outlined the general procedure for performing the ladder iterative technique. This section will address how that procedure can be used for an unbalanced three-phase feeder.

Figure 6.33 is the one-line diagram of an unbalanced three-phase feeder.

The topology of the feeder in Fig. 6.33 is the same as the feeder in Fig. 6.32. Figure 6.33 shows more detail of the feeder however. The feeder in Fig. 6.33 can be broken into the “series” components and the “shunt” components.

Series Components

The “series” components of a distribution feeder are:

- Line segments
- Transformers
- Voltage regulators

Models for each of the series components have been developed in prior areas of this section. In all cases, models (three-phase, two-phase, and single-phase) were developed in such a manner that they can be generalized. Figure 6.34 shows the “general model” for each of the series components.

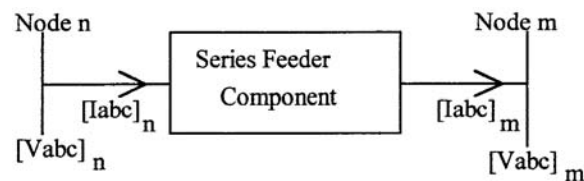


FIGURE 6.34 Series feeder component.

The general equations defining the “input” (Node n) and “output” (Node m) voltages and currents are given by:

$$\begin{bmatrix} V_{abc} \end{bmatrix}_n = \begin{bmatrix} a \end{bmatrix} \cdot \begin{bmatrix} V_{abc} \end{bmatrix}_m + \begin{bmatrix} b \end{bmatrix} \cdot \begin{bmatrix} I_{abc} \end{bmatrix}_m \quad (6.199)$$

$$\begin{bmatrix} I_{abc} \end{bmatrix}_n = \begin{bmatrix} c \end{bmatrix} \cdot \begin{bmatrix} V_{abc} \end{bmatrix}_m + \begin{bmatrix} d \end{bmatrix} \cdot \begin{bmatrix} I_{abc} \end{bmatrix}_m \quad (6.200)$$

The general equation relating the “output” (Node m) and “input” (Node n) voltages is given by:

$$\begin{bmatrix} V_{abc} \end{bmatrix}_m = \begin{bmatrix} A \end{bmatrix} \cdot \begin{bmatrix} V_{abc} \end{bmatrix}_n - \begin{bmatrix} B \end{bmatrix} \cdot \begin{bmatrix} I_{abc} \end{bmatrix}_m \quad (6.201)$$

In Eqs. (6.199), (6.200), and (6.201), the voltages are line-to-neutral for a four-wire wye feeder and “equivalent” line-to-neutral for a three-wire delta system. For transformers and voltage regulators, the voltages are line-to-neutral for terminals that are connected to a four-wire wye and line-to-line when connected to a three-wire delta.

Shunt Components

The shunt components of a distribution feeder are:

- Spot loads
- Distributed loads
- Capacitor banks

“Spot” loads are located at a node and can be three-phase, two-phase, or single-phase and connected in either a wye or a delta connection. The loads can be modeled as constant complex power, constant current, constant impedance, or a combination of the three.

“Distributed” loads are located at the mid-section of a line segment. A distributed load is modeled when the loads on a line segment are uniformly distributed along the length of the segment. As in the spot load, the distributed load can be three-phase, two-phase, or single-phase and connected in either a wye or a delta connection. The loads can be modeled as constant complex power, constant current, constant impedance, or a combination of the three. To model the distributed load, a “dummy” node is created in the center of a line segment with the distributed load of the line section modeled at this dummy node.

Capacitor banks are located at a node and can be three-phase, two-phase, or single-phase and can be connected in a wye or delta. Capacitor banks are modeled as constant admittances.

In Fig. 6.33 the solid line segments represent overhead lines while the dashed lines represent underground lines. Note that the phasing is shown for all of the line segments. In the area of this section entitled “Line Impedances”, the application of Carson’s equations for computing the line impedances for overhead and underground lines was presented. There it was pointed out that two-phase and single-phase lines are represented by a three-by-three matrix with zeros set in the rows and columns of the missing phases.

In the area of this section entitled “Line Admittances”, the method for the computation of the shunt capacitive susceptance for overhead and underground lines was presented. Most of the time the shunt capacitance of the line segment can be ignored; however, for long underground segments, the shunt capacitance should be included.

The “node” currents may be three-phase, two-phase, or single-phase and consist of the sum of the load current at the node plus the capacitor current (if any) at the node.

Applying the Ladder Iterative Technique

The previous section outlined the steps required for the application of the ladder iterative technique. For the general feeder of Fig. 6.33 the same outline applies. The only difference is that Eq. (6.199) and (6.200) are used for computing the node voltages on the “forward sweep” and Eq. (6.201) is used for computing

the downstream voltages on the “backward sweep.” The $[a]$, $[b]$, $[c]$, $[d]$, $[A]$, and $[B]$ matrices for the various series components are defined in the following areas of this section:

- Line Segments: Line Segment Models
- Voltage Regulators: Step-Voltage Regulators
- Transformer Banks: Transformer Bank Connections

The node currents are defined in the following area:

- Loads: Load Models
- Capacitors: Shunt Capacitor Models

Final Notes

Line Segment Impedances

It is extremely important that the impedances and admittances of the line segments be computed using the exact spacings and phasing. Because of the unbalanced loading and resulting unbalanced line currents, the voltage drops due to the mutual coupling of the lines become very important. It is not unusual to observe a voltage rise on a lightly loaded phase of a line segment that has an extreme current unbalance.

Power Loss

The real power losses of a line segment must be computed as the difference (by phase) of the input power to a line segment minus the output power of the line segment. It is possible to observe a negative power loss on a phase that is lightly loaded compared to the other two phases. Computing power loss as the phase current squared times the phase resistance does not give the actual real power loss in the phases.

Load Allocation

Many times the input complex power (kW and kVAr) to a feeder is known because of the metering at the substation. This information can be either total three-phase or for each individual phase. In some cases the metered data may be the current and power factor in each phase.

It is desirable to have the computed input to the feeder match the metered input. This can be accomplished (following a converged iterative solution) by computing the ratio of the metered input to the computed input. The phase loads can now be modified by multiplying the loads by this ratio. Because the losses of the feeder will change when the loads are changed, it is necessary to go through the ladder iterative process to determine a new computed input to the feeder. This new computed input will be closer to the metered input, but most likely not within a specified tolerance. Again, a ratio can be determined and the loads modified. This process is repeated until the computed input is within a specified tolerance of the metered input.

Short Circuit Analysis

The computation of short-circuit currents for unbalanced faults in a normally balanced three-phase system has traditionally been accomplished by the application of symmetrical components. However, this method is not well-suited to a distribution feeder that is inherently unbalanced. The unequal mutual coupling between phases leads to mutual coupling between sequence networks. When this happens, there is no advantage to using symmetrical components. Another reason for not using symmetrical components is that the phases between which faults occur is limited. For example, using symmetrical components, line-to-ground faults are limited to **phase a to ground**. What happens if a single-phase lateral is connected to phase **b** or **c**? This section will present a method for short circuit analysis of an unbalanced three-phase distribution feeder using the phase frame (Kersting, 1980).

General Theory

Figure 6.35 shows the unbalanced feeder as modeled for short-circuit calculations.

In Fig. 6.35, the voltage sources E_a , E_b , and E_c represent the Thevenin Equivalent line-to-ground voltages at the faulted bus. The matrix $[Z_{TOT}]$ represents the Thevenin Equivalent impedance matrix at the faulted bus. The fault impedance is represented by Z_f in Fig. 6.35.

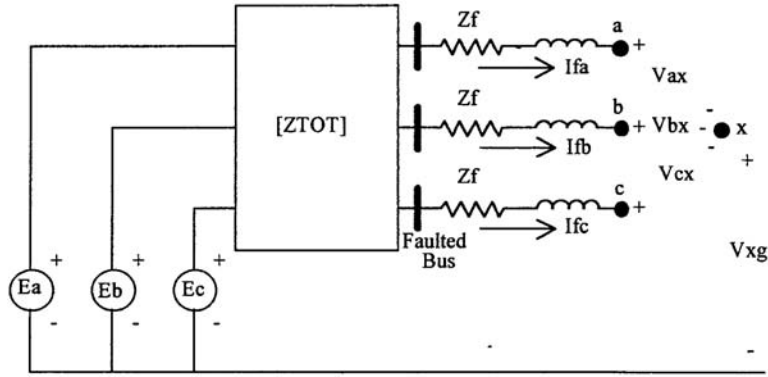


FIGURE 6.35 Unbalanced feeder short-circuit analysis model.

Kirchhoff's Voltage Law in matrix form can be applied to the circuit of Fig. 6.35.

$$\begin{bmatrix} E_a \\ E_b \\ E_c \end{bmatrix} = \begin{bmatrix} Z_{aa} & Z_{ab} & Z_{ac} \\ Z_{ba} & Z_{bb} & Z_{bc} \\ Z_{ca} & Z_{cb} & Z_{cc} \end{bmatrix} \cdot \begin{bmatrix} I_{fa} \\ I_{fb} \\ I_{fc} \end{bmatrix} + \begin{bmatrix} Z_f & 0 & 0 \\ 0 & Z_f & 0 \\ 0 & 0 & Z_f \end{bmatrix} \cdot \begin{bmatrix} I_{fa} \\ I_{fb} \\ I_{fc} \end{bmatrix} + \begin{bmatrix} V_{ax} \\ V_{bx} \\ V_{cx} \end{bmatrix} + \begin{bmatrix} V_{xg} \\ V_{xg} \\ V_{xg} \end{bmatrix} \quad (6.202)$$

Equation (6.202) can be written in compressed form as:

$$\begin{bmatrix} E_{abc} \end{bmatrix} = \begin{bmatrix} ZTOT \end{bmatrix} \cdot \begin{bmatrix} I_{abc} \end{bmatrix} + \begin{bmatrix} ZF \end{bmatrix} \cdot \begin{bmatrix} I_{abc} \end{bmatrix} + \begin{bmatrix} V_{abcx} \end{bmatrix} + \begin{bmatrix} V_{xg} \end{bmatrix} \quad (6.203)$$

Combine terms in Eq. (6.203).

$$\begin{bmatrix} E_{abc} \end{bmatrix} = \begin{bmatrix} ZEQ \end{bmatrix} \cdot \begin{bmatrix} I_{abc} \end{bmatrix} + \begin{bmatrix} V_{abcx} \end{bmatrix} + \begin{bmatrix} V_{xg} \end{bmatrix} \quad (6.204)$$

where:

$$\begin{bmatrix} ZEQ \end{bmatrix} = \begin{bmatrix} ZTOT \end{bmatrix} + \begin{bmatrix} ZF \end{bmatrix} \quad (6.205)$$

Solve Eq. (6.204) for the fault currents:

$$\begin{bmatrix} I_{abc} \end{bmatrix} = \begin{bmatrix} YEQ \end{bmatrix} \cdot \begin{bmatrix} E_{abc} \end{bmatrix} - \begin{bmatrix} YEQ \end{bmatrix} \cdot \begin{bmatrix} V_{abcx} \end{bmatrix} - \begin{bmatrix} YEQ \end{bmatrix} \cdot \begin{bmatrix} V_{xg} \end{bmatrix} \quad (6.206)$$

where

$$\begin{bmatrix} YEQ \end{bmatrix} = \begin{bmatrix} ZEQ \end{bmatrix}^{-1} \quad (6.207)$$

Since the matrices $\begin{bmatrix} YEQ \end{bmatrix}$ and $\begin{bmatrix} E_{abc} \end{bmatrix}$ are known, define:

$$\begin{bmatrix} IP_{abc} \end{bmatrix} = \begin{bmatrix} YEQ \end{bmatrix} \cdot \begin{bmatrix} E_{abc} \end{bmatrix} \quad (6.208)$$

Substituting Eq. (6.208) into Eq. (6.206) results in the expanded Eq. (6.209).

$$\begin{bmatrix} I_{fa} \\ I_{fb} \\ I_{fc} \end{bmatrix} = \begin{bmatrix} IP_a \\ IP_b \\ IP_c \end{bmatrix} - \begin{bmatrix} Y_{aa} & Y_{ab} & Y_{ac} \\ Y_{ba} & Y_{bb} & Y_{bc} \\ Y_{ca} & Y_{cb} & Y_{cc} \end{bmatrix} \cdot \begin{bmatrix} V_{ax} \\ V_{bx} \\ V_{cx} \end{bmatrix} - \begin{bmatrix} Y_{aa} & Y_{ab} & Y_{ac} \\ Y_{ba} & Y_{bb} & Y_{bc} \\ Y_{ca} & Y_{cb} & Y_{cc} \end{bmatrix} \cdot \begin{bmatrix} V_{xg} \\ V_{xg} \\ V_{xg} \end{bmatrix} \quad (6.209)$$

Performing the matrix operations in Eq. (6.209):

$$\begin{aligned} If_a &= IP_a - (Y_{aa} \cdot V_{ax} + Y_{ab} \cdot V_{bx} + Y_{ac} \cdot V_{cx}) - Y_a \cdot V_{xg} \\ If_b &= IP_b - (Y_{ba} \cdot V_{ax} + Y_{bb} \cdot V_{bx} + Y_{bc} \cdot V_{cx}) - Y_b \cdot V_{xg} \\ If_c &= IP_c - (Y_{ca} \cdot V_{ax} + Y_{cb} \cdot V_{bx} + Y_{cc} \cdot V_{cx}) - Y_c \cdot V_{xg} \end{aligned} \quad (6.210)$$

$$Y_a = Y_{aa} + Y_{ab} + Y_{ac}$$

where

$$Y_b = Y_{ba} + Y_{bb} + Y_{bc} \quad (6.211)$$

$$Y_c = Y_{ca} + Y_{cb} + Y_{cc}$$

Equations (6.210) become the general equations that are used to simulate all types of short circuits. Basically there are three equations and seven unknowns (If_a , If_b , If_c , V_{ax} , V_{bx} , V_{cx} , and V_{xg}). The other three variables in the equations (IP_a , IP_b , and IP_c) are functions of the total impedance and the Thevenin voltages and are therefore known. In order to solve Eq. (6.210), it will be necessary to specify four of the seven unknowns. These specifications are functions of the type of fault being simulated. The additional required four knowns for various types of faults are given below:

Three-phase faults

$$\begin{aligned} V_{ax} &= V_{bx} = V_{cx} = 0 \\ I_a + I_b + I_c &= 0 \end{aligned} \quad (6.212)$$

Three-phase-to-ground faults

$$V_{ax} = V_{bx} = V_{cx} = V_{xg} = 0 \quad (6.213)$$

Line-to-line faults (assume **i-j** fault with phase **k** unfaulted)

$$\begin{aligned} V_{ix} &= V_{jx} = 0 \\ If_k &= 0 \\ If_i + If_j &= 0 \end{aligned} \quad (6.214)$$

Line-to-line-to-ground faults (assume **i-j** to ground fault with **k** unfaulted)

$$\begin{aligned} V_{ix} &= V_{jx} = V_{xg} = 0 \\ V_{kx} &= \frac{IP_k}{Y_{kk}} \end{aligned} \quad (6.215)$$

Line-to-ground faults (assume phase **k** fault with phases **i** and **j** unfaulted)

$$\begin{aligned} V_{kx} &= V_{xg} = 0 \\ If_i &= If_j = 0 \end{aligned} \quad (6.216)$$

Notice that Eqs. (6.214), (6.215), and (6.216) will allow the simulation of line-to-line, line-to-line-to-ground, and line-to-ground faults for all phases. There is no limitation to **b-c** faults for line-to-line and **a-g** for line-to-ground as is the case when the method of symmetrical components is employed.

References

- Carson, J. R., Wave propagation in overhead wires with ground return, *Bell Syst. Tech. J.*, 5, 1926.
- Glover, J. D. and Sarma, M., *Power System Analysis and Design*, 2nd ed., PWS Publishing Company, Boston, 1994, chap. 5.
- Kersting, W. H., Distribution system short circuit analysis, *25th Intersociety Energy Conversion Conference*, Reno, Nevada, August 1980.
- Kersting, W. H., *Milsoft Transformer Models — Theory*, Research Report, Milsoft Integrated Solutions, Inc., Abilene, TX, 1999.
- Kersting, W. H. and Mendive, D. L., An application of ladder network theory to the solution of three-phase radial load-flow problems, IEEE Conference Paper presented at the *IEEE Winter Power Meeting*, New York, January 1976.
- Kron, G., Tensorial analysis of integrated transmission systems, Part I: The six basic reference frames, *AIEE Trans.*, 71, 1952.
- Trevino, C., Cases of difficult convergence in load-flow problems, IEEE Paper n. 71-62-PWR, presented at the IEEE Summer Power Meeting, Los Angeles, CA, 1970.

6.3 Power System Operation and Control

George L. Clark and Simon W. Bowen

Implementation of Distribution Automation

The implementation of “distribution automation” within the continental U.S. is as diverse and numerous as the utilities themselves. Particular strategies of implementation utilized by various utilities have depended heavily on environmental variables such as size of the utility, urbanization, and available communication paths. The current level of interest in distribution automation is the result of:

- The maturation of technologies within the past 10 years in the areas of communication and RTUs/PLCs.
- Increased performance in host servers for the same or lower cost; lower cost of memory.
- The threat of deregulation and competition as a catalyst to automate.
- Strategic benefits to be derived (e.g., potential of reduced labor costs, better planning from better information, optimizing of capital expenditures, reduced outage time, increased customer satisfaction).

While not meant to be all-inclusive, this section on distribution automation attempts to provide some dimension to the various alternatives available to the utility engineer. The focus will be on providing insight on the elements of automation that should be included in a scalable and extensible system. The approach will be to describe the elements of a “typical” distribution automation system in a simple manner, offering practical observations as required.

For the electric utility, justification for automating the distribution system, while being highly desirable, was not readily attainable based on a cost/benefit ratio due to the size of the distribution infrastructure and cost of communication circuits. Still there have been tactical applications deployed on parts of distribution systems that were enough to keep the dream alive. The development of the PC (based on the Intel architecture) and VME systems (based on the Motorola architecture) provided the first low-cost SCADA master systems that were sized appropriately for the small co-ops and municipality utilities. New SCADA vendors then entered the market targeting solutions for small to medium-sized utilities.

Eventually the SCADA vendors who had been providing transmission SCADA took notice of the distribution market. These vendors provided host architectures based on VAX/VMS (and later Alpha/Open-VMS) platforms and on UNIX platforms from IBM and Hewlett-Packard. These systems were required for the large distribution utility (100,000–250,000 point ranges). These systems often resided on company-owned LANs with communication front-end processors and user interface attached either locally on the same LAN or across a WAN.

Distribution SCADA History

Supervisory Control And Data Acquisition (SCADA) is the foundation for the distribution automation system. The ability to remotely monitor and control electric power system facilities found its first application within the power generation and transmission sectors of the electric utility industry. The ability to significantly influence the utility bottom line through the effective dispatch of generation and the marketing of excess generating capacity provided economic incentive. The interconnection of large power grids in the midwestern and the southern U.S. (1962) created the largest synchronized system in the world. The blackout of 1965 prompted the U.S. Federal Power Commission to recommend closer coordination between regional coordination groups (Electric Power Reliability Act of 1967), and gave impetus to the subsequent formation of the National Electric Reliability Council (1970). From that time (1970) forward, the priority of the electric utility has been to engineer and build a highly reliable and secure transmission infrastructure. Transmission SCADA became the base for the large Energy Management Systems that were required to manage the transmission grid. Distribution SCADA languished during this period.

In the mid-1980s, EPRI published definitions for distribution automation and associated elements. The industry generally associates distribution automation with the installation of automated distribution line devices, such as switches, reclosers, sectionalizers, etc. The author's definition of distribution automation encompasses the automation of the distribution substations and the distribution line devices. The automated distribution substations and the automated distribution line devices are then operated as a system to facilitate the operation of the electric distribution system.

SCADA System Elements

At a high level, the elements of a distribution automation system can be divided into three main areas:

- SCADA application and server(s)
- DMS applications and server(s)
- Trouble management applications and server(s)

Distribution SCADA

As was stated in the introduction, the Supervisory Control And Data Acquisition (SCADA) system is the heart of Distribution Management System (DMS) architecture. A SCADA system should have all of the infrastructure elements to support the multifaceted nature of distribution automation and the higher level applications of a DMS. A Distribution SCADA system's primary function is in support of distribution operations telemetry, alarming, event recording, and remote control of field equipment. Historically, SCADA systems have been notorious for their lack of support for the import, and more importantly, the export of power system data values. A modern SCADA system should support the engineering budgeting and planning functions by providing access to power system data without having to have possession of an operational workstation. The main elements of a SCADA system are:

- Host equipment
- Communication infrastructure (network and serial communications)
- Field devices (in sufficient quantity to support operations and telemetry requirements of a DMS platform)

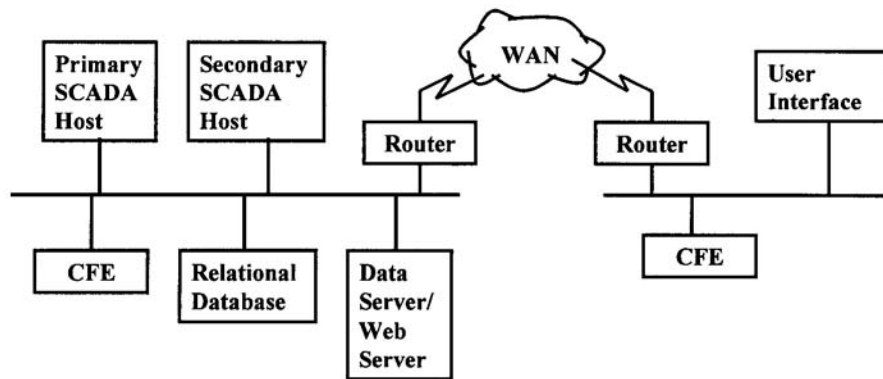


FIGURE 6.36 DA system architecture.

Host Equipment

The authors feel that the essential elements of a distribution SCADA host are:

- Host servers (redundant servers with backup/failover capability).
- Communication front-end nodes (network based).
- Full graphics user interfaces.
- Relational database server (for archival of historical power system values) and data server/Web server (for access to near real time values and events).

The elements and components of the typical distribution automation system are illustrated in [Fig. 6.36](#).

Host Computer System

SCADA Servers

As SCADA has proven its value in operation during inclement weather conditions, service restoration, and daily operations, the dependency on SCADA has created a requirement for highly available and high-performance systems. Redundant server hardware operating in a “live” backup/failover mode is required to meet the high availability criteria. High-performance servers with abundant physical memory, RAID hard disk systems, and interconnected by 10/100 baseT switched Ethernet are typical of today’s SCADA servers.

Communication Front-End (CFE) Processors

The current state of host to field device communications still depends heavily on serial communications. This requirement is filled by the CFE. The CFE can come in several forms based on bus architecture (e.g., VME or PCI) and operating system. Location of the CFE in relation to the SCADA server can vary based on requirement. In some configurations the CFE is located on the LAN with the SCADA server. In other cases, existing communications hubs may dictate that the CFE reside at the communication hub. The incorporation of the WAN into the architecture requires a more robust CFE application to compensate for less reliable communications (in comparison to LAN). In general the CFE will include three functional devices: a network/CPU board, serial cards, and possibly a time code receiver. Functionality should include the ability to download configuration and scan tables. The CFE should also support the ability to dead band values (i.e., report only those analog values that have changed by a user-defined amount). CFE, network, and SCADA servers should be capable of supporting worst-case conditions (i.e., all points changing outside of the dead band limits), which typically occur during severe system disturbances.

Full Graphics User Interface

The current trend in the user interface (UI) is toward a full graphics (FG) user interface. While character graphics consoles are still in use by many utilities today, SCADA vendors are aggressively moving their

platforms to a full graphics UI. Quite often the SCADA vendors have implemented their new full graphics user interface on low-cost NT workstations using third-party applications to emulate the X11 window system. Full graphic displays provide the ability to display power system data along with the electric distribution facilities in a geographical (or semigeographical) perspective. The advantage of using a full graphics interface becomes evident (particularly for distribution utilities) as SCADA is deployed beyond the substation fence where feeder diagrams become critical to distribution operations.

Relational Databases, Data Servers, and Web Servers

The traditional SCADA systems were poor providers of data to anyone not connected to the SCADA system by an operational console. This occurred due to the proprietary nature of the performance (in memory) database and its design optimization for putting scanned data in and pushing display values out. Power system quantities such as: bank and feeder loading (MW, MWH, MQH, and ampere loading), and bus volts provide valuable information to the distribution planning engineer. The availability of event (log) data is important in postmortem analysis. The use of relational databases, data servers, and Web servers by the corporate and engineering functions provides access to power system information and data while isolating the SCADA server from nonoperations personnel.

Host to Field Communications

Serial communications to field devices can occur over several mediums: copper wire, fiber, radio, and even satellite. Telephone circuits, fiber, and satellites have a relatively high cost. New radio technologies offer good communications value. One such technology is the Multiple Address Radio System (MAS). The MAS operates in the 900 MHz range and is omnidirectional, providing radio coverage in an area with radius up to 20–25 miles depending on terrain. A single MAS master radio can communicate with many remote sites. Protocol and bandwidth limit the number of remote terminal units that can be communicated with by a master radio. The protocol limit is simply the address range supported by the protocol. Bandwidth limitations can be offset by the use of efficient protocols, or slowing down the scan rate to include more remote units. Spread-spectrum and point-to-point radio (in combination with MAS) offers an opportunity to address specific communication problems. At the present time MAS radio is preferred (authors' opinion) to packet radio (another new radio technology); MAS radio communications tend to be more deterministic providing for smaller timeout values on communication no-responses and controls.

Field Devices

Distribution Automation (DA) field devices are multi-featured installations meeting a broad range of control, operations, planning, and system performance issues for the utility personnel. Each device provides specific functionality, supports system operations, includes fault detection, captures planning data and records power quality information. These devices are found in the distribution substation and at selected locations along the distribution line. The multifeatured capability of the DA device increases its ability to be integrated into the electric distribution system. The functionality and operations capabilities complement each other with regard to the control and operation of the electric distribution system. The fault detection feature is the “eyes and ears” for the operating personnel. The fault detection capability becomes increasingly more useful with the penetration of DA devices on the distribution line.

The real-time data collected by the SCADA system is provided to the planning engineers for inclusion in the radial distribution line studies. As the distribution system continues to grow, the utility makes annual investments to improve the electric distribution system to maintain adequate facilities to meet the increasing load requirements. The use of the real-time data permits the planning engineers to optimize the annual capital expenditures required to meet the growing needs of the electric distribution system.

The power quality information includes capturing harmonic content to the 15th harmonic and recording Percent Total Harmonic Distortion (%THD). This information is used to monitor the performance of the distribution electric system.

Modern RTU

Today's modern RTU is modular in construction with advanced capabilities to support functions that heretofore were not included in the RTU design. The modular design supports installation configurations ranging from the small point count required for the distribution line pole-mounted units to the very large point count required for large bulk-power substations and power plant switchyard installations. The modern RTU modules include analog units with 9 points, control units with 4 control pair points, status units with 16 points, and communication units with power supply. The RTU installation requirements are met by accumulating the necessary number of modern RTU modules to support the analog, control, status, and communication requirements for the site to be automated. Packaging of the minimum point count RTUs is available for the distribution line requirement. The substation automation requirement has the option of installing the traditional RTU in one cabinet with connections to the substation devices or distributing the RTU modules at the devices within the substation with fiberoptic communications between the modules. The distributed RTU modules are connected to a data concentrating unit which in turn communicates with the host SCADA computer system.

The modern RTU accepts direct AC inputs from a variety of measurement devices including line-post sensors, current transformers, potential transformers, station service transformers, and transducers. Direct AC inputs with the processing capability in the modern RTU supports fault current detection and harmonic content measurements. The modern RTU has the capability to report the magnitude, direction, and duration of fault current with time tagging of the fault event to 1-millisecond resolution. Monitoring and reporting of harmonic content in the distribution electric circuit are capabilities that are included in the modern RTU. The digital signal processing capability of the modern RTU supports the necessary calculations to report %THD for each voltage and current measurement at the automated distribution line or substation site.

The modern RTU includes logic capability to support the creation of algorithms to meet specific operating needs. Automatic transfer schemes have been built using automated switches and modern RTUs with the logic capability. This capability provides another option to the distribution line engineer when developing the method of service and addressing critical load concerns. The logic capability in the modern RTU has been used to create the algorithm to control distribution line switched capacitors for operation on a per phase basis. The capacitors are switched on at zero voltage crossing and switched off at zero current crossing. The algorithm can be designed to switch the capacitors for various system parameters, such as voltage, reactive load, time, etc. The remote control capability of the modern RTU then allows the system operator to take control of the capacitors to meet system reactive load needs.

The modern RTU has become a dynamic device with increased capabilities. The new logic and input capabilities are being exploited to expand the uses and applications of the modern RTU.

PLCs and IEDs

Programmable Logic Controllers (PLCs) and Intelligent Electronic Devices (IEDs) are components of the distribution automation system, which meet specific operating and data gathering requirements. While there is some overlap in capability with the modern RTU, the authors are familiar with the use of PLCs for automatic isolation of the faulted power transformer in a two-bank substation and automatic transfer of load to the unfaulted power transformer to maintain an increased degree of reliability. The PLC communicates with the modern RTU in the substation to facilitate the remote operation of the substation facility. The typical PLC can support serial communications to a SCADA server. The modern RTU has the capability to communicate via an RS-232 interface with the PLC.

IEDs include electronic meters, electronic relays, and controls on specific substation equipment, such as breakers, regulators, LTC on power transformers, etc. The IEDs also have the capability to support serial communications to a SCADA server. However, the authors' experience indicates that the IEDs are typically reporting to the modern RTU via an RS-232 interface or via status output contact points. As its communicating capability improves and achieves equal status with the functionality capability, the IED has the potential to become an equal player in the automation communication environment.

However, in the opinion of the authors, the limited processing capability for supporting the communication requirement, in addition to its functional requirements (i.e., relays, meters, etc.), hampers the widespread use of the IEDs in the distribution automation system.

Substation

The installation of the SCADA technology in the DA substation provides for the full automation of the distribution substation functions and features. The modular RTU supports the various substation sizes and configuration. The load on the power transformer is monitored and reported on a per-phase basis. The substation low-side bus voltage is monitored on a per phase basis. The distribution feeder breaker is fully automated. Control of all breaker control points is provided including the ability to remotely set up the distribution feeder breaker to support energized distribution line work. The switched capacitor banks and substation regulation are controlled from the typical modular RTU installation. The load on the distribution feeder breaker is monitored and reported on a per-phase basis as well as on a three-phase basis. This capability is used to support the normal operations of the electric distribution system and to respond to system disturbances. The installation of the SCADA technology in the DA substation eliminates the need to dispatch personnel to the substation except for periodic maintenance and equipment failure.

Line

The DA distribution line applications include line monitoring, pole-mounted reclosers, gang-operated switches equipped with motor operators, switched capacitor banks, and pad-mounted automatic transfer switchgear. The modular RTU facilitates the automation of the distribution line applications. The use of the line post sensor facilitates the monitoring capability on a per-phase basis. The direct AC input from the sensors to the RTU supports monitoring of the normal load, voltage and power factor measurements, and also the detection of fault current. The multifeatured distribution line DA device can be used effectively to identify the faulted sections of the distribution circuit during system disturbances, isolate the faulted sections, and restore service to the unfaulted sections of the distribution circuit. The direct AC inputs to the RTU also support the detection and reporting of harmonics to the 15th harmonic and the %THD per phase for voltage and current.

Tactical and Strategic Implementation Issues

As the threat of deregulation and competition emerges, retention of industrial and large commercial customers will become the priority for the electric utility. Every advantage will be sought by the electric utility to differentiate itself from other utilities. Reliable service, customer satisfaction, fast storm restorations, and power quality will be the goals of the utility. Differing strategies will be employed based on the customer in question and the particular mix of goals that the utility perceives will bring customer loyalty.

For large industrial and commercial customers, where the reliability of the electric service is important and outages of more than a few seconds can mean lost production runs or lost revenue, tactical automation solutions may be required. Tactical solutions are typically transfer schemes or switching schemes that can respond independently of operator action, reporting the actions that were initiated in response to loss of preferred service and/or line faults. The requirement to transfer source power, or reconfigure a section of the electric distribution system to isolate and reconnect in a matter of seconds is the primary criteria. Tactical automation based on local processing provides the solution.

In cases where there are particularly sensitive customer requirements, tactical solutions are appropriate. When the same requirements are applied to a large area and/or customer base, a strategic solution based on a distribution management platform is preferred. This solution requires a DMS with a system operational model that reflects the current configuration of the electric distribution system. Automatic fault isolation and restoration applications that can reconfigure the electric distribution system, require a “whole system” model in order to operate correctly and efficiently.

So while tactical automation requirements exist and have significant impact and high profile, goals that target system issues (reduction of system losses, voltage programs, storm restoration) require a strategic solution.

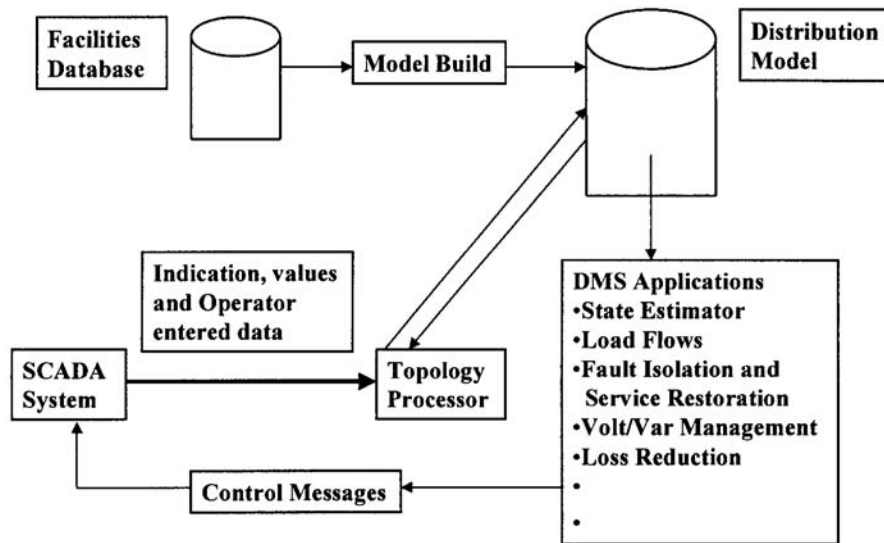


FIGURE 6.37 A DMS platform with SCADA interface.

Distribution Management Platform

Distribution Management System

A functional Distribution Management System (DMS) platform should be fully integrated with the distribution SCADA system. The SCADA-DMS interface should be fully implemented with the capability of passing data [discrete indication (status) and values (analog)] bidirectionally. The SCADA interface should also support device control. Figure 6.37 details the components of a DMS.

Trouble Management Platform

Trouble Management System

In addition to the base SCADA functionality and high-level DMS applications, the complete distribution automation system will include a Trouble Management System (TMS). Trouble Management Systems collect trouble calls received by human operators and Interactive Voice Recorders (IVR). The trouble calls are fed to an analysis/prediction engine that has a model of the distribution system with customer to electrical address relationships. Outage prediction is presented on a full graphics display that overlays the distribution system on CAD base information. A TMS also provides for the dispatch and management of crews, customer callbacks, accounting, and reports. A SCADA interface to a TMS provides the means to provide confirmed (SCADA telemetry) outage information to the prediction engine. Figure 6.38 shows a typical TMS.

Practical Considerations

Choosing the Vendor

Choosing a Platform Vendor

In choosing a platform (SCADA, DMS, TMS) vendor there are several characteristics that should be kept in mind (these should be considered as rule of thumb based on experience of what works and what does not). Choosing the right vendor is as important as choosing the right software package.

Vendor characteristics that the authors consider important are:

- A strong “product” philosophy. Having a strong product philosophy is typically a chicken and egg proposition. Which came first, the product or the philosophy? Having a baseline SCADA application

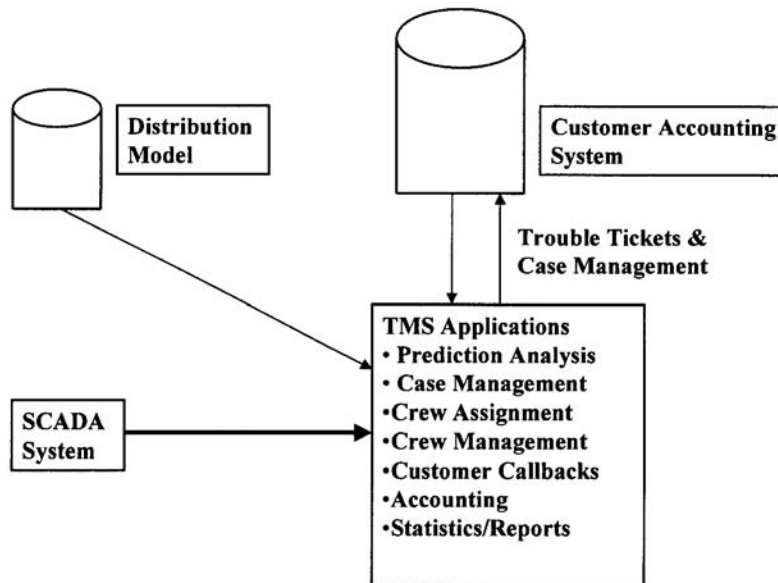


FIGURE 6.38 A TMS platform with SCADA interface.

can be a sign of maturity and stability. Did the platform vendor get there by design or did they back into it? Evidence of a product philosophy include a baseline system that is in production and enhancements that are integrated in a planned manner with thorough testing on the enhancement and regression testing on the product along with complete and comprehensive documentation.

- A documented development and release path projected three to five years into the future.
- By inference from the first two bullets, a vendor who funds planned product enhancements from internal funds.
- A strong and active User Group that is representative of the industry and industry drivers.
- A platform vendor that actively encourages its User Group by incentive (e.g., dedicating part of its enhancement funding to User Group initiatives).
- A vendor that is generally conservative in moving its platform to a new technology; one that does not overextend its own resources.

Other Considerations

- As much as possible, purchase the platform as an off-the-shelf product (i.e., resist the urge to ask for customs that drive your system away from the vendor's baseline).
- If possible, maintain/develop your own support staff.

All "customization" should be built around the inherent capabilities and flexibility of the system (i.e., do not generate excessive amounts of new code). Remember, you will have to reapply any code that you may have developed to every new release; or worse, you will have to pay the vendor to do it for you.

Standards

Internal Standards

The authors highly recommend the use of standards (internal to your organization) as a basis for ensuring a successful distribution automation or SCADA program. Well-documented construction standards that specify installation of RTUs, switches, and line sensors with mechanical and electrical specifications will ensure consistent equipment installations from site to site. Standards that cover nontrivial, but often overlooked issues can often spell the difference between acceptance and rejection by operational users

and provide the additional benefit of having a system that is “maintainable” over the 10–20 year (or more) life of a system. Standards that fall in this category include standards that cover point-naming conventions, symbol standards, display standards, and the all-important Operations Manual.

Industry Standards

In general, standards fall into two categories: standards that are developed by organizations and commissions (e.g., EPRI, IEEE, ANSI, CCITT, ISO, etc.) and *de facto* standards that become standards by virtue of widespread acceptance. As an example of what can occur, the reader is invited to consider what has happened in network protocols over the recent past with regard to the OSI model and TCP/IP.

Past history of SCADA and automation has been dominated by the proprietary nature of the various system vendor offerings. Database schemas and RTU communication protocols are exemplary of proprietary design philosophies utilized by SCADA platform and RTU vendors. Electric utilities that operate as part of the interconnected power grid have been frustrated by the lack of ability to share power system data between dissimilar energy management systems. The same frustration exists at the device level; RTU vendors, PLC vendors, electronic relay vendors, and meter vendors each having their own product protocols have created a “Tower of Babel” problem for utilities. Recently several communications standards organizations and vendor consortiums have proposed standards to address these deficiencies in intersystem data exchange, intrasystem data exchange (corporate data exchange), and device level interconnectivity. Some of the more notable examples of network protocol communication standards are ICCP (Inter Control Center Protocol), UCA (Utility Communication Architecture), CCAPI (Control Center Applications Interface), and UIB (Utility Integration Bus). For database schemas, EPRI’s CIM (Common Information Model) is gaining supporters. In RTU, PLC, and IED communications, DNP 3.0 has also received much industry press.

In light of the number of standards that have appeared (and then disappeared) and the number of possibly competing “standards” that are available today, the authors, while acknowledging the value of standards, prefer to take (and recommend) a cautious approach to standards. A wait-and-see posture may be an effective strategy. Standards by definition must have proven themselves over time. Difficulties in immediately embracing new standards are due in part to vendors having been allowed to implement only portions of a standard, thereby nullifying the hopefully “plug-and-play” aspect for adding new devices. Also, the trend in communication protocols has been to add functionality in an attempt to be all-inclusive, which has resulted in an increased requirement on bandwidth. Practically speaking, utilities that have already existing infrastructure may find it economical to resist the deployment of new protocols. In the final analysis, as in any business decision, a “standard” should be accepted only if it adds value and benefit that exceeds the cost of implementation and deployment.

Deployment Considerations

The definition of the automation technology to be deployed should be clearly delineated. This definition includes the specification of the host systems, the communication infrastructure, the automated end-use devices, and the support infrastructure. This effort begins with the development of a detailed installation plan that takes into consideration the available resources. The pilot installation will never be any more than a pilot project until funding and manpower resources are identified and dedicated to the enterprise of implementing the technologies required to automate the electric distribution system. The implementation effort is best managed on an annual basis with stated incremental goals and objectives for the installation of automated devices. With the annual goals and objectives identified, then the budget process begins to ensure that adequate funding is available to support the implementation plan. To ensure adequate time to complete the initial project tasks, the planning should begin 18 to 24 months prior to the budget year. During this period, the identification of specific automation projects is completed. The initial design work is commenced with the specification of field automation equipment (e.g., substation RTU based on specific point count requirements and distribution line RTU). The verification of the communication to the selected automation site is an urgent early consideration in order to minimize the cost of achieving effective remote communications. As the installation year approaches, the associated

automation equipment (e.g., switches, motor-operators, sensors, etc.) must be verified to ensure that adequate supplies are stocked to support the implementation plan.

The creation of a SCADA database and display is on the critical path for new automated sites. The database and display are critical to the efficient completion of the installation and checkout tasks. Data must be provided to the database and display team with sufficient lead time to create the database and display for the automated site. The database and display are subsequently used to checkout the completed automated field device. The Point Assignment (PA) sheet is a project activity that merits serious attention. The PA sheet is the basis for the creation of the site-specific database in the SCADA system. The PA sheet should be created in a consistent and standard fashion. The importance of an accurate database and display cannot be overemphasized. The database and display form the basis for the remote operational decisions for the electric distribution system using the SCADA capability. Careful coordination of these project tasks is essential to the successful completion of the annual automation plans.

Training is another important consideration during the deployment of the automation technology. The training topics are as varied as the multidisciplinary nature of the distribution automation project. Initial training requirements include the system support personnel in the use and deployment of the automation platform, the end-user (operator) training, and installation teams. Many utilities now install new distribution facilities using energized line construction techniques. The automated field device adds a degree of complexity to the construction techniques to ensure adherence to safe practices and construction standards. These training issues should be addressed at the outset of the planning effort to ensure a successful distribution automation project.

Support Organization

The support organization must be as multidisciplinary as the distribution automation system is multifaceted. The support to maintain a deployed distribution automation system should not be underestimated. Functional teams should be formed to address each discipline represented within the distribution automation system. The authors recommend forming a core team that is made up of representation from each area of discipline or area of responsibility within the distribution automation project. These areas of discipline include the following:

- Host SCADA system
- User interface
- Communication infrastructure
- Facilities design personnel for automated distribution substation and distribution line devices
- System software and interface developments
- Installation teams for automated distribution substation and distribution line devices
- End-users (i.e., the operating personnel)

The remaining requirement for the core team is project leadership with responsibility for the project budget, scheduling, management reports, and overall direction of the distribution automation project. The interaction of the various disciplines within the distribution automation team will ensure that all project decisions are supporting the overall project goals. The close coordination of the various project teams through the core team is essential to minimizing decision conflict and maximizing the synergy of project decisions. The involvement of the end-user at the very outset of the distribution automation project planning cannot be overemphasized. The operating personnel are the primary users of the distribution automation technology. The participation of the end-user in all project decisions is essential to ensure that the distribution automation product meets business needs and improves the operating environment in the operating centers. One measure of good project decisions is found in the response of the end-user. When the end-user says, "I like it," then the project decision is clearly targeting the end-user's business requirements. With this goal achieved, then the distribution automation system is in position to begin meeting other corporate business needs for real-time data from the electric distribution system.